Deltares

Enabling Delta Life

North Sea conditions on 1 and 2 January 2019

Metocean conditions during the incident with the MSC Zoe

Prepared for Dutch Safety Board

Deltares

North Sea conditions on 1 and 2 January 2019

Metocean conditions during the incident with the MSC Zoe

S.P. Reijmerink
M.P.C. de Jong
A.J. van der Hout

Photo cover: MSC Zoe after loss of containers (Source : Kustwacht Nederland)

Deltares

Title
North Sea conditions on 1 and 2 January 2019

Client	Project	Attribute	Pages
Dutch Safety Board	11204419-002	11204419-002-HYE-0001	65

Classification
Secret until further notice

Keywords
MSC Zoe, containers, incident, storm, shallow water, ground seas, grondzee

Project context
The Dutch Safety Board (Onderzoeksraad voor Veiligheid, OVV) is performing an investigation into the incident involving container vessel 'MSC Zoe' on 1 and 2 of January 2019, when that ship lost several containers in an area north of the Dutch Wadden Islands. This report describes the contents and outcomes of related tasks performed by Deltares under assignment by OVV.

The tasks by Deltares were focused on 1) deriving the metocean conditions (wind, waves, water levels, currents) that occurred in the area north of the Dutch and German Wadden Islands during the days of the event and 2) which conditions the vessel encountered along its track. The exceptionality of those conditions was assessed by comparing them to reference statistics of wind and wave conditions for the area. Furthermore, variations in time and space of metocean conditions were considered by comparing the conditions encountered by the vessel along its track to conditions during the storm at other moments in time and in other parts of the considered area.

The tasks by Deltares also involved the translation of the derived conditions to representative parameter values to be considered for physical scale model tests, performed by MARIN within the same project context (MARIN, 2019). As a final confirmation, the generated wave conditions inside the laboratory basin were checked by Deltares for their representativeness of the metocean conditions as derived for the area north of the Wadden Islands on 1-2 January 2019.

The detailed project approach, results and conclusions are described in an Executive Summary included on the following pages. Section 1.5 of the main report text includes a reading guide directing the reader to specific parts of the report for further background information.

References
Deltares offer 11204419-001-HYE-0001, dated 18 July 2019
Summary document actions and agreements by OVV, dated 24 July 2019
Contract award 'Overeenkomst 0004/2019/100077', dated 15 August 2019

Version	Date	Author	Initials	Review	Initials	Approval	Initials
1 - draft (excl. Sec 6.3)	Sep. 2019	S.P. Reijmerink et al.		S. Caires		J. Schouten	
2 - draft (complete)	Oct. 2019	S.P. Reijmerink et. al.		S. Caires		J. Schouten	
3 – draft (feedback DSB)	Nov. 2019	S.P. Reijmerink et. al.		S. Caires		J. Schouten	
4 – final	June 2020	S.P. Reijmerink M.P.C. de Jong A.J. van der Hout		S. Caires		J. Schouten	

Status
Final

Executive summary

The Dutch Safety Board (Onderzoeksraad voor Veiligheid, OVV) is performing an investigation into the incident involving container vessel 'MSC Zoe' on 1 and 2 of January 2019, when that ship lost several containers in an area north of the Dutch Wadden Islands. OVV has asked the Dutch knowledge institutes Deltares and MARIN to contribute to the research by providing insight in:

- the metocean conditions (wind, waves, currents) during the accident,
- the vessel motion behaviour under such conditions,
- how frequent these metocean conditions can be expected to occur.

Overall (and eventually), the investigation is foreseen to answer the following research questions:

1. What were the local environmental conditions during the incident (1-2 January 2019) in the North Sea region north of the Dutch Wadden islands, both on the selected route of MSC Zoe, and in the area of the sea route further north in deeper water?
2. How will specific environmental conditions and vessel properties (of large container vessels) contribute to the risk of losing containers?
3. Which parameters (vessel parameters and/or environmental conditions) are important for route selection and which of these parameters will provide vessel crew members insight in the specific sailing conditions north of the Wadden Islands and their possible consequences for vessel motions?

The present project phase covers Research Questions 1 and 2. Deltares has performed tasks aimed at providing the answers to Question 1 and MARIN worked on answering the different elements of Question 2 (MARIN, 2019).

This report describes the approach, results and conclusions of the tasks carried out by Deltares within the project. It is a technical advice report that deals with complex phenomena such as wave growth, dissipation and propagation. This Executive Summary and the Conclusions chapter (Chapter 7) are aimed at a broad readers audience. Other chapters in the main report provide background information for readers interested in further details of the work performed and of the results.

Data from operational measurement stations in the area were considered first to analyse local conditions in the area (wind, waves, water levels) on 1-2 January 2019 and surrounding days. These data gave valuable information for general characterisation of the storm event[1]. However, that measured information is only available at a compact set of observation points, most of them located at some distance from where the incident occurred. Therefore, numerical models and model output were used to derive the conditions along the track of the vessel and to obtain detailed spatial maps of metocean conditions (currents, wind, waves) for further analyses. The areas covered with these numerical models included the southern and the northern west-east sailing routes north of the Wadden Islands.

[1] *Please note that in this report we use the term 'storm' as a common label used in coastal engineering (and possibly in laymen's terms) to refer to an interval of increased windspeeds. In a formal meteorological definition, the situation as encountered by the MSC Zoe on 1-2 January 2018 corresponded to "(near) gale conditions" and not to a full storm force.*

Spatial distributions of wind, water levels and currents at regular intervals in time were obtained from operational model sources, i.e. numerical models that are run and applied daily for weather forecasts (by organisations such as Rijkswaterstaat) and climate studies and of which results are archived. Those were used as input to force a detailed local numerical wave model, which was used to produce spatial distributions of waves in the area. The ship track (location and timing) was projected on the different model outputs to establish which conditions the vessel had encountered north of the Wadden Islands along its route. The results are summarised in the table below (MSL means Mean Sea Level). These most severe conditions were experienced by the MSC Zoe within the time interval 1 January 18:00 h to 2 January 06:00 h.

Table ES.1 Most severe metocean conditions experienced by MSC Zoe on 1-2 January 2019 (numerical outcomes).

Parameter	Representative value (range) along the track of the ship on 1-2 January 2019	Frequency of occurrence, exceptionality
Current speed	up to 0.5 m/s (1 kn)	Very common, occur daily
Water level	MSL + 0 m – MSL + 1 m	
Wind speed	16 – 18 m/s	Are exceeded on average one to two times in a year
Significant wave height (H_s)	5 – 6.5 m	
Peak wave period (T_p)	11 – 13 s	

Statistical descriptions of local wave and wind conditions were derived to serve as reference for assessing the exceptionality of these conditions. This showed that the metocean conditions that occurred in the studied area on 1-2 January 2019 are not very extreme or exceptional: the derived water levels and current conditions occur daily, and these storm and resulting wave conditions are exceeded on average one to two times in a year.

Currents during the most critical part of the voyage of the MSC Zoe (i.e. the area where most containers were recovered and where most intense wave impacts were reported by the crew) were directed towards the west, leading to a counter current experienced by the vessel of moderate and fairly constant magnitude (Table ES.1). Wave-current interactions in principle could have enhanced the intensity and complexity of the wave conditions. However, such interactions will have been minimal, given that the main wave direction was approximately perpendicular to the (tidal) flow direction. The tide was falling (ebb tidal phase) and the vessel experienced slowly dropping water levels as it progressed along its track. The presence of a wind-induced storm surge, offsetting the total tidal cycle upwards, resulted in water levels not dropping below mean sea level around the moment of low tide. The timing of the water levels, combined with the sea bed levels along the route, resulted in the vessel experiencing relatively small water depths at two locations along the sailed track on those days (around 20-22 m). Water depths experienced by the vessel could have been even smaller, if the lowest tidal water levels would have occurred while the vessel was at the shallowest location.

The local wave conditions were influenced by the shallower depths. Particularly the highest and longest waves will have showed steepened (enlarged) crests and flattened troughs. Mariners have reported that such conditions are known to occur along the southern sailing route north of the Wadden Islands. Such wave conditions are referred to by them as ‘ground seas’, or ‘Grondzee’ in Dutch. Steepening of wave crests will have enhanced wave breaking by foamy, spilling wave crests. Even though this type of wave energy dissipation is very common out at the open sea, it may have contributed to the complexity of the wave conditions encountered by the vessel.

Spatial distributions of wind and waves during the storm proved to be fairly uniform in the area north of the Wadden Islands, with similar overall wave conditions along the sailing route further north of the Wadden Islands compared to those along the southern sailing route originally taken by MSC Zoe. For a representative output location on the northern sailing route metocean conditions have been determined and it has been established that the most severe conditions at this location are similar to the ranges presented in Table ES.1. Along the northern sailing route, shallow-water effects will have been weaker because of the larger depths present along that route. In principle, that may have resulted in less adverse sailing conditions. However, the intensity of breaking wave crests was also large there. This shows that further analyses are required to reach definitive conclusions on recommendations or preferences for sailing routes related to specific metocean conditions. An important factor in such an assessment will be the larger water depths available along the northern route, which could mean around 10-15 m more under-keel clearance compared to the shallowest sections of the southern sailing route.

The accuracy and validity of the numerical results used to derive the abovementioned information and data has been verified as part of this study. This showed that the general physics of the natural system have been captured well by the numerical models used. This means that results are suitable for assessing the overall storm situation and to analyse the metocean conditions during the event of 1-2 January 2019. However, some underestimations were found around the peak of the storm (2 January, 00:00 h) in wave heights and periods. This has been linked to the archived spatial wind fields available from external sources to drive the wave model and which already included an underestimation in wind speed. Since an unambiguous calibration (tuning) of the wind fields was not possible, the available wind fields were used unchanged. The resulting underestimation in wave parameters has been covered as part of the laboratory tests, following a recommendation by Deltares, by considering a set of wave conditions that also included slightly elevated values of wave height and period. Furthermore, the observed underestimation of the wind speeds does not affect the conclusions of this study regarding exceptionality of the conditions on 1 and 2 January 2019, given that it affected all considered locations and that the severity of the storm conditions (frequency of occurrence) was determined consistently, i.e. relative to reference information from the same dataset.

Deltares provided information on the metocean conditions during 1-2 January 2019 along the southern and northern sailing route to MARIN. Deltares and MARIN have discussed those conditions and how they should be used to define the wave and water depth conditions in the scale model basin of MARIN.

Deltares has verified that the wave conditions as prescribed at the wave maker of MARIN have been created correctly within their basin, including the relevant non-linear shallow water effects. In this way the generated wave conditions are representative for typical conditions as computed for the North Sea wave conditions north of the Wadden Islands on 1-2 January 2019.

Contents

1 Introduction

1.1 Project context

The Dutch Safety Board (Onderzoeksraad voor Veiligheid, OVV) is performing an investigation into the incident involving container vessel 'MSC Zoe' on 1 and 2 of January 2019, when that ship lost several containers in an area north of the Dutch Wadden Islands.

OVV has asked the Dutch knowledge institutes Deltares and MARIN to contribute to the investigation by providing insight into:

- the metocean conditions (wind, waves, currents) during the accident,
- the vessel motion behaviour under such conditions,
- how frequently these metocean conditions can be expected to occur.

Overall (and eventually), the investigation is foreseen to answer the following research questions:

1. What were the local environmental conditions during the incident (1-2 January 2019) in the North Sea region north of the Dutch Wadden islands, both on the selected route of MSC Zoe, and in the area of the sea route further north in deeper water?
2. How will specific environmental conditions and vessel properties (of large container vessels) contribute to the risk of losing containers?
3. Which parameters (vessel parameters and/or environmental conditions) are important for route selection and which of these parameters will provide vessel crew members insight in the specific sailing conditions north of the Wadden Islands and their possible consequences for vessel motions?

The present project phase covers Research Questions 1 and 2. Deltares has performed tasks aimed at providing the answers to Question 1 and MARIN worked on answering the different elements of Question 2 (MARIN, 2019).

1.2 Aim of the tasks by Deltares

The first main aim of the tasks by Deltares is establishing the metocean conditions as they occurred during the incident of the MSC Zoe on 1-2 January 2019[2]. In addition, the accuracy of the derived conditions needs to be verified. The work should also show how exceptional these conditions were (Do conditions like these occur often?) and how variable they were in space and time (Would encountered conditions have been much different if the vessel would have sailed elsewhere in the area or at the same location but somewhat later or earlier?).

The second main aim is to translate these metocean conditions to representative conditions to be simulated in the physical scale model basin at MARIN, including possible shallow-water and non-linear wave effects. The finite dimensions of the physical modelling basin and practical requirements to the maximum duration of such tests mean that choices need to be made in how to create conditions in the wave basin that meet those practical requirements but that are still representative of the conditions that occurred in the studied area on 1 and 2 January 2019.

[2] *Please note that in this report we use the term 'storm' as a common label used in coastal engineering (and possibly in laymen's terms) to refer to an interval of increased windspeeds. In a formal meteorological definition, the situation as encountered by the MSC Zoe on 1-2 January 2018 corresponded to "(near) gale conditions" and not to a full storm force.*

1.3 Scope of work by Deltares

The present scope of work by Deltares within the overall investigation of OVV consists of the following two main study tasks (further described in Chapter 2):

1. Determining the metocean conditions north of the Wadden Islands during 1-2 January 2019 and of their relative severity (frequency of occurrence);
2. Providing recommendations for, and verification of, the wave conditions as included in the scale model tests by MARIN for this project.

1.4 Project team

The following Deltares team members have worked on the different aspects of the assessment and have contributed to the present report:

Name	Expertise	Role
A.J. van der Hout	Sr. Advisor hydrodynamics + nautical, project leader	Analyses, coordination
S.P. Reijmerink	Wave modelling and data analysis expert	Modelling, analyses, reporting
M.P.C. de Jong	Expert Advisor coastal and port hydrodynamics	Analyses, reporting
S. Caires	Metocean Expert	Quality assurance

A.J. van der Hout is the primary contact person in Deltares for this project. However, any inquiries related to this report should first be addressed to OVV.

1.5 Report outline

The present report is a description of a high-level technical assessment. General readers interested in the overall findings and a general summary of the work are referred to the Executive Summary on the first pages of this report. The chapters of the main text of this report (Chapters 2–6) give detailed background information on the work performed and on the outcomes.

Some sections of the main report text are intended for recording of the approach taken and of the modelling choices made. Other sections mainly present results and conclusions. The report outline on the next page is provided to readers interested in the details of the work performed, to aid them in selecting the sections that will be of most relevance to them. The characteristics of the work performed result in some of the chapters having a larger technical complexity level, since they provide detailed descriptions supporting the contents of other chapters and of the main study conclusions. This is indicated in the rightmost column of the outline table on the next page.

Chapter	Contents	Technical complexity level
Executive summary	Gives a general overview of the work performed, the results and main conclusions.	Low
1 – Introduction	Describes the background and the context of the project including task aims.	Low
2 – Study approach	Summarises the technical approach taken to reach the aims of the tasks by Deltares (outlined in Section 1.2).	Low
3 – Available data	Gives an overview of the input data and information that were available to Deltares to perform the work.	Average
4 – Numerical modelling	Describes the numerical models considered to derived and compute the metocean conditions that were present during the days of the incident with the MSC Zoe (1-2 January 2019). It also describes the validation of the accuracy of the results calculated.	High
5 – Conditions 1-2 January	Describes how the computed model results from Chapter 4 have been processed to derive the conditions experienced by the MSC Zoe along its track north of the Wadden Islands. This chapter also describes how exceptional the conditions on 1-2 January 2019 were relative to local reference statistics of waves and wind.	High
6 – Basin test conditions	Considers how the conditions as they occurred during the days of the incident have been interpreted for representation in the physical scale model tests performed under the same project context by MARIN (2019). The wave conditions as generated in the scale model basin have also been verified for their representativeness of the actual situation in the field.	Average
7 – Conclusions	Summarises the main conclusions related to the tasks by Deltares.	Low

2 Study approach

2.1 Overall study approach

The project is coordinated by the investigation team of OVV. Deltares and MARIN have been requested to contribute to the project from their specific fields of expertise. Separate research reports have been created, describing the contributions by these knowledge organisations. The investigation team of OVV writes the overall investigation report.

The project has been performed in close cooperation between all parties. Meetings took place between the two knowledge organisations during the project to brief the technical project teams on progress and results. This included a meeting prior to performing the scale model tests, used for interpreting the metocean conditions as derived by Deltares in preparation of those laboratory activities. Later meetings took place during the scale model tests (witness tests) and following the tests, for discussing the analyses and verifications of the model test results.

The following sections describe the approach taken for the specific technical tasks performed by Deltares. The outcomes of those tasks are reported in the following chapters. Where fitting, some sections in those later chapters may cover more than one of the tasks described below.

Where parameters and other technical elements are first mentioned in this report they will be introduced. Throughout the report wave heights will mostly be reported as the 'significant wave height' (H_s). This is a measure of the average of the highest one-third of the waves occurring in a sea state (wave field). This is a commonly applied parameter to describe a representative height of a wave condition, in which the wave field is the combined effect of many wave components with different heights and periods. Part of the reason why this wave height parameter is used often in wave studies is that historically this parameter proved to correspond to visual wave height estimates made by experienced mariners. For more information on wave propagation, numerical wave modelling and related subjects the reader is referred to textbooks such as Holthuijsen (2007).

All times mentioned throughout this report are expressed relative to UTC (Coordinated Universal Time). During winter the local time in The Netherlands is UTC + 1 hour.

2.2 Task 1: establishing the metocean conditions of 1-2 January 2019 (Chapters 4 + 5)

2.2.1 Task 1.1 – validated numerical modelling of the metocean conditions

The measured metocean conditions on the North Sea during 1-2 January 2019 have been analysed and interpreted. They are available at several platforms and buoy locations throughout the North Sea area. They provide a good characterisation of the overall conditions in the area during the incident with the MSC Zoe. However, measured information is only available at the observation locations and not along the full sailing routes in the area north of the Wadden Islands. Therefore, a numerical model has been setup and applied by Deltares to compute the corresponding conditions along the sailing routes as they occurred during those days. Measurements available from the observation locations have been used to verify the computed results. The computed results also allow for an assessment of the spatial extent and variation in time of the different metocean conditions.

For this modelling the following numerical models, i.e. software packages and area descriptions, have been applied (described in full detail in later chapters):

- Waves: SWAN – DCSM + a dedicated local model grid
- Water level + currents: Delft3D-FLOW – DCSMv6

The local wave model has been forced by offshore boundary conditions taken from the most reliable global metocean dataset presently available (ERA5, describing metocean conditions from 1979 until 2018, see later chapters). In addition, spatial and temporal information has been obtained from databases with results of (operational) numerical models by others (all the sources of information applied are described in more detail in later chapters).

Available information on conditions computed by numerical models includes waves, wind, and currents. Detailed results have been derived at output locations along the track of the vessel and for the times that the ship was present there. In this way it is as if the vessel 'moves through the simulated area' in the course of the computation by considering the precise track and timing of the ship. The output generated in this way includes full 2D wave spectra, describing the distribution of wave energy over wave frequencies (short or long wave periods) and directions (from where the waves reach the location considered).

The applied numerical wave model is a spectral wave model. Such a model efficiently and accurately simulates how wave energy at sea is generated, moves forward in space (propagates and interacts), changes due to bed level influences and dissipates (e.g. by breaking). This model produces wave spectra without having to model each individual wave crest. This makes this type of wave model very computationally efficient. It is specifically intended for application in coastal areas because it can cover larger areas, such as considered in the present study. However, the spectral outcomes will need to be interpreted in post-processing to derive what the results mean for time series of wave conditions (described in later chapters).

The reliability and accuracy of the modelling approach and its results have been assessed by comparing computed wave results for the days of the incident to measurements recorded during those days at measurement locations closest to the vessel track. It should be noted that these measurement locations are not located on the track of the vessel and will often correspond to different water depths (higher or lower). Nevertheless, comparing computed and measured wave data at such observation locations provides a good indication for the reliability of the computed metocean conditions. This comparison will verify whether the overall wave patterns in the area have been captured accurately and that the transformation from the offshore reference data (from ERA5) all the way up to the coastal measurement locations has been done successfully and accurately. Since the area of the track of the vessel is located 'in the middle', i.e. in between the different measurement locations used for the validation, this forms an indirect verification of the results along the track. Any discrepancies found between computed and measured data have been interpreted and explained.

2.2.2 Task 1.2 – exceptionality of the conditions

To assess how exceptional the conditions during 1-2 January 2019 have been, first local statistics of relevant parameters have been derived to serve as reference. These reference statistics are based on the full ERA5 dataset (from 1979 until 2018). Because of its long duration, these data provide the most reliable statistical basis available. The conditions that occurred on 1-2 January 2019 have been compared to the statistical information derived. This makes it possible to derive whether the conditions during the event are exceeded – on average – multiple times per year, or only once every so many years.

The statistical probability, or exceptionality, of a metocean condition is often expressed as a 'return period', as is done in the present study. This value indicates that if one would be able to consider a very long time series of measurements of a specific parameter, say 1000+ years, then the value considered will *on average* be exceeded once very N years. This does not mean that extreme events of that magnitude will always be N years apart, since a calm interval may be followed by an interval with more of such events. Nevertheless, this average return period gives a practical measure of how exceptional an event is and whether it is to be expected to occur typically every year or only every several years.

2.2.3 Task 1.3 – analysis of spatial and temporal variation metocean conditions

The influence of the variability in space and time of the metocean conditions has also been considered. Would the vessel have experienced much different metocean conditions if it would have taken a different route, or if it would have taken the same route but slightly earlier or later? Were the overall environmental conditions changing so rapidly that the vessel crew was taken by surprised? Information on wave patterns in the modelled area at different moments in time (taken from the numerical wave modelling) have been considered to answer these questions.

The most recent bathymetry data available has been applied in the numerical models. The long-term variability of the bed levels has been assessed to estimate the likelihood that bed levels may have significantly changed in the area of the incident since the latest bed level survey. The outcome of that assessment indicated whether such potential recent bed level changes should be kept in mind when interpreting the model outcomes. This assessment was made by considering the static draft of the vessel to derive the under-keel clearance from the numerical model results, i.e. the local computed water depth minus that static draft value. These results were compared to measured keel clearance values. Even though in reality the vessel will also show motions in waves, and because of the lost containers the draft will not have been constant, still this check was performed as an additional form of model validation, i.e. a quality and consistency check.

2.3 Task 2: wave conditions for in the scale model basin (Chapter 6)

2.3.1 Task 2.1 – input and recommendations scale model test conditions

The outcomes of Task 1 have been used to select a set of wave conditions representative for typical conditions encountered by the MSC Zoe along the most critical section of its track. The provided information consists of 2D wave spectra (describing the distribution of wave energy over direction and frequency). MARIN has converted these spectra into sea surface elevation time signals to be used in their basin. Note that the tests by MARIN aim for representative wave conditions and not necessarily an exact copy of the conditions during the incident with the MSC Zoe. The tests are aimed at generating general insights into the effect of such conditions (including water depths) on large container vessels[3]. As indicated in Chapter 1, the overall study context is not aimed at identifying the cause of the incident with the MSC Zoe on 1-2 January 2019.

By providing data and by participating in technical meetings, Deltares delivered data specifications and advised on the following aspects in relation to the conditions to be tested in the physical scale model:

- Water depth
- Wave conditions
- Wind conditions

[3] *For similar reasons MARIN used a scale model ship similar to the hull of the MSC Zoe, but not exactly the same.*

- Current conditions

Please note that currents were considered as part of Task 1, including the possible influence of currents on waves, but that currents have not been directly imposed in the scale model tests by MARIN. Deltares has advised MARIN on which wave parameters to consider for representing the relevant wave conditions best. The experts of the physical test facilities at MARIN have used that information to set up their tests within their selected basin approach.

2.3.2 Task 2.2 – detailed analyses of wave field complexities

Complexities in the wave fields may have influenced the local heights and wave shapes reaching the vessel along its track. These may include non-linearity of the waves (shallow-water effects), breaking intensity, influence of currents on the wave propagation and wave heights, directional spreading (short-crestedness) of the waves. The computed wave conditions from Task 1 (spectral representations) have been considered in more detail to ensure that the wave signals simulated in the basin are representative of the conditions as those occurred on the studied part of the North Sea on 1-2 January 2019.

2.3.3 Task 2.3 – verifying the conditions created in the scale model basin

MARIN has provided Deltares with multiple measured wave signals from their scale model basin tests. These have been processed by Deltares to derive wave spectra from these signals. Those spectra have been compared to the conditions as encountered by the MSC Zoe on 1-2 January 2019 (Task 1) and to the target spectra as provided by Deltares to MARIN (Task 2.1). Where differences have been found, Deltares assessed whether the differences were small enough for the simulated conditions to still be representative for the situation as derived by Deltares.

3 Available data and information

3.1 Information on the incident

3.1.1 Vessel track data and draft

OVV has made available to Deltares information on the track of the MSC Zoe. The information provided included: time, coordinates, speed, available keel clearance (as measured from the ship) and heading. Figure 3.1 – on the next page – gives an overview of these data. The track as sailed by the vessel has been presented as a map figure in the left panel of Figure 3.1 (dotted blue line) together with the centre lines of the standard sailing routes on the North Sea area north of the Wadden Islands (dashed black lines). The first part of the vessel transit was along the southern of the two sailing routes. In a normal situation the vessel would have continued to follow this route until it reached the port in Germany. However, after issues were detected/experienced, north of the Wadden Island Borkum (Germany) the crew steered the ship into the incoming wave direction and sailed north to then continue its voyage eastward along the northern sailing route. The other parameters have been presented as timeseries in the right panels of Figure 3.1. Note that for visualisation purposes, the raw measured timeseries of the vessel speed, vessel heading, and keel clearance have been averaged at a 1-minute interval. This removes high-frequency disturbances from the signal for clarity of plotting while leaving the essence of the information intact. Please also note that the plotted timeseries of these parameters end at 02-01-2019 21:00h UTC, since the part of the voyage after that moment (sailing into the port of Bremerhaven) is not part of the focus area of this study.

The mean draft of the MSC Zoe was 12.41 m (source: stability summary at the departure port).

3.1.2 Locations of lost containers

OVV has shared figures showing the approximate locations of where most of the lost containers have been found. Combined with the information from the VDR, these data have been used to identify the critical sections of the track of the vessel. Main output locations in the numerical model were targeted at those critical sections. Furthermore, OVV has provided Deltares with a set of suggested output locations along the southern route, which Deltares has applied together with an additional output location along the northern route for comparison.

3.2 General experiences by mariners

As part of the research team of MARIN, Capt. J. Krijt shared general experiences of sailing along the route directly north of the Wadden Islands. The area is known among mariners because it includes shallower sections and because it is an area in which so-called ‘ground seas’ occur (in Dutch: ‘grondzee’).

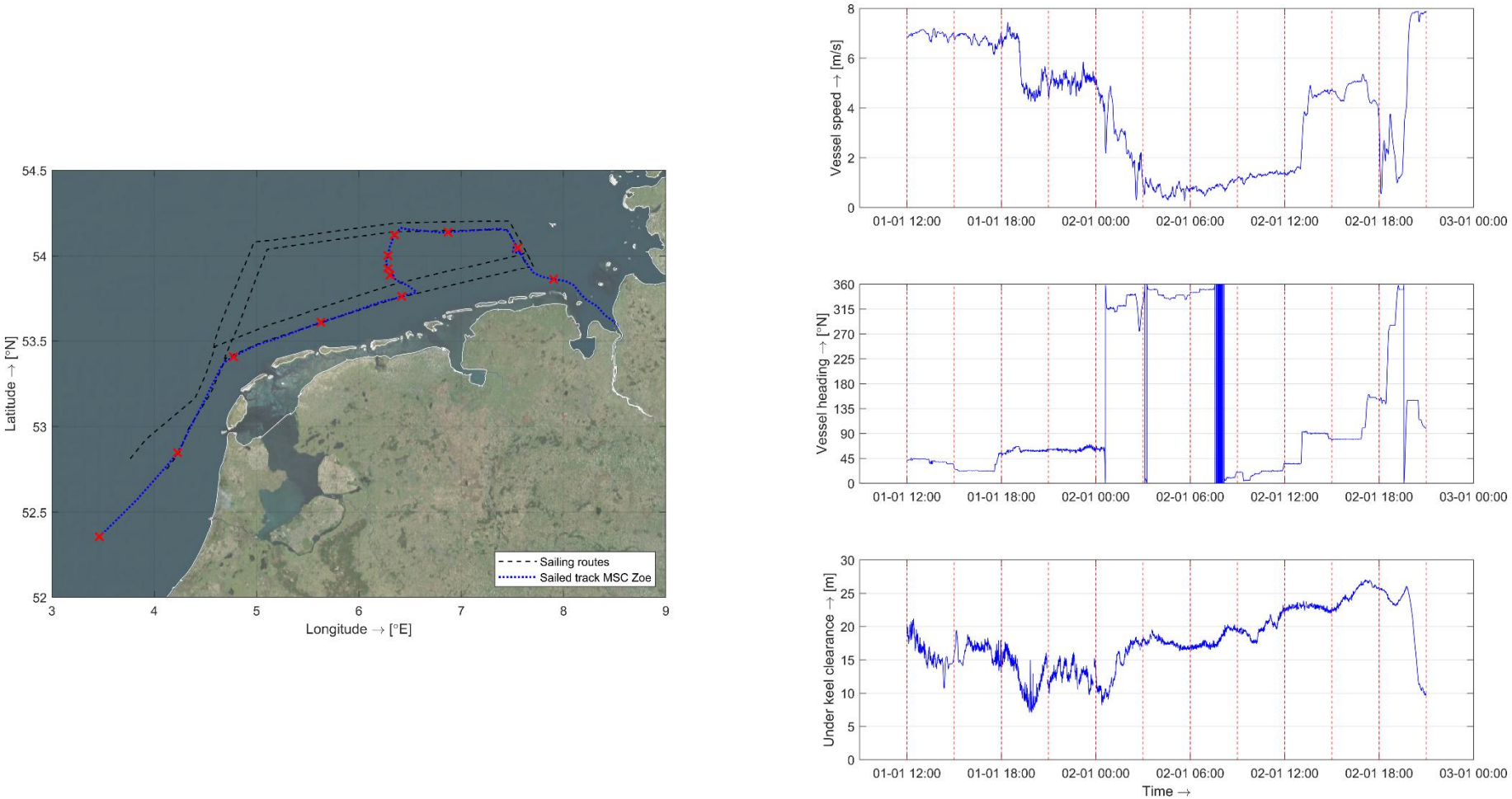

Figure 3.1 Track information of the MSC Zoe during the 1-2 January 2019 event. Left: sailed track of the MSC Zoe (blue line); the black dashed lines represent the centre lines of the main shipping channels. Right: panels with timeseries of 1-minute averages of the recorded vessel speed (top) vessel heading (middle) and under keel clearance (bottom). For reference, the dashed red lines in the right panels correspond to the locations indicated by red crosses in the left panel (the first dashed red line at 01-01 12:00h corresponds to the westernmost red cross).

Different definitions of ‘grondzee’ exist among mariners, either ‘wave conditions that steepen in wave height because of the interaction of the waves with a shallow water depth’ or ‘a wave condition in which a vessel is prone to touch the seabed due to local wave action’. The interaction of the waves with the seabed during a state of ‘grondzee’, according to Capt. Krijt, can be severe enough to result in suspended soil particles in the water visible at the water surface. This may be another explanation of the term ‘grondzee’ (since the direct translation from Dutch can be “Soil sea” / “Ground Sea”).

In this study we have adopted the first definition mentioned, primarily since it relates the term directly to the wave conditions, which makes it the most fitting for the present report on metocean conditions.

3.3 Local bathymetry

The bathymetry (bed levels) of the North Sea is surveyed by the Dutch government at a regular interval (every 3-5 years), depending on the mobility (dynamics) of the bed. These data are then made publicly available for downloading via several databases on the internet. An example of such a database is the EMODNET[4] database (European Marine Observation and Data Network). In the EMODNET database multiple bathymetry survey datasets of European countries are combined into one large connected consistent dataset (i.e. corrected for differences in vertical reference systems).

For this project the most recent bathymetry data in the area around and including the recorded ship track (Figure 3.1) has been downloaded from the EMODNET database (status July 2019) for use in the numerical models. This dataset contains survey data from approximately 2008 up to 2018; with the data within the shipping routes updated most often (see Deltares, 2011).

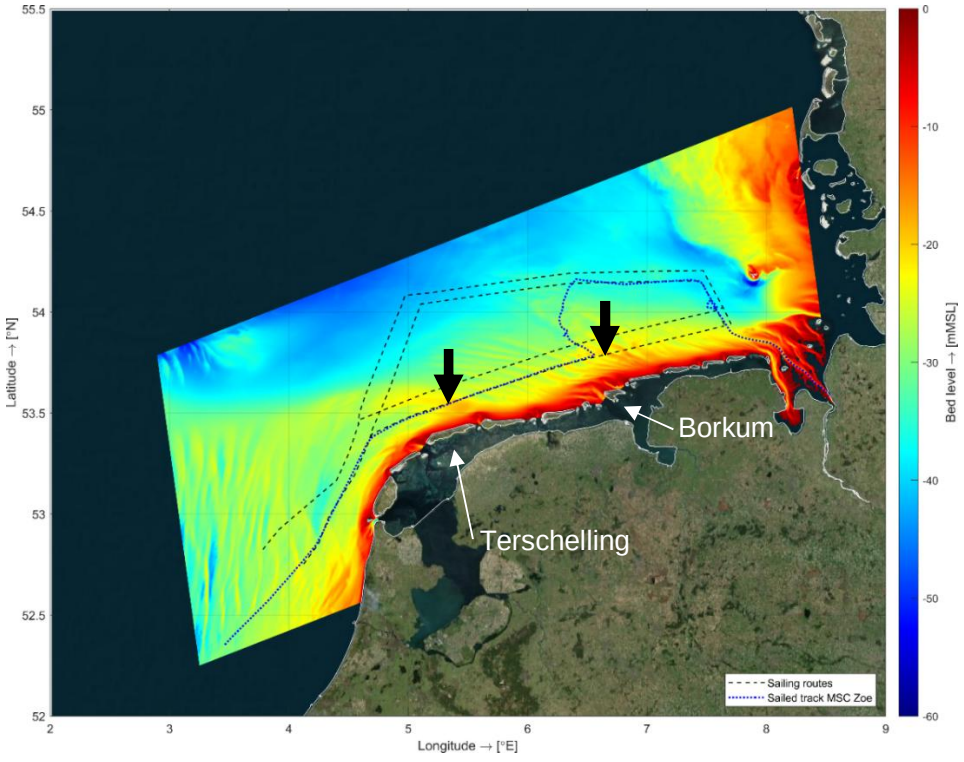

Figure 3.2 EMODNET bathymetry along the sailed track of the MSC Zoe.

[4] https://www.emodnet-bathymetry.eu/

It has been verified that bathymetric changes between subsequent surveys in the area of interest are rather small and that vertical bed level changes are typically less than 0.10 m/year. As will be shown in Section 5.1.4, the dataset can be considered as accurate and representative for the 1-2 January 2019 event. Figure 3.2 presents these data, the track of the vessel (finely dashed blue line) and the centre lines of the main shipping routes (coarsely dashed black lines). The vertical reference level used for this figure is the local Mean Sea Level (MSL[5]), which is commonly applied as vertical reference in coastal wave and current modelling. Results from the models are used with that reference, or they are converted to Chart Datum (CD[6]). Figure 3.2 shows the shallow areas along the southern of the two main shipping routes, mentioned in Section 3.2, located north of Terschelling and north of Borkum (Germany). Their locations are indicated by the two vertical black arrows included in that figure.

3.4 General description of the weather pattern during the event

Figure 3.3, on the next page, summarises the available meteorological information related to the storm of 1-2 January 2019. On these days a pattern of high- and low-pressure fields occurred above Northern Europe, resulting to a North-westerly storm above the North Sea. Weather maps of the KNMI (Royal Dutch Meteorological Institute) of this event are presented in the left panels of Figure 3.3. These panels show that a high-pressure field was present over Iceland and the British Isles together with a low-pressure field east of the Scandinavian Peninsula, leading to large pressure gradients (cf. isobars close to each other) and high wind speeds over the North Sea. This is confirmed by the right panels of Figure 3.3, showing the corresponding wind forecasts by the Hirlam atmospheric numerical model of the KNMI (KNMI, 2019). The highest wind speeds in that forecast occurred (and were observed, considered in later sections) along the Norwegian coast, where the isobars were located closest to each other. The highest wind speeds in the forecast, were foreseen (and observed) in the night from the 1st to the 2nd of January. This is confirmed by measurements of wind (Section 3.5).

3.5 Wind measurements

Wind measurement data (hourly averaged values of wind speed at 10 m height and of wind direction) for an interval of a number of days around the event on 1-2 January 2019 (28-12-2018 – 04-01-2019) were collected for five offshore platforms located on the North Sea[7]. Of these five platforms, four platforms are in Dutch territorial waters (platforms A121, F161, L91[8] and AWG) and one in Norwegian waters (Troll-A)[9]. The coordinates of these locations are presented in Table 3.1. The table also presents the bed levels at these locations as derived from the bathymetric information available (Section 3.3). Please note that waves are not measured at all these wind measurement locations (Section 3.6).

---

[5] *This reference level is used in the remainder of this report as vertical reference level for all related variables (i.e. water levels and bed levels). Please note that the specific vertical reference applied does not influence the modelling results or related analyses provided that all values are consistently applied so that the proper water depth is considered.*

[6] *Chart Datum is a commonly applied vertical reference level for shipping applications, such as nautical charts. It differs from region to region and is set at the lowest water level that typically occurs in an area, indicating that a vessel can expect at least that water depth – or higher – to be present.*

[7] *Data downloaded from the Matroos data portal: http://matroos.rws.nl.*

[8] *For platform L91, wind data were collected for a 10-year period (2010-2019) for validation purposes (see Chapter 5).*

[9] *Data downloaded from the ASOS (Automated Surface Observing System) network for Norway, via the Iowa State University: https://mesonet.agron.iastate.edu/request/download.phtml?network=NO__ASOS. Data presented is corrected for measurement height (hub at 20 m height) and sampling rate (30 min) using API (2000) guidelines.*

Table 3.1 Coordinates and local bed levels for the considered offshore platforms.

Platform name	Longitude [°E]	Latitude [°N]	Bed level [mMSL]
Troll-A (Norway)	3.609700	60.885800	-301.06
A121	3.810108	55.398942	-33.92
F161	4.011096	54.115934	-51.02
L91	4.966667	53.616669	-25.13
Q1	4.150608	52.926411	-27.03
AWG	5.940429	53.491983	-8.41

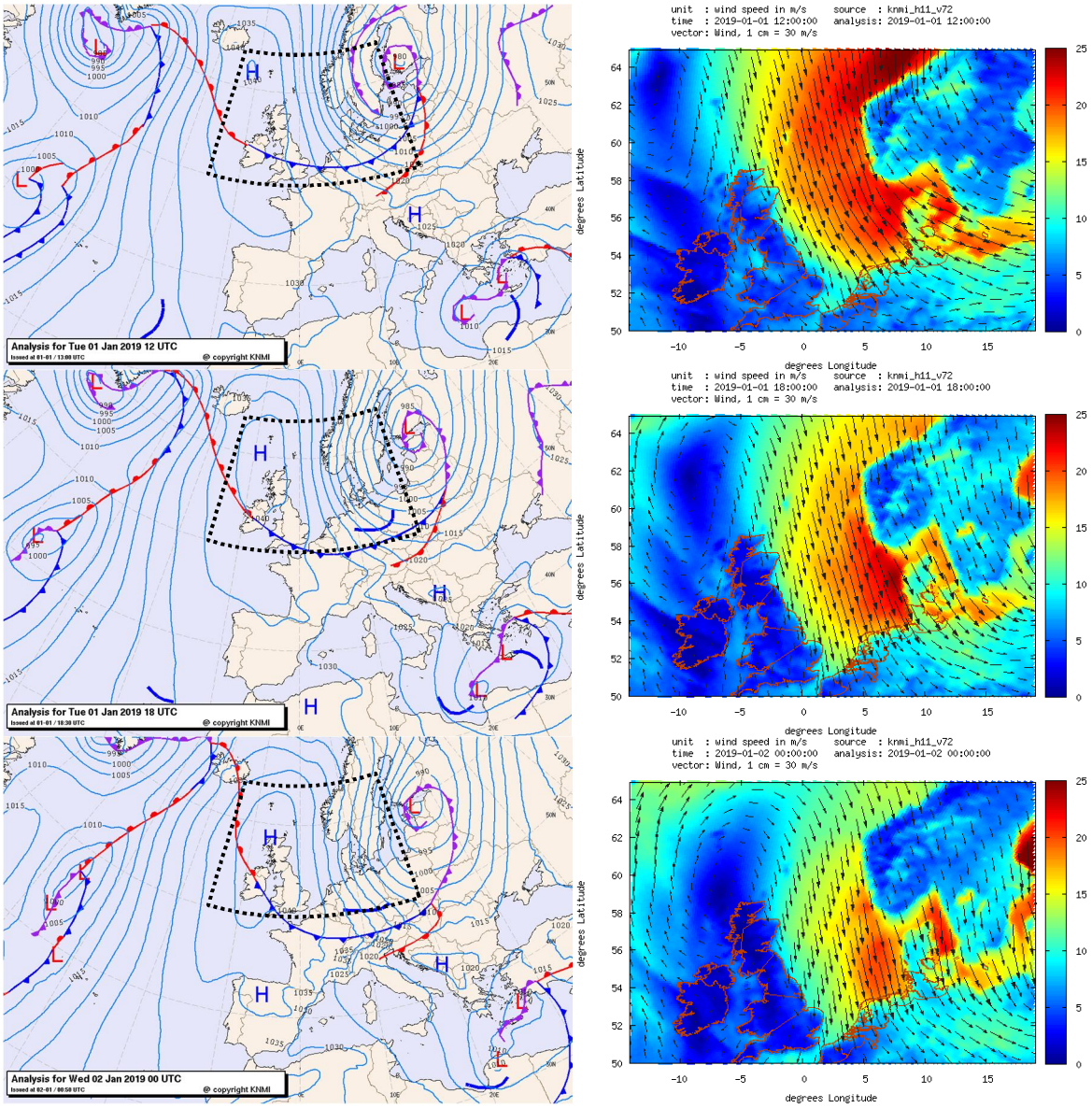

Figure 3.3 Weather maps (left panels) and wind forecasts (right panels) during the period of the storm of 1-2 January 2019 (Source: KNMI). Top panels 01-01-2019 12 UTC. Middle panels: 01-01-2019 18 UTC. Bottom panels: 02-01-2019 00 UTC. The dotted black trapezium in the left panels indicate the approximate spatial extent of the right panels. The trapezium shape of the area in the left panels is the result of the curvature of the earth surface and how that is projected onto the 2D image shown.

These platform locations are presented in Figure 3.4 together with the measured time series of wind recorded at those locations for the period of 31-12-2018 – 04-01-2019. The highest wind speeds during 01 - 02 January 2019 were measured near Norway, in line with the wind forecasts presented in the previous section. At station Troll-A hourly averaged wind speeds (at 10 m height) up to 22 m/s were measured (≈Bft 9). More towards the Dutch coast hourly averaged winds speeds up to 18 m/s were measured (≈Bft 8). With the wind mainly coming from 330°N (NNW) a long fetch (i.e. the stretch of area available to the wind for generating waves) was available over the North Sea (see next section).

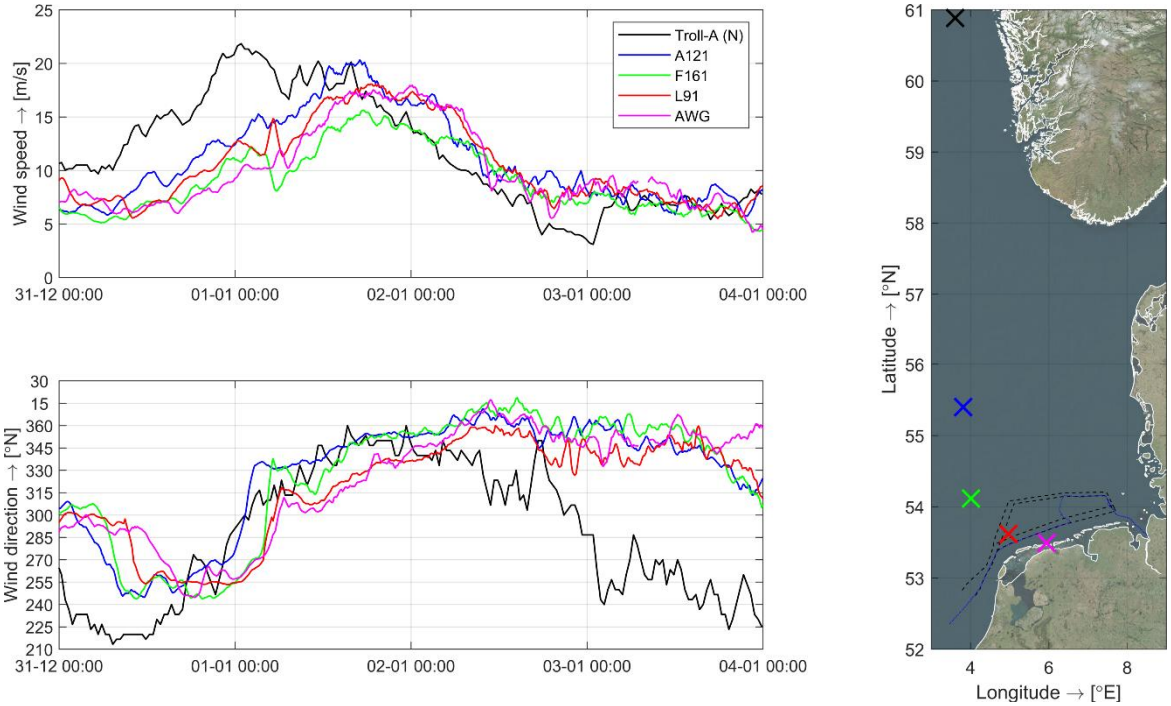

Figure 3.4 Measurement data of wind speed (recorded at 10 m height) and wind direction recorded on 1-2 January at North Sea platforms Troll-A (Norway), A121, F161, L91 and AWG. The locations of these platforms are visualised in the right panel by crosses with colours corresponding to the timeseries in the left panels. Note the black cross furthest north indicating the location of the Norwegian platform.

3.6 Wave measurements

Wave data for 1-2 January 2019 were obtained from online databases (see Footnote 7). These data included the following parameters: H_s, peak wave period (T_p), spectral wave periods ($T_{m0,1}$; $T_{m0,2}$; $T_{m-1,0}$) and the Mean Wave Direction, MWD. The peak wave period is the wave period at which the highest energy density is present in the wave spectrum describing the distribution of wave energy over the different wave frequencies (wave periods). The different '$T_{mx,x}$' values are different ways of weighing the energy distribution in the wave spectrum over the different frequencies[10]. These different values for a representative wave period of a sea state give an indication of the distribution of the energy within the wave spectrum and are commonly considered in different hydraulic and coastal engineering applications. Measurement wave data were obtained from locations where this type of information is recorded, either close to the track

[10] *The spectral wave period $T_{m0,2}$ corresponds to T_z, i.e. the mean wave period that follows from a temporal wave-by-wave analysis, with waves being separated by crossings of the zero water-level line. $T_{m0,1}$ represents the centre of gravity of the 1D wave spectrum (computed by dividing the spectral zeroth order moment by the spectral first order moment: m0/m1), it gives more weight to the longer waves than $T_{m0,2}$ (√(zeroth order moment/second order moment): √(m0/m2)). Tm-1,0 gives even more weight to the longer waves (m-1/m0).*

of the vessel or in the up-wind direction of the storm. These locations correspond to five offshore platforms (A121, F161, Q1, L91[11] and AWG) and three wave buoys (Eierlandse Gat (EiG), Schiermonnikoog Noord (SoN) and Amelander Zeegat Boei 1-2 (AZ 1-2)), all located in Dutch territorial waters.

The coordinates of the considered measurement platforms were presented in Table 3.1. Table 3.2 contains the coordinates of the wave measurement buoys. The table also presents the bed levels at these locations as derived from the bathymetric information available (Section 3.3).

Table 3.2 Coordinates and local bed levels for the considered measurement buoys.

Buoy name	Longitude [°E]	Latitude [°N]	Bed level [mMSL]
Eierlandse Gat (EiG)	4.661667	53.276944	-27.97
Amelander Zeegat 1-2 (AZ 1-2)	5.484865	53.508745	-18.94
Schiermonnikoog Noord (SoN)	6.166667	53.595556	-20.25

The measurements for H_s, T_p and MWD, together with the platform/buoy locations, are presented in Figure 3.5 for the interval of 31-12-2018 00:00 h – 04-01-2019 00:00 h. Note that the mean wave direction is only available from the wave buoys, since the instruments at the platform locations do not record that parameter. The wave heights at AWG are lower than at the other locations because of the proximity of that location to the shoreline; the shallower depth present at that location means that higher waves will break and lose energy before reaching that observation point.

At the peak of the storm (along the sailing track of the MSC Zoe this was between 01-01-2019 21:00 and 02-01-2019 00:00) waves were recorded with H_s values ranging between 5.5 - 6.5 m, with T_p values ranging between 12 - 14 s. During that time interval, the MWD at all buoys was 330 - 340°N (defined as waves 'coming from' the direction mentioned).

[11] *For platform L91, wave data were collected for a 10-year period (2010-2019) for validation purposes (see Chapter 5).*

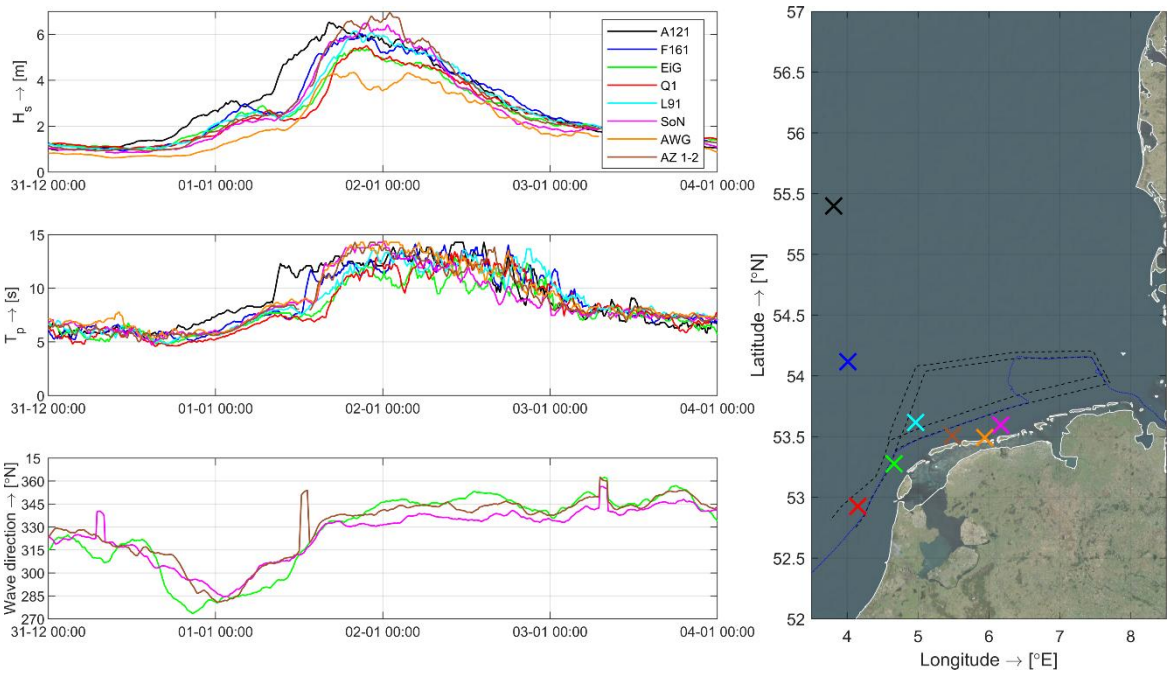

Figure 3.5 Measurement data of H_s, T_p and MWD during 1-2 January 2019 at selected North Sea platforms and wave buoys. The locations of these platforms/buoys are visualised in the right panel by crosses with colours corresponding to those indicated in the legend of the left panels.

3.7 Water level measurements

Measured water level data were obtained from online databases (Footnote 7) for three measurement platforms (F161, L91 and AWG), located in the vicinity the track of the MSC Zoe (see Section 3.5 for their coordinates). Unfortunately, currents (velocities, directions) are not recorded at these platforms or elsewhere in the area of interest.

Figure 3.6 presents the platform locations together with recorded water level time series at those locations for the interval of 31-12-2018 – 04-01-2019. The measurements show that during 1-2 January 2019 the tidal signal was elevated as a result of the wind pushing water up towards the coast (i.e. a wind-induced surge), causing the tidal high and low water levels to be shifted upwards during approximately three tidal cycles. During the peak intensity of the storm (01-01-2019 21:00 – 02-01-2019 00:00) the tidal water level was falling (ebb tidal phase) and the moment that the highest waves were observed in the main area considered (02-01-2019 00:00), approximately coincides with the time of astronomical low-water. In this specific situation the low water level was ≈MSL +0.0 m, instead of below MSL as in the adjacent tidal cycles plotted in the left panel of Figure 3.6, because of the positive offset caused by the wind-induced surge present in the area during the storm.

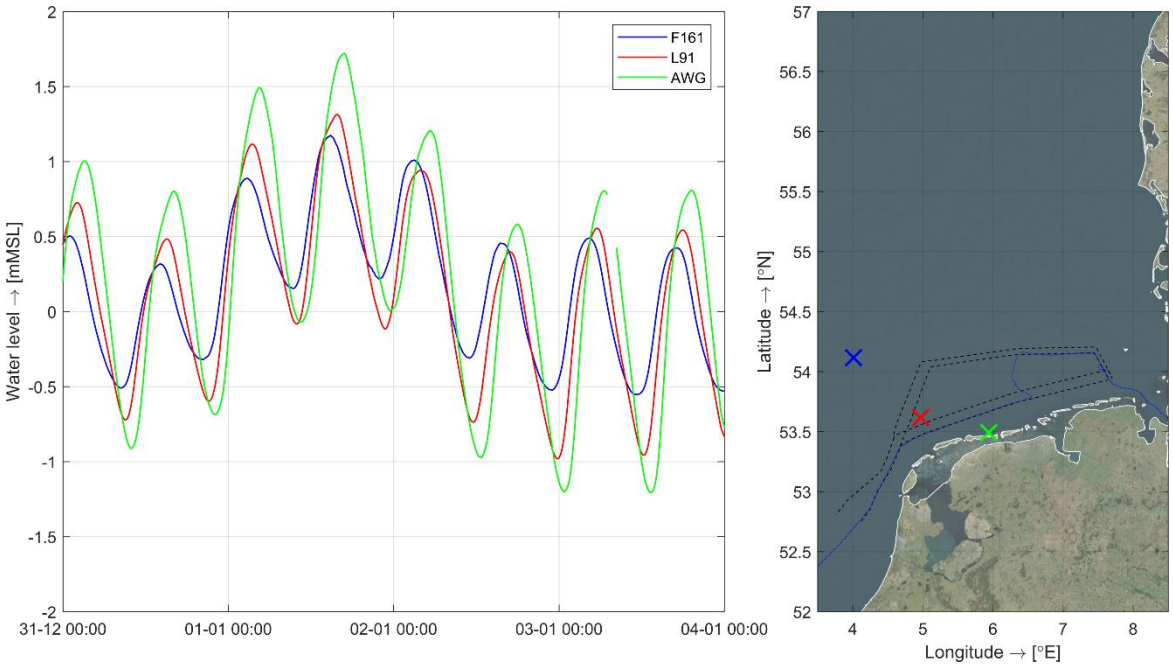

Figure 3.6 Measurement data of total water levels during 1-2 January 2019 at selected North Sea platforms. The locations of these platforms are given in the right panel by crosses with colours corresponding to those of the timeseries in the left panels.

4 Numerical modelling

As introduced in Chapter 2, numerical models have been used to determine the metocean conditions along the track of the ship and at other locations in the area where no measurements are available. Computations with state-of-the-art numerical models have been considered for hydrodynamics (water level and currents) and for waves. Some model setups and computations were made specifically for the present study, some data and modelling results were obtained from archived data from other (operational) models (developed by Deltares or others). This chapter describes the different models applied, the computational outcomes and the validation of the model results by comparing computed results at locations for which measurements are available. The flow model (describing the hydrodynamics) is considered in Section 4.1; model wind data are considered in Section 4.2; and the wave model is the topic of Section 4.3. The chapter ends with a discussion on the different model outcomes (Section 4.4).

4.1 Flow conditions (water levels and currents)

4.1.1 Numerical flow model

The (tidal and storm surge) flow conditions in the area were derived from an existing numerical modelling configuration called the DCSM flow model, which is based on the Delft3D-FLOW software of Deltares, simulating the shallow-water (tidal) flow equations. This model (Version 6) is part of the 5th generation of forecast models (RWsOS North Sea) developed by Deltares for operational use by Rijkswaterstaat[12]. It consists of two model domains that are two-way coupled. Here we only used water level and current data of the overall domain because that model has been most widely calibrated, based on observation locations throughout the full region. More background information on DCSM V6 is available on the websites mentioned in Footnote 12. Below only the main characteristics of the model schematisation relevant to the present study purpose are summarised.

The model extents and the bathymetry of the DCSM V6 overall model domain are presented in Figure 4.1. This model has a resolution of 1/40 (angular) degree (≈2.0-1.2 km) in longitudinal (East-West) direction and of 1/60 (angular) degree (≈1.85 km) in lateral direction (North-South). It has approximately 850.000 active computational cells. The bathymetry included in this model is based on the gridded NOOS[13] (North West Shelf Operational Oceanographic System) bathymetry dataset supplemented with bathymetry data from the ETOPO2 dataset from NOAA[14]. Please note that this bathymetry information has been included in this model to optimise the accuracy of these flow computations in the larger area modelled. The wave model developed with this study (Section 4.3) focusses on a smaller area and therefore may use bed level information from other sources that provide the best data in that particular area modelled.

The flow model is atmospherically forced with data (i.e. atmospheric pressure and wind) from the HIRLAM meteorological model of the KNMI (Dutch Meteorological Institute). Along the open boundaries, the DCSM flow model is forced at 205 locations with time series of tidal water levels and local surge due to atmospheric pressure differences (estimated by using Inverse Barometer Correction based on local air pressure). Wind-induced surge is not considered along

[12] https://www.helpdeskwater.nl/publish/pages/132741/factsheet-dcsm_zuno-generatie_5_v2017_01.pdf
https://www.deltares.nl/en/projects/rwsos-north-sea-operational-forecasting-system-north-sea/

[13] www.noos.cc

[14] https://www.ngdc.noaa.gov/mgg/global/etopo2.html

the outer boundaries of the flow model, since those boundaries are located far from the coast and at deeper water, therefore they will not show large wind-induced surge values. The tidal signal consists of several different oscillating components as a result of the influence of the sun and the moon, but also because of changes to the tidal wave propagating in shallow water, resulting in additional components. In these computations the amplitudes and phases of 38 harmonic tidal components/constituents were applied, which is enough to represent accurately the local tidal signal.

Kalman filtering is used to integrate measured water levels from 32 measurement stations into the hydrodynamics model to improve the accuracy of the computations (Tiessen and Zijl, 2015). This data-assimilation method is a commonly applied approach to improving numerical modelling results by taking along information from measurements into the computational process. The applied measurement points are located throughout the computational domain but with an emphasis on the Dutch coastal region, given its original purpose for the Dutch coastal region.

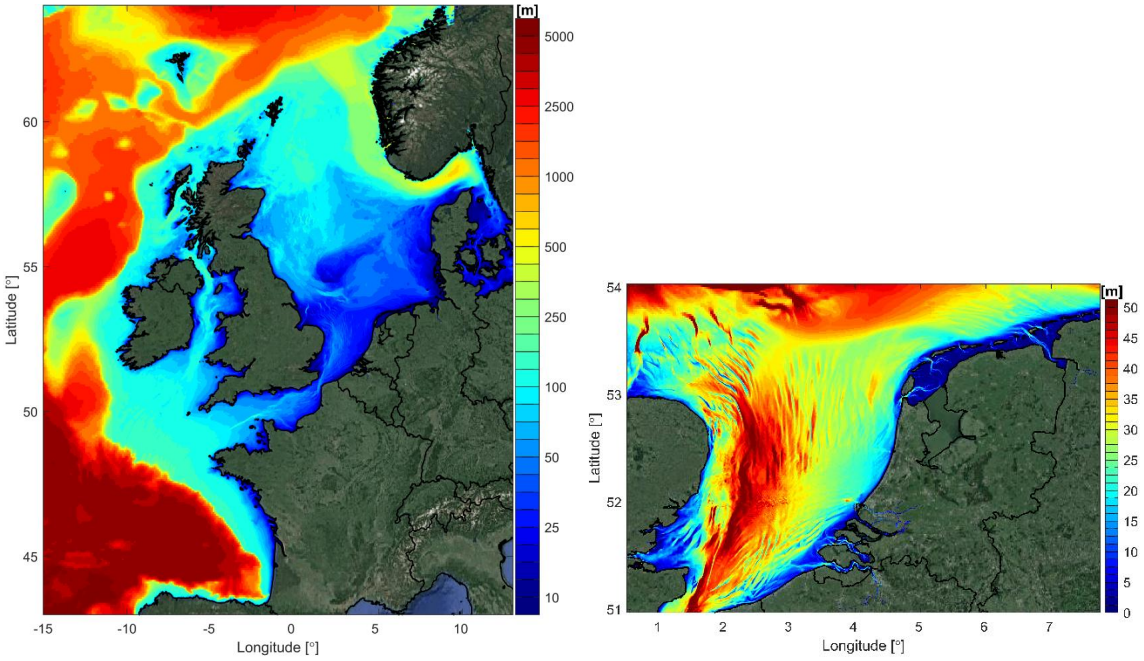

Figure 4.1 Extents and bathymetry of DCSM v6 model (left panel, please note the non-linear scale in the colour bar, applied for visibility purposes). Right panel: Zoom in of the Dutch coastal zone.

In this study the hourly spatial water level and current fields from the DCSM V6 model have been obtained for the period of 28-12-2018 until 04-01-2019 to serve as input to the analysis of the metocean conditions of Task 1 (Footnote 7). These data are applied in the wave modelling and analysed in Chapter 5.

4.1.2 Validation of hydrodynamics

To check the validity of the DCSM hydrodynamic data, the operational data have been validated against measured values at three measurement stations out at sea (platforms F161, L91 and AWG, see Section 3.7). From the available locations recording this parameter, these are the closest to the area of interest or located up-wind of the storm conditions. Even though measured time series already have been used to improve and calibrate the flow model when it was originally developed, it still is useful to consider these measurements here since the calibration of the numerical model was done based on longer and other time intervals than the time interval

studied in the present project. Therefore, comparing computed to measured results is a good verification of the quality and accuracy of the model in representing the specific conditions that occurred on 1-2 January 2019 and in this specific area of interest.

Figure 4.2 presents density scatter plots of the hourly measured and modelled water levels for the period of 30-12-2018 – 04-01-2019 at the three selected platforms, together with error statistics (grey-box).

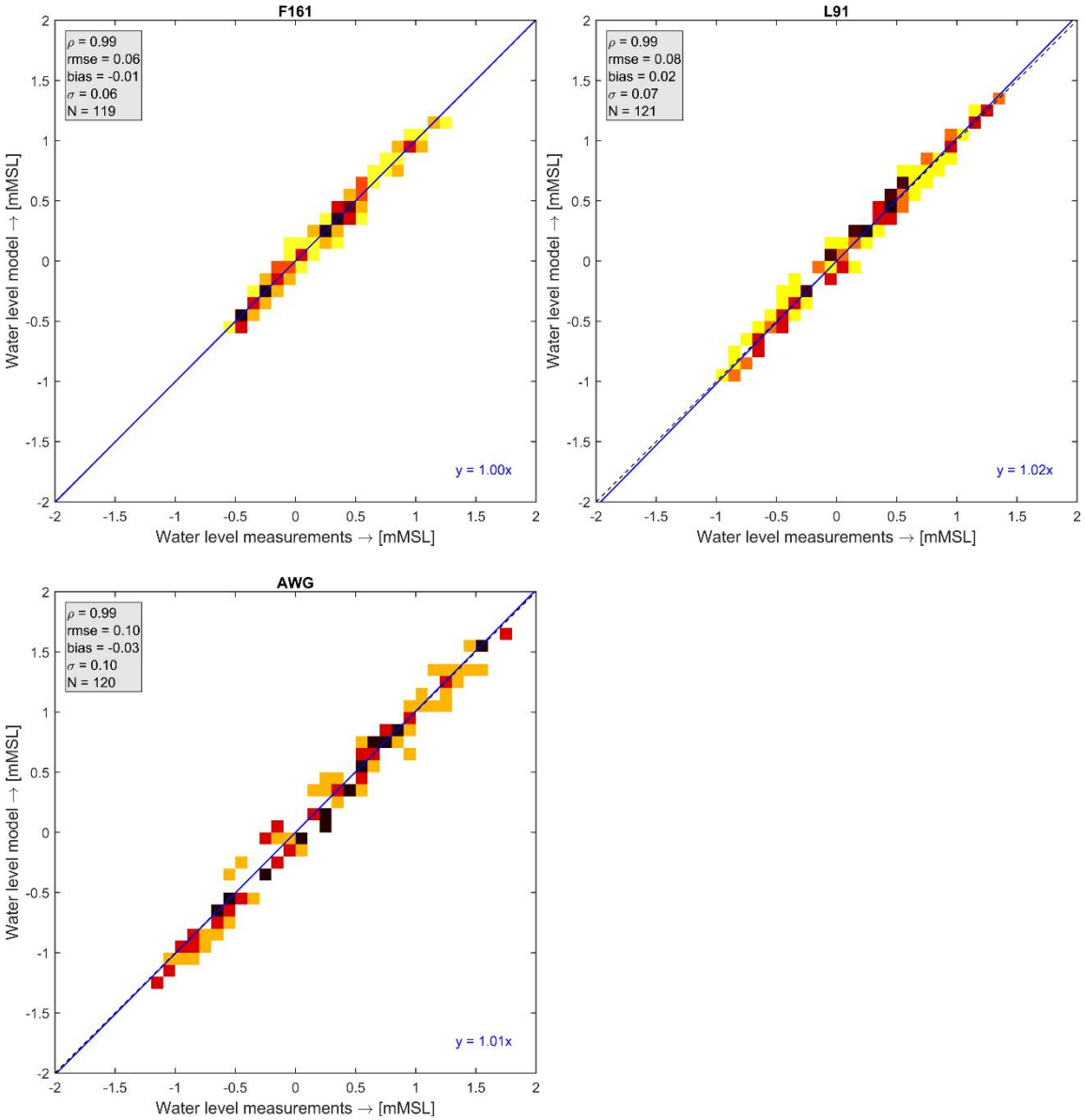

Figure 4.2 Scatter plots of water level measurements against numerical model data for platforms F161, L91 and AWG (period: 30-12-2018 – 04-01-2019). The coloured squares, ranging from yellow (low density) to black (high density), indicate the data density in the scatter plot. Each panel includes information on error statistics (grey box in top left corner, see main text for further information and units) and an origin-crossing linear fit (blue line + the relation given in the bottom right corner).

These error statistics are:

- correlation factor (dimensionless): indicating to what extent a change in one parameter is a prediction for a similar change in the other parameter;
- root-mean-square error (m): a measure of the absolute and accumulated error between computed and measured results;
- bias (m): a measure of the mean offset between computed and measured values;
- standard deviation (m): a measure of the spreading of the errors;
- and number of data points: the number of instances/samples considered.

The figure shows that the comparison in water levels at the three platforms is excellent with very high correlation values and very small errors values. This high level of quality is expected to be valid for the full area of interest, including the main shipping routes. This is considered further in Section 5.1.4.

As described in Section 3.7, no current measurements are available in the area of interest for 1-2 January 2019 so available information on currents cannot be verified. Even though currents are a derivative of (spatial variations in) the water levels, the fact that the water levels are modelled very accurately by the numerical model is not necessarily a guarantee that also the flow velocities and directions are equally accurate. However, in absence of measurement data, and knowing that the DCSM V6 model has been extensively calibrated and validated for a large set of observation locations throughout a large area, the computed results are considered the most accurate source of flow information available for the present study.

4.2 Wind conditions

4.2.1 ERA5 hindcast database

Reanalysis[15] spatial data of wind and wave conditions were obtained from the European Centre for Medium-Range Weather Forecasts' (ECMWF) ERA5 dataset[16]. The ERA5 dataset is ECMWF's latest and most advanced reanalysis dataset available. It provides information with a timestep of one hour. This information includes analyses of many atmospheric, land and oceanic climate variables such as wind parameters (wind speed at 10 m height and wind directions) and multiple wave parameters on a large-scale, relatively coarse calculation grid and with a schematised bathymetry description. ERA5 combines large amounts of historical observations into global estimates using advanced modelling and data assimilation systems. The hourly data are available globally on a grid of 0.25º for atmospheric parameters and 0.50º for wave parameters from 1979 up to present (this will soon be extended backwards to 1950). Following our experience, the wind data from ERA5 often requires almost no correction when validated against in-situ measurements on the North Sea. This validation is discussed in the next section. The wave data from ERA5 is used to force the applied detailed local wave model at its outer (incoming) wave boundaries (Section 4.3).

4.2.2 Validation of wind data

To check the validity of the ERA5 wind data for the present study, these data have been validated here against observed values at five offshore measurement stations (platforms Troll-A (Norway), A121, F161, L91 and AWG, see Section 3.5). From the available locations recording this parameter, these are the closest to the area of interest or located up-wind of the

[15] *A hindcast is a model computation of past conditions using measurements and other data available for the interval simulated. An analysis is the result of correcting a model result with observations (data assimilation). A reanalysis is a hindcast with data assimilation, leading to conditions that are as close to reality as possible.*

[16] https://www.ecmwf.int/en/forecasts/datasets/reanalysis-datasets/era5

storm conditions. Even though the ERA5 model has been fed with large amounts of measurement data to calibrate and validate the model during its development, still it is useful to assess its quality and accuracy of that model for representing the conditions for 1-2 January 2019 and for these locations specifically. Figure 4.3 to Figure 4.7 present scatter plots of the hourly measured and modelled wind speeds and directions for the period of 30-12-2018 – 04-01-2019 at the five platforms together with error statistics of the comparison in the grey-box. These statistics are: correlation (dimensionless), root-mean-square error (m/s or angular degrees), bias (m/s or angular degrees), standard deviation (m/s or angular degrees) and number of data points/samples considered.

Wind speed

The figures show that the agreement in wind speed at the five platforms is generally quite good, with very high correlation values and with quite limited scatter. However, looking in detail at the results, at platform F161 the wind speeds are overestimated in general by approximately 15%, while at platform AWG the wind is underestimated by approximately 9%. At the other three platforms there is no structural over- or underestimation over the full range of values present in the time series considered. However, during the peak of the storm the wind is underestimated at all platforms in the Dutch territory by approximately 5%. Since the bias found in wind conditions during this event is not constant throughout the full domain, correcting for this deviation cannot be done unambiguously. This makes that any adjustment or correction to the wind computed wind fields could be considered arbitrary. Therefore, it was decided that no correction (scaling of wind speed) would be applied on the ERA5 wind fields when used to drive to the local wave model. This needs to be kept in mind when interpreting the model results and when applying the computed outcomes in further study tasks (see also Section 4.3.7).

Wind direction

The comparison of measured and modelled wind directions shows that the quality of the ERA5 wind directions is excellent on that parameter. Only a little amount of scatter is observed, indicating that the wind directions are generally very well described by the available ERA5 wind data and therefore suitable for use in the present study.

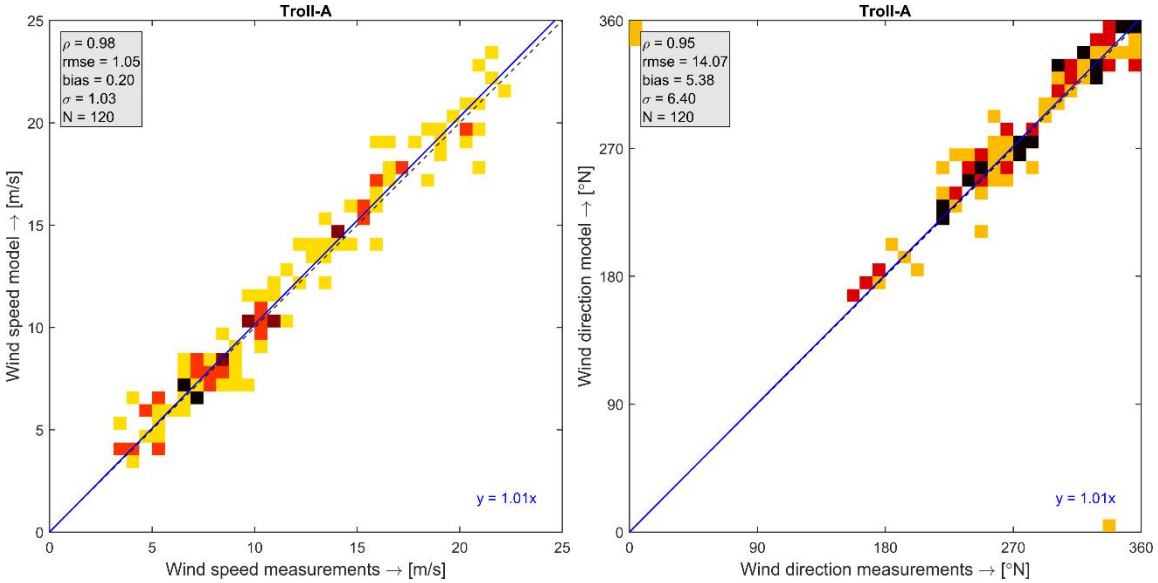

Figure 4.3 As Figure 4.2, now for wind speed (left panel) and direction (right panel) measurements against numerical model data (ERA5) for platform Troll-A.

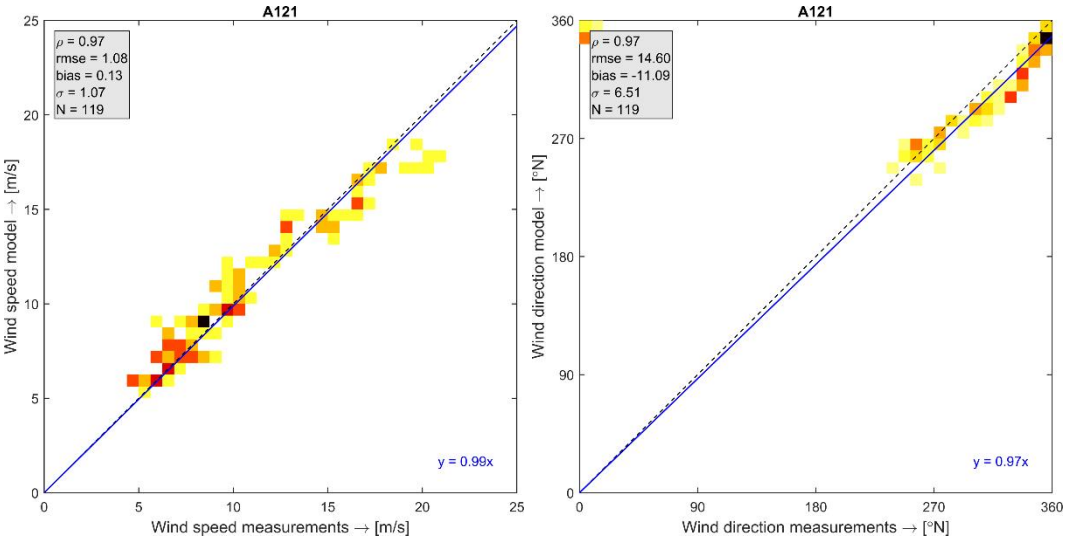

Figure 4.4 As Figure 4.3, now for platform A121.

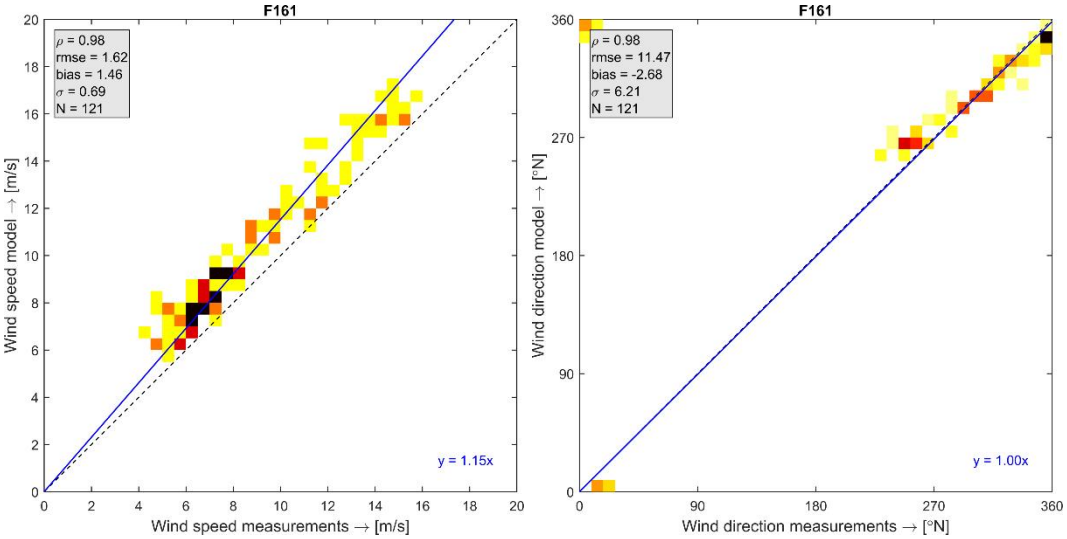

Figure 4.5 As Figure 4.3, now for platform F161.

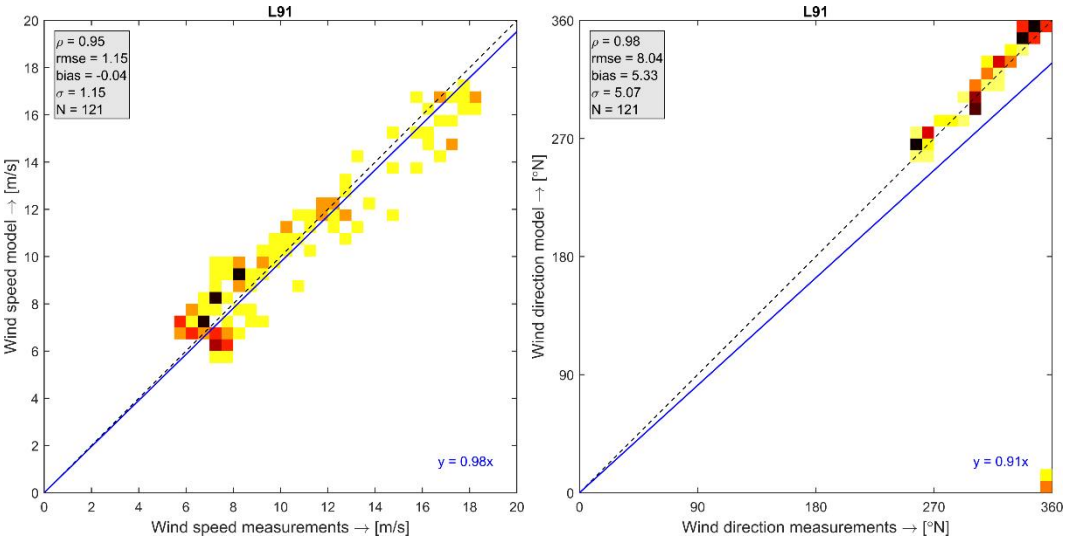

Figure 4.6 As Figure 4.3, now for platform L91.

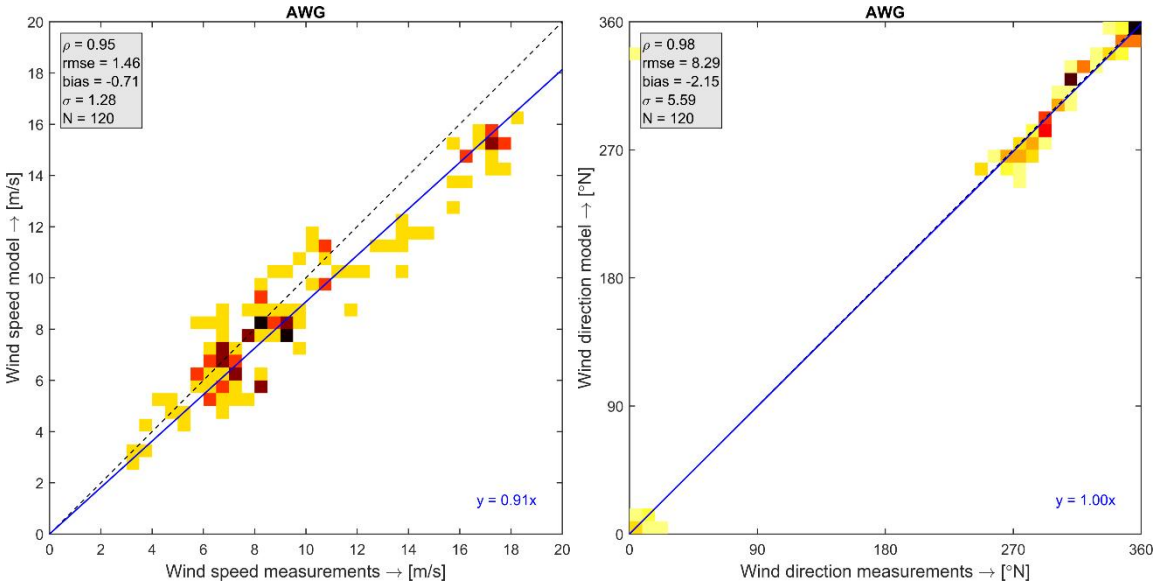

Figure 4.7 As Figure 4.3, now for platform AWG.

4.3 Wave conditions

4.3.1 Introduction

Numerical wave modelling has been performed to reproduce the wave conditions during 1-2 January 2019. The dedicated local numerical wave model has been forced by the available offshore wave, wind, current and water level conditions described and validated in the previous sections.

The third-generation shallow water wave model SWAN (Simulating WAves Nearshore; Booij et al, 1999) has been used for the numerical modelling of waves in the area north of the Wadden Islands. SWAN has been developed at the Delft University of Technology (e.g., Van der Westhuysen, 2010 and Zijlema, 2010) with contributions by Deltares. It computes wave propagation and wave energy evolution efficiently and accurately and it describes several non-linear effects via parameterised formulations. More specifically, SWAN can account for several wave propagation phenomena, including (only the most relevant for the present project mentioned):

- Wave propagation in time and space, shoaling[17], refraction[18] due to current and depth, frequency shifting due to currents and non-uniform depth;
- Wave generation by wind;
- Three- and four-wave interactions[19];
- Energy dissipation by: white-capping, bottom friction and depth-induced breaking.

White-capping is the phenomenon that waves show foam effects at the wave crests due to dissipation of wave energy. It is sometimes called deep-water wave breaking, as opposite to shallow-water wave breaking that can be observed at the beach (depth-induced breaking).

[17] *Shoaling is the steepening of waves as they approach the coast and reach shallower water. This increases the energy density of the waves, leading to an increase in wave height.*

[18] *Refraction is the effect that (non-uniform) bed levels have on the propagation direction of waves.*

[19] *Multiple wave components at different frequencies can interact (in deeper water 4 components, in shallow water 3), leading to a redistribution of wave energy over different wave frequencies. Since it causes energy transfer between components/frequencies these are non-linear processes.*

Bottom friction causes dissipation of wave energy when the waves are long enough to be influenced by the roughness of the sea bed while propagating. At shallow depths and for longer wave periods bed friction has the largest influence.

SWAN is widely used for nearshore wave modelling in the international coastal engineering community and has been successfully validated under a large variety of field cases and conditions. The software is continually undergoing further development; see www.swan.tudelft.nl for more information. For this study we have used the latest operational version that includes the most recent insights and model developments (SWAN Version 41.20).

4.3.2 Model domains

SWAN requires the specification of three types of grids:

1 computational grid, which defines the 2D geographical locations of the nodes in the calculation grid;
2 directional grid, which defines the wave directional range (usually 360°) and resolution;
3 spectral grid, which defines the range and resolution of the computations in the wave frequency space.

The following two computational grids (spatial domains) were used in this study:

- Overall: an overall domain with a spatial resolution of 1/20 degree (≈4.0-2.4 km) in longitudinal (East-West) direction and of 1/30 degree (≈3.7 km) in lateral direction (North-South), and
- Detailed: a nested detailed domain with a spatial resolution of 0.5 km by 0.5 km covering the considered section of the track sailed by the MSC Zoe.

The two domains are presented in Figure 4.8 and Figure 4.9, with the overall model grid in green and the detailed model grid in red[20]. The overall domain provides input for boundary conditions along the outer edges of the detailed calculation grid (this approach is called 'nesting'). For reasons of computational efficiency, the Irish Sea is not considered in the model (by not including that area in the bathymetry schematisation, see Section 4.3.3). This is because the conditions in that area do not influence the wave conditions in the Dutch section of the North Sea. The trapezium-shaped extent of the local model is the result of the curvature of the earth in combination with how the grid is plotted onto this 2D image.

The directional grid in SWAN covers the full circle (360°). The number of directional bins was set to 45, resulting in a directional resolution of 8°. This is a typical and often used directional resolution in these kinds of nearshore wave studies.

The spectral grid of the numerical model covers a frequency range from 0.03 Hz to 0.6 Hz, allowing for representation of wave periods ranging from 1.67 s to 33.33 s. The distribution of the frequencies, f, is logarithmic with a constant relative resolution, Δf/f, close to 0.1. This results in a total number of frequency bins of 32. This way of distributing the modelled frequencies over the extent of the considered frequency range ensures that the resolution at lower frequencies is not as coarse as it would have been if an equidistant distribution of frequencies had been applied.

[20] *The overall domain extent is equal to that of the overall domain of the DCSM operational* wave *forecast model of Rijkswaterstaat (part of RWsOS North Sea, see Footnote 12). Note that the wave model domain is smaller than that of the DCSM flow model (see Section 4.1.1). This has no implications for the present study.*

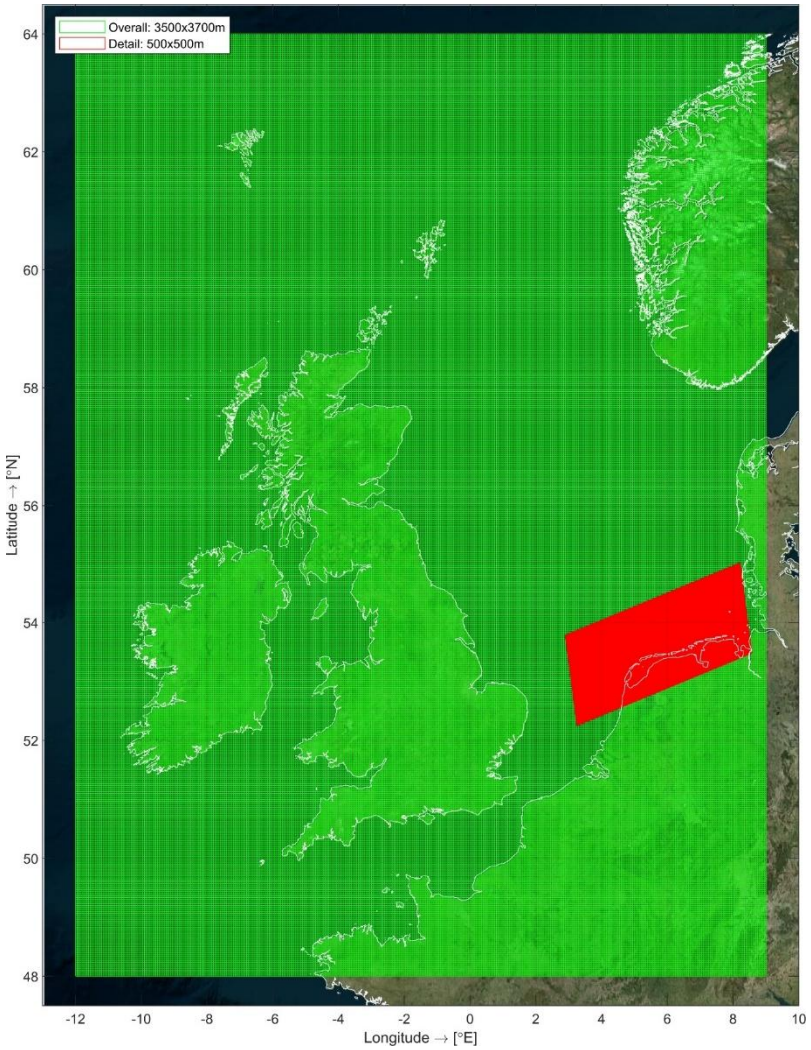

Figure 4.8 Computational SWAN domains.

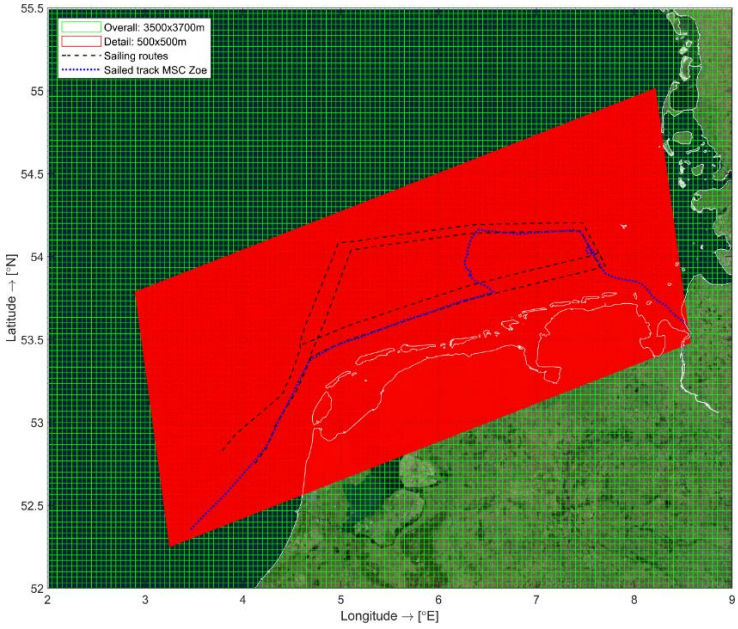

Figure 4.9 Zoom of detailed computational SWAN domain.

4.3.3 Bathymetry

The bathymetry information included in the DCSM flow model (Section 4.1.1) has also been used for the depth schematization of the overall wave model. The bathymetry of the overall wave domain is shown in Figure 4.10. Note in this image that the Irish Sea is not included in the depth information for computational efficiency reasons (Section 4.3.2).

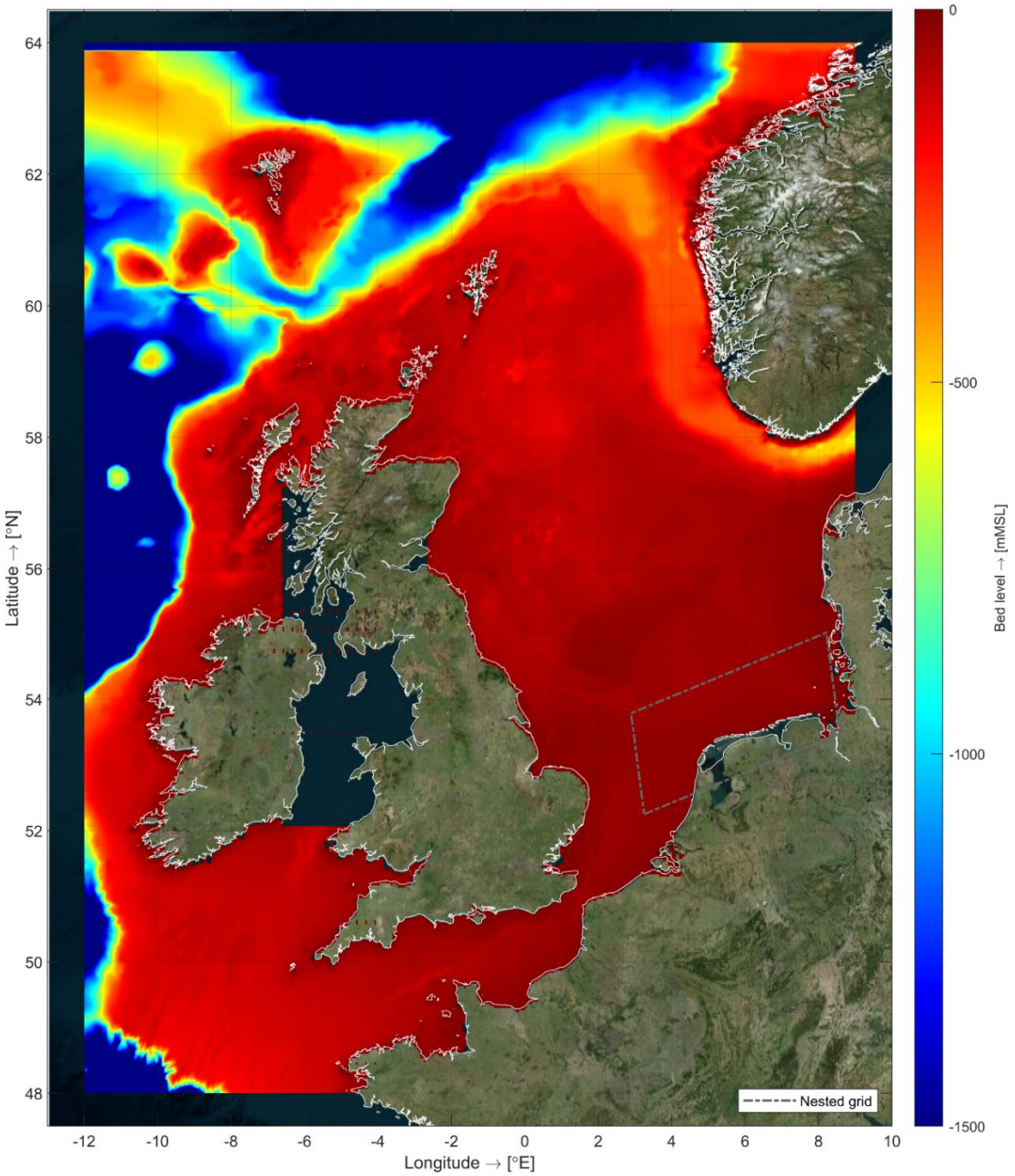

Figure 4.10 Bed levels relative to MSL as used in the overall grid of the wave model. The depth colour scale is cut-off at MSL -1500 m for visualisation purposes. In the deepest parts, bed levels go down to MSL -4200 m.

The depth schematization of the detailed wave grid is based on the EMODnet DTM (European Marine Observation and Data Network Digital Terrain Model) for 2018 (cf. Section 3.3). This additional source of bed level information was consulted since it provides the most recent and accurate information for this focused model area. Consistency between the overall and the

detailed wave model domain (including vertical and horizontal references used) was checked and corrected for, where required.

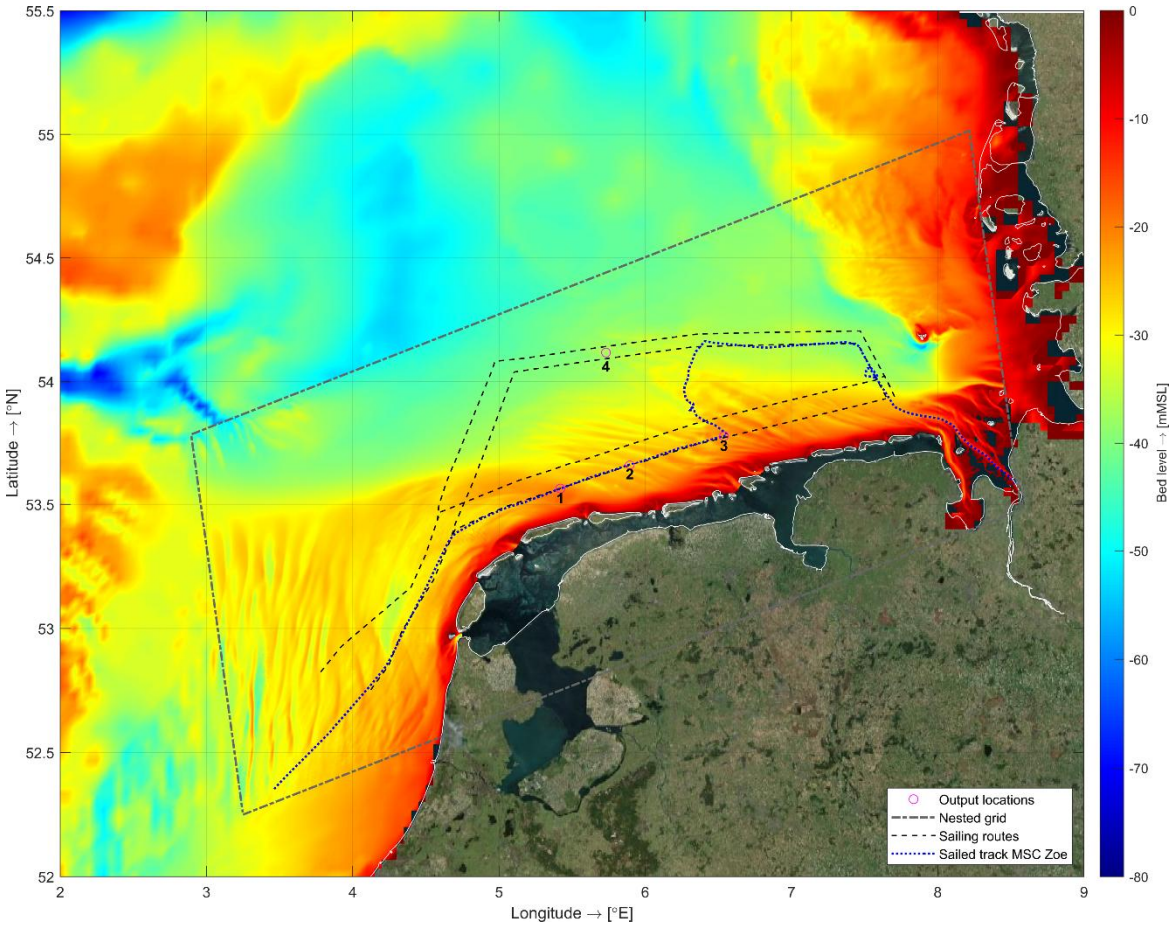

Figure 4.11 Bed levels relative to MSL as used in the detailed grid of the wave model and the locations of the considered output points (described in Section 4.3.6).

4.3.4 Boundary and input conditions

The wave model was run in non-stationary mode (i.e. taking evolution of the wave conditions in time into account) for a total of 8 simulated days (28-12-2018 – 04-01-2019). The model uses a timestep of one hour, which is equal to the time step of the (ERA5) input wind fields (Section 4.2). The first 48 hours simulated time are considered as the spin-up period of the model[21]. First the total time interval was modelled for the overall domain, generating the boundary input for the detailed domain. After the modelling for that domain was finished, the run for the detailed domain started in an automated computational process.

Incoming boundary conditions

The SWAN model was forced at the outer boundaries of the overall domain with parameterized wave spectra described by ERA5 timeseries of five wave parameters (described in more detail below this list):

[21] *The spin-up period is the modelling interval which is required for the model to start up and initialise. This includes allowing the wave energy from the boundary to distribute over the total modelling domain. A spin-up period of 48 hours (2 days) is typically used. Results for the spin-up period may not be reliable and are discarded.*

- Significant wave height, H_s
- Peak wave period, T_p
- Mean wave direction (coming from), MWD
- Directional spreading, σ or m
- Spectral shape, γ (an enhancement factor of the peak in the wave spectrum)

The spectral shape, γ, was assumed to be constant for all computations, being a JONSWAP shape (Hasselmann et al., 1973) with a value of γ = 3.3. The exact value of γ prescribed along the boundary is not critical, since the model will automatically properly redistribute the wave energy in the frequency domain and in balance with the wind forcing. The amount of directional spreading present at the incoming boundaries was derived from the ERA5 timeseries for "wave spectral directional width". For numerical reasons, this value was capped at a maximum of σ = 37.5° (one-sided directional spreading level from the mean direction), which corresponds to a cosine-m power of m = 1 in SWAN[22]. Also for this boundary parameter, the exact value prescribed is not critical, since the model will automatically properly redistribute in the computed domain the wave energy over the different directions.

Reflecting/transmitting boundaries
No reflecting or transmitting boundaries were defined in both modelling domains. All wave energy reaching an outer boundary or land boundary is assumed in the model to be fully absorbed at that location. For sloping shorelines and beaches that is a fitting and often applied approach. At the sections bordering the Irish Sea waves propagate out of the computational domain uninfluenced (as if they move into the Irish Sea).

Wind input
Both the SWAN model domains were forced spatially using the ERA5 wind fields as described in Section 4.2. As discussed in Section 4.2.2, no corrections on the wind speeds or directions have been applied. This is mainly because the quality of the wind data is in general high and the discrepancies found were not consistent over all measurement locations considered (some showed overestimations and some showed underestimations of the wind speeds included in the spatial wave fields).

Hydrodynamics input
The spatially varying hourly water level and current fields, from the model described in Section 4.1, have been used as input to both SWAN wave modelling domains. This means that the wave model simulates how the spatially distributed water levels and currents (speeds and directions) influence the wave propagation and evolution.

4.3.5 Numerical and physics parameter settings

This section lists detailed settings for physics parameters and numerical aspects within the SWAN model. It is primarily included here for recording purposes, e.g. for possible future interpretation or reproduction of results. General readers may opt to skip this section.

The modelling was carried out using SWAN, version 41.20, in non-stationary mode. The most relevant applied wave physics settings in the computations are:

- Dissipation of wave energy by bottom friction and wave breaking (wave steepness-induced and depth-induced) have both been applied in the SWAN computations.

[22] *This power is used to describe directional distribution shape description according to $\cos^m(\theta)$, with θ representing the wave directions.*

  - For dissipation by bottom friction the JONSWAP formulation (Hasselmann et al., 1973) with a friction coefficient of 0.038 m^2s^{-3} (Zijlema et al., 2012) has been applied.
  - For dissipation by depth-induced wave breaking the Battjes-Janssen formulation (Battjes and Janssen, 1978) with a proportionality coefficient of 0.73 has been applied.
- For representing the effects of white-capping, the formulations by Rogers et al. (2003) have been applied, which is default setting since SWAN version 40.91.
- For the wind drag the default Wu (1982) approximation of the Charnock relation has been applied, which describes the effect of the wind over the corrugated water surface.

The criteria for numerical accuracy thresholds were set as follows:
- the computation is finished in case of changes of less than 1% in H_s and $T_{m0,1}$ at 99.5% of the grid points relatively to the previous computational iteration rounds, and
- a maximal number of 30 iterations is computed.

These settings mean that the computation will continue until a stable outcome has been reached for the modelled moment in time, with a maximum of 30 iterations to reach the result for that time step. Typically, 30 iteration steps will be sufficient, if not then often a setting in the model is incorrect or the computational grid is not optimal. In the computations performed for the present study, all timesteps after the two days spin-up period have been verified to have converged within 30 iterations, i.e. the computation has reached the proper numerical outcomes.

4.3.6 Output definitions

Spatial and time varying fields of multiple wave (-related) parameters (H_s, T_p, other spectral wave periods and MWD) were produced by the model as output at a time step of 1 hour (i.e. the computational time step). In addition, location-specific timeseries of the same set of parameters were generated in the numerical model at all platform and buoy locations mentioned in Chapter 3 to allow for a detailed validation of the model outcomes. Comparing measured and computed values at those locations gives an indirect verification of the accuracy of the results in the full domain modelled.

Output timeseries as well as two-dimensional wave variance spectra (describing the wave-energy distribution over frequencies and directions) have been generated for every running kilometre along the sailing route of the MSC Zoe. Special attention has been given to three of these locations, corresponding to key moments/locations as suggested by OVV (Locations 1 to 3 in Table 4.1). Note that the time stamps considered have been rounded off to the corresponding nearest wave modelling timestep (linked to the resolution of the available wind fields to drive the numerical wave model). The time that the vessel was at Location 3 is exactly in between two output time stamps (00:00 h and 01:00 h). The time stamp with the highest wave conditions from those two was selected for Location 3 (00:00 h).

Table 4.1 Information on the considered main output locations along the sailed track of the MSC Zoe.

Loc. ID + *Time*	**Longitude [°E]**	**Latitude [°N]**	**Bed level [mMSL]**
1: *1-1-19 20:00 (20:10)*	5.420370	53.563703	-20.93
2: *1-1-19 22:00 (22:01)*	5.895292	53.660787	-26.52
3: *2-1-19 00:00 (00:30)*	6.538329	53.779176	-21.67
4: *2-1-19 00:00 (00:00)*	5.731791	54.117485	-37.37

OVV requested Deltares to consider also a location along the northern sailing route for comparison to conditions at the three locations selected for the southern sailing route.

Figure 4.11 presents the locations of all four main output points. Location 4 was selected by going northward from Location 2 in the direction of the incoming wind (up-wave, or up-wind into the storm condition, i.e. towards 330°N). Location 4 was then defined in between the traffic lanes of the northern sailing routes (the dashed lines in Figure 4.11 correspond to the centre lines of those traffic lanes). Preliminary calculations with the numerical model indicated that the wave conditions at that location were representative for the full west-east stretch of the northern sailing route.

The bed level at Location 4 (MSL -37.37 m) is representative for the bathymetry along the northern route. Along the west-east stretch of the northern sailing route the bed level gradually shifts from around MSL -41 m in the west to around MSL –35 m in the east (derived from the model bathymetry). This is deep enough for an average value to be considered for representative wave parameter values. The timestamp of 00:00 considered for Location 4 corresponds to the moment on which the peak of the storm at that location is computed (i.e. highest wind speeds in combination with highest and longest waves). Coincidently, it is the same (rounded-off) time stamp as is considered for Location 3.

4.3.7 Results and validation

In this section the computed wave results at the selected wave measurement locations (Chapter 3) are presented and discussed as a validation (quality check) of the modelling performed. The analysis of the metocean conditions (including waves) experienced by the MSC Zoe during its voyage on 1-2 January 2019 and the spatial and temporal variations of these conditions are considered separately, in Chapter 5.

Appendix A presents density scatter plots of measured and modelled wave parameters for all platforms and buoys with wave information (cf. Section 4.3.6 and Chapter 3). At those locations the following measured wave parameters are available:

- significant wave height, H_s [m],
- peak wave period, T_p [s],
- spectral wave period, $T_{m0,2}$ [s],
- spectral wave period, $T_{m-1,0}$ [s], and
- mean wave direction, MWD [°N] (only available for wave buoys).

Data entries that fall on the central black dashed line in those figures indicate a perfect match between the computed and measured value; the further away from that central line, the larger the discrepancy between the computational value and the measured entry. The data in the scatter plots in Appendix A cover the five-day period of 30-12-2018 00:00 to 04-01-2019 00:00. This interval corresponds to up to 121 data entries (5 days of 24 hourly values each). Some of the scatter plots contain a lower number of data entries because of unavailability of some of the measured entries (e.g. as a result of measurement errors or data loss due to communication problems).

The scatter plots in Appendix A show that the numerical wave model generally reproduces the wave conditions fairly well, i.e. most of the data entries are along, or close to, the central black dashed line. Table 4.2 presents an overview of the correlation coefficients (ρ) for the different considered parameters and locations, collected from the scatted plots in Appendix A. A correlation coefficient of 1.0 indicates a perfectly correlated result, whereas a correlation of 0 indicates that there is no relation. The correlation of the results varies between 0.92 and 0.99 for all variables and all locations, indicating an excellent correspondence between measured and computed values.

Table 4.2 Correlation coefficients (dimensionless) between computed and measured wave parameters for the considered measurement locations.

	Platforms					Buoys		
Param.	**A121**	**F161**	**L91**	**Q1**	**AWG**	**EiG**	**AZ 1-2**	**SoN**
H_s	0.99	0.98	0.98	0.98	0.98	0.98	0.99	0.99
T_p	0.95	0.96	0.96	0.92	0.95	0.94	0.96	0.96
$T_{m-1,0}$	0.95	0.94	0.95	0.95	0.97	0.96	0.98	0.98
$T_{m0,2}$	0.97	0.94	0.95	0.93	0.97	0.95	0.98	0.98
MWD	n.a.	n.a.	n.a.	n.a.	n.a.	0.95	0.95	0.96

For a further quantification of discrepancies between the measured and computed values Table 4.3 presents the RMSE (Root-Mean-Square Error) values collected from the scatted plots in Appendix A. This parameter is a measure for the mismatch between the measurements and the calculated results, whereby extra weight is given to larger errors. The Bias, although useful for assessing any structural offsets, is considered a less suitable parameter for assessing the overall accuracy of the results here, since in that parameter in principle an underestimation in one part of the simulation could be 'compensated' by an overestimation later in the computation.

Table 4.3 RMSE values for the considered measurement locations.

	Platforms					Buoys		
Param.	**A121**	**F161**	**L91**	**Q1**	**AWG**	**EiG**	**AZ 1-2**	**SoN**
H_s [m]	0.29	0.32	0.29	0.29	0.24	0.25	0.46	0.34
T_p [s]	0.96	0.94	0.82	0.98	0.94	0.66	0.90	0.71
$T_{m-1,0}$ [s]	0.80	0.86	0.82	0.64	0.64	0.57	0.52	0.44
$T_{m0,2}$ [s]	1.03	1.08	1.03	0.87	1.19	0.82	0.79	0.80
MWD [º]	n.a.	n.a.	n.a.	n.a.	n.a.	7.09	6.86	5.56

The RMSE values in Table 4.3 should be seen in relation to the H_s and T_p values that occurred during the storm, i.e. up to 6.5 m and 14 s (Section 3.6). This means that these weighted errors are in the order of 5-10% of the computed values for H_s and the different wave period parameters. The error for the wave directions should be seen in relation to the directional resolution of the SWAN computations (8º), i.e. the deviations fall within one computational bin. Overall, the accuracy level found is typical for these kinds of computations, in which the accuracy of the computational results will be strongly dependent on the accuracy of the input (forcing) data.

In addition to the accuracy assessment on the overall time series computed, also details within the time series have been analysed. A general observation is that at all locations H_s is systematically underestimated by 2-8% on average. And at buoy 'AZ 1-2' a larger underestimation of approximately 13% in H_s is found during the peak of the storm, while the errors in the other parameters at that location are much smaller during that time. In Figure 4.12 the measured and modelled timeseries for that location ('AZ 1-2') are plotted. The figure shows that no such underestimation is found during calmer conditions and the overall agreement of results during those intervals is rather good.

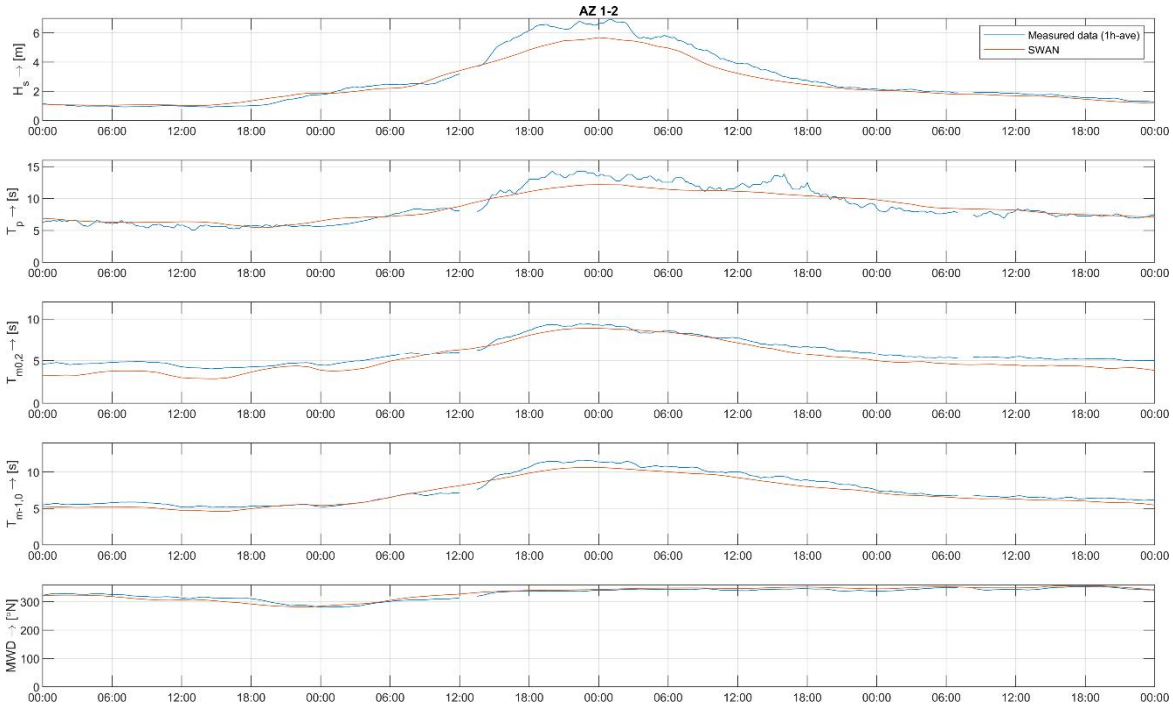

Figure 4.12 Timeseries of measured and modelled wave parameters for buoy 'AZ 1-2' (31-12-2018 00:00 – 04-01-2019 00:00).

Another general observation is that during the peak of the storm SWAN underestimates T_p at all locations (by approximately 2-3 s), while during calmer conditions the match in T_p is often excellent. Besides Figure 4.12, a second example of this is shown in Figure 4.13 for the timeseries for platform L91. The results for T_p in both figures are in the second panel from the top[23]. These two locations have been selected to highlight representative results because they are located closest to the main critical section of the track of the MSC Zoe, i.e. where the main incident was reported to have occurred. The mismatch found at these locations around the peak of the storm was much smaller (or even absent) at some of the other observation locations further out into the North Sea.

The model does reproduce accurately the overall trends in all the parameter values (also at the locations not shown in detail here), indicating that the general physics of the natural system are captured well by the numerical model. The general outcomes of the computations are therefore trustworthy and suitable for analyses and interpretations of the types of conditions that the MSC Zoe has experienced while transiting this area (considered in Chapter 5). Nevertheless, the differences found should be kept in mind while interpreting those conditions, particularly for the wave heights and periods around the peak of the storm.

As discussed in Section 4.2.2, underestimations in wind speed (≈5%) were identified in the available input data for the time that the peak of the storm reached the Dutch measurement locations. These wind fields directly drive (force) the wave model. The observed underestimations in the wave parameters during the peak of the storm are therefore (at least partially) ascribed to these underestimated wind speeds, which have limited the generation of higher and longer waves during that part of the simulation.

[23] *Please note that at the measurement platforms wave directions are not registered, hence only 4 panels with data are included in Figure 4.13, whereas Figure 4.12 also includes a fifth panel showing MWD, since the data presented in that figure have been registered by a wave buoy.*

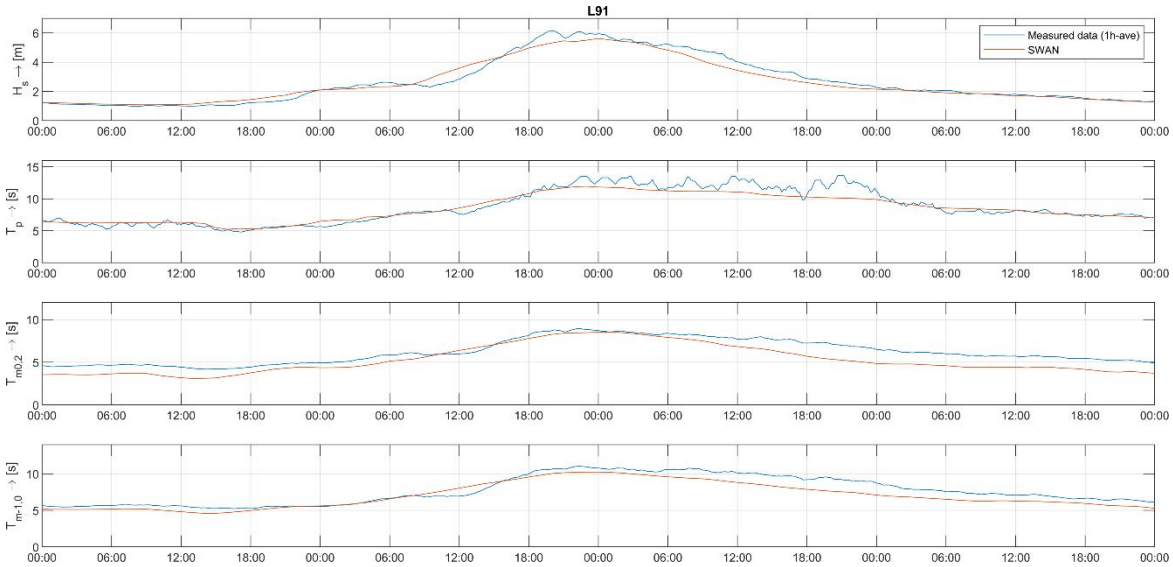

Figure 4.13 Timeseries of measured and modelled wave parameters for platform L91 (31-12-2018 00:00 – 04-01-2019 00:00).

4.4 Discussion

Water levels and currents

The water levels computed proved to be very accurate. No measured information on currents was available, but the numerical results are considered the best available source available. They are therefore suitable for further analyses and have been used as input for the wave modelling performed.

Wave and wind conditions

The comparison made in earlier sections between measured and computed wave conditions for the considered time interval around 1-2 January 2019 shows that the numerical wave model is generally capable of reproducing the conditions as occurred and the trends in the evolving wave parameters. However, it is unfortunate that particularly during the peak of the storm values for H_s and T_p at some of the observation locations show a discrepancy with the measurements (on average an underestimation of around 6% in H_s and around 2 s in T_p). As discussed in previous sections, this can at least partially be ascribed to underestimations in wind speeds included in the wind fields available to force the numerical wave model. This underestimation (around 5% in wind speed) is not equally present throughout the simulated days and occurs particularly around the time of the peak of the storm. As concluded earlier, these wind fields, obtained from available hindcast archives of such parameters, could not be corrected unambiguously and without arbitrary measures. Furthermore, deviations were largest at some of the measurement locations closer to shore (including the locations considered in detail in this chapter), whereas results for observation locations further out at sea were in many cases much better and not requiring a tuning correction of the same magnitude. Therefore, a deliberate decision was made not to tweak the wind fields and to apply them without alterations.

Regardless, using the computed wave conditions as basis for further tasks and analyses is considered justified since the overall physics of the natural wave system have been captured correctly. As a practical solution to account for the uncertainty in the available wind fields and in the corresponding wave model results, Deltares advised MARIN to consider also waves with 10% higher values for H_s and waves with approximately 2 s higher values for T_p in their set of

conditions applied for their physical scale modelling task[24]. By considering additional tests with elevated values for H_s and T_p, the laboratory tests will show whether such adjusted conditions would lead to other results and conclusions than those that result from using the wave parameter values as computed.

[24] *This has also been discussed during the progress meeting of 19-09-2019 at MARIN (Wageningen) with the project teams of both MARIN and Deltares. During that meeting the two-dimensional wave variance spectra at the four main output locations (Table 4.1) were delivered to MARIN and the test program for the scale model tests was discussed.*

5 Metocean conditions during the incident on 1-2 January 2019

The first sections of this chapter present the metocean conditions that the MSC Zoe experienced along its track on 1-2 January 2019 (Section 5.1) and how exceptional those conditions have been (Section 5.2). The information listed in those sections are combined, discussed and interpreted in the final section of this chapter (Section 5.3).

5.1 Metocean conditions experienced by the vessel

5.1.1 Flow conditions

Conditions considered by the vessel along the track

The current speeds and directions, the water levels and the corresponding water depths experienced by the MSC Zoe have been determined by deriving the model results along the track of the vessel (coordinates and timing). Figure 5.1 shows the outcome, with time plotted along the horizontal axis. In this and subsequent figures the magenta circles represent the timestamps corresponding to the three main output locations along the sailing route of the MSC Zoe (Table 4.1). The data show that during the critical part of the transit, i.e. the time range stretched by the magenta circles, the water level was dropping (ebb tidal phase) and that the lowest (tidal) water level occurred around the easternmost of the three key locations (i.e. the latest of the three). This is considered further in Section 5.1.4.

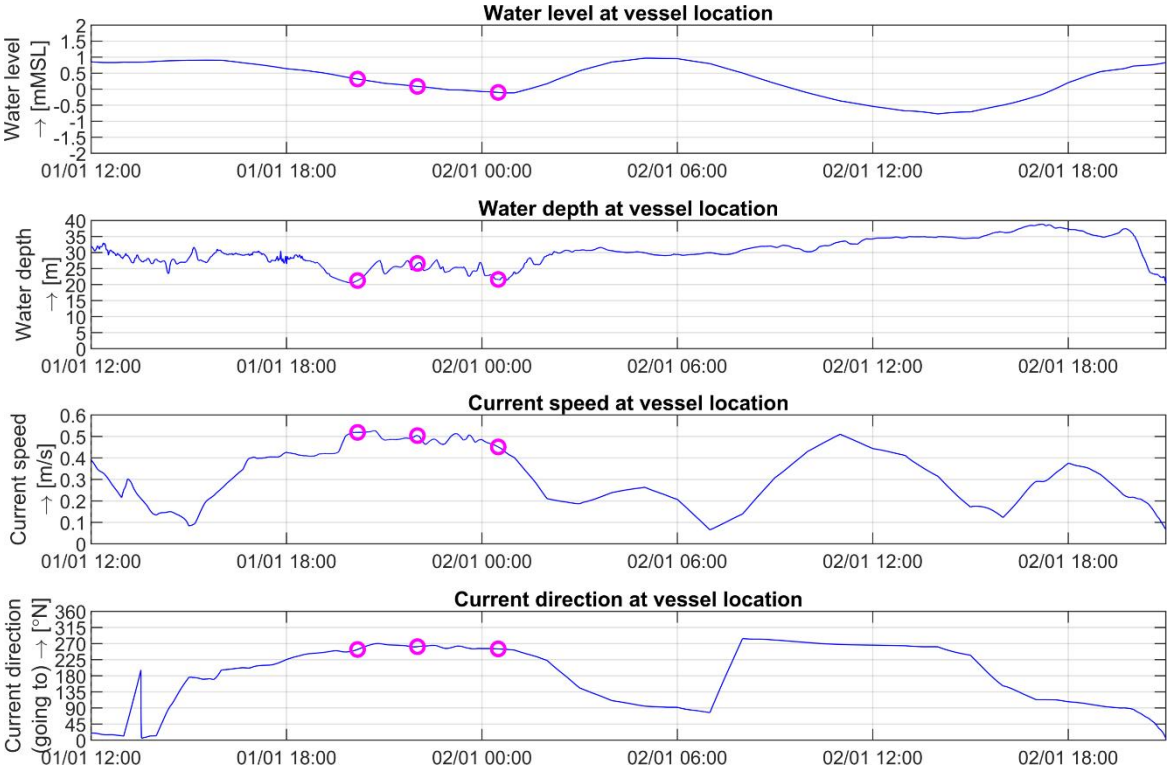

Figure 5.1 Timeseries of hydrodynamic conditions experienced by the MSC Zoe.

Table 5.1 summarises the hydrodynamic conditions at the four main output locations for the modelling timestep nearest to the moment in time associated with the vessel being present at that location:

- water level, WL, in m relative to MSL,
- local water depth, d, in m (derived from the water and bed levels in the model),
- current speed (depth averaged), U_{cur}, in m/s, and
- current direction (depth averaged), $U_{cur,dir}$, in °N (going to).

Table 5.1 Hydrodynamic parameters at the four considered output locations.

Loc. ID + *Time*	Lon. [°E]	Lat. [°N]	WL [mMSL]	d [m]	U_{cur} [m/s]	$U_{cur,dir}$ [°N] (going to)
1: *1-1-19 20:00*	5.420370	53.563703	0.37	21.30	0.50	253
2: *1-1-19 22:00*	5.895292	53.660787	0.09	26.61	0.50	261
3: *2-1-19 00:00*	6.538329	53.779176	-0.06	21.61	0.50	257
4: *2-1-19 00:00*	5.731791	54.117485	0.18	37.55	0.49	259

Spatial variation in hydrodynamic conditions in the area

Appendix B.1 includes spatial plots of water levels and depth-averaged current speeds and directions. These plots show that during the considered days the water level in the area north of the Wadden Islands was generally quite (spatially) uniform for a given moment in time. The current speeds are lowest at the location where the tide is turning, and this location is slowly progressing north(east)ward as the ship is moving east. Since the vessel moved along north-eastward with this flow-field evolution, while sailing in an area of a depth-averaged current of around 0.5 m/s, it experienced a quite constant flow condition.

5.1.2 Wind

Conditions considered by the vessel along the track

The wind conditions as experienced by the vessel have been derived along the route in a similar way as for the flow conditions, i.e. using the ship track information to derive the relevant information from the numerical model output. Figure 5.2 shows as results of this approach the wind speed (top panel) and direction (bottom panel) as experienced by the MSC Zoe. The panels in this figure indicate that the wind direction was rather constant during the critical section of the transit (around 330º, coming from). The wind speed experienced by the vessel slightly increased as the vessel progressed along its west-east transit.

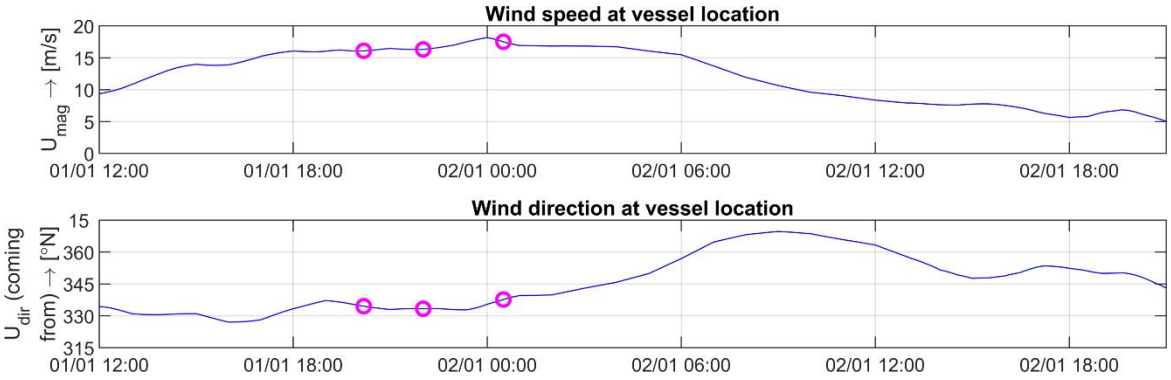

Figure 5.2 Timeseries of wind conditions experienced by the MSC Zoe.

Table 5.2 summarises the wind conditions at the four main output locations for the modelling timestep nearest to the moment in time associated with that location:

- wind speed at 10 m above mean sea level, U_{mag} in m/s, and
- wind direction at 10 m above mean sea level, U_{dir} in °N (coming from).

Table 5.2 Wind parameters at the four considered output locations.

Loc. ID + *Time*	Lon. [°E]	Lat. [°N]	U_{mag} [m/s]	U_{dir} [°N] (coming from)
1: *1-1-19 20:00*	5.420370	53.563703	16.00	335
2: *1-1-19 22:00*	5.895292	53.660787	16.31	333
3: *2-1-19 00:00*	6.538329	53.779176	18.18	336
4: *2-1-19 00:00*	5.731791	54.117485	17.93	339

Spatial variations in wind conditions in the area

Appendix B.2 presents spatial plots of the wind conditions north of the Wadden Islands at the moments in time corresponding to the vessel being at the different main output locations (and for Location 4 the same time as Location 3). These figures show spatially quite uniform wind conditions, with somewhat higher wind speeds to the east. Although the uniformity in the conditions may be partially due to the coarse resolution of the ERA5 data, we presently see no strong reasons to suspect otherwise. While progressing along its track between the main output locations the vessel experiences increasing wind speeds. This is because of two reasons: 1) the overall wind speeds are still gradually increasing in time and 2) at the same time the vessel moves into the eastern area with slightly higher wind speeds.

5.1.3 Waves

Conditions considered by the vessel along the track

The wave conditions experienced by the MSC Zoe are shown in Figure 5.3. The values for H_s (top panel) and T_p (middle panel) increased as the vessel made its transit along the shipping channel. The bottom panel of this figure shows that the wave direction experienced by the vessel was rather constant at 330º (coming from).

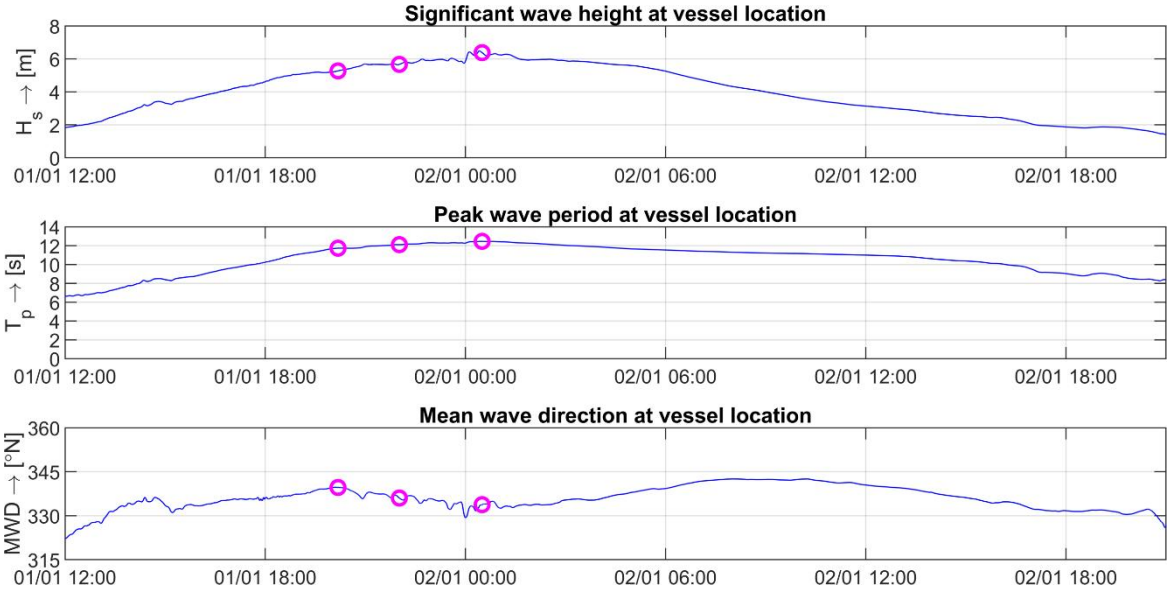

Figure 5.3 Timeseries of wave conditions experienced by the MSC Zoe.

Table 5.3 summarises the following wave parameter values for the four main output locations:

- significant wave height, H_s in m,
- maximum wave height[25], H_{max} in m,
- crest height of maximum wave[26], h_{cr} in m,
- trough depth of maximum wave, h_{tr} in m (= H_{max}-h_{cr}),
- peak wave period, T_p in s,
- spectral wave period, $T_{m0,1}$ in s,
- spectral wave period, $T_{m0,2}$ in s,
- spectral wave period, $T_{m-1,0}$ in s,
- peak wave length, L_p, in m,
- mean wave direction, MWD in °N (coming from),
- one-sided directional spread of the waves, σ in ° and m-power ($\cos^m(\theta)$), and
- peak enhancement factor of a JONSWAP spectrum[27], γ: Pierson Moskowitz spectrum corresponds to γ = 1 (i.e. fully-grown sea state) and standard JONSWAP to γ = 3.3 (i.e. young sea state).

Table 5.3 Wave parameters at the four considered output locations derived from the computed 2D wave spectra by SWAN for the respective selected moments in time.

Loc. ID + *Time*	H_s [m]	H_{max} [m]	h_{cr} [m]	h_{tr} [m]	T_p [s]	$T_{m0,1}$ [s]	$T_{m0,2}$ [s]	$T_{m-1,0}$ [s]	L_p [m]	MWD [°N]	σ [°] (m [-])	γ [-]
1: *1-1-19 20:00*	5.23	9.59	6.48	3.11	11.77	9.07	8.36	10.20	153	340	20.93 (6.2)	1.15
2: *1-1-19 22:00*	5.66	10.50	6.74	3.76	12.10	9.40	8.69	10.51	172	336	22.55 (5.2)	1.40
3: *2-1-19 00:00*	6.46	11.53	8.25	3.28	12.43	10.03	9.33	11.08	164	333	23.77 (4.6)	1.67
4: *2-1-19 00:00*	6.37	11.84	7.09	4.75	12.25	9.54	8.88	10.57	196	336	23.48 (4.7)	1.53

The significant wave height experienced by the vessel increases from 5.23 m (Location 1) to 6.46 m (Location 3), with peak wave periods ranging from 11.77 s to 12.43 s. The spectral wave periods ($T_{mx,x}$, see Footnote 10 on page 13) show approximately the same range of values for the different locations, indicating that the shape of the spectrum is not significantly changed. The spectrum mostly shifts along with changes in T_p. The MWD is fairly constant and practically speaking remains unchanged over the considered locations, i.e. the difference falls within a typical wave model resolution required for an accurate description of wave conditions (Section 4.3.2). Based on the values found for the peak enhancement factors at the four locations (between 1-2), it is concluded that the sea states at the main output locations can be considered as near fully-grown[28]. The inequality between the crest heights and relatively small trough depths of the maximum waves (i.e the value for h_{cr} is larger than for h_{tr}) indicates that non-linear shallow-water effects have influenced the waves. This causes a steepening of the

[25] *The maximum wave height (H_{max}) is defined as the largest individual wave height in 1,000 waves (H0.1%) during a given sea state (characterized by the representative wave height H_s). To determine this H_{max} we have used a wave distribution proposed by Wu et al. (2016), which is referred to as the 'LOWISH distribution'.*

[26] *The extreme crest height (h_{cr}) of the maximal wave height, is determined using the Rienecker-Fenton wave theory (Rienecker and Fenton, 1981).*

[27] *Based on a least-square fit of the 1D representation of the spectra calculated by SWAN with the 1D JONSWAP spectrum function (see also Section 6.1).*

[28] *Fully-grown sea states, or saturated or mature seas, typically show peak enhancement factors of around 1.*

crests and a reduction (and stretching) of the troughs, whereas for deep-water linear waves the crest height and the trough depth would be equal, as illustrated in Figure 5.4.

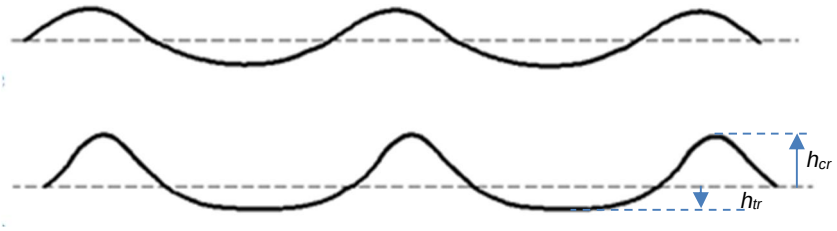

Figure 5.4 Schematized typical wave shapes of deep (top) and shallow water waves (bottom). For shallow water waves (or very nonlinear deep-water waves), the crest height h_{cr} is larger than the trough depth h_{tr} as illustrated in the bottom panel.

Table 5.4 presents an overview the magnitudes of different wave energy dissipation effects at the four considered main output locations for the exact moment in time at which the ship was at that location (Locations 1 to 3) or for the moment in time of the maximum of the storm at that location (Location 4). The total amount of wave energy dissipation is split up in three considered types of wave energy dissipation (cf. Figure 5.5): dissipation by white-capping (steepness-induced breaking), by bottom friction and by surf breaking (depth-induced breaking). For each of the types of dissipation, the percentage of the total is also presented in the table cells in parentheses. From Table 5.4 it is concluded that at the considered locations and moments in time the dissipation of wave energy by surf breaking (depth-induced breaking) is very small, with only at Location 3 a practically significant effect found of around 5% of the total dissipation. This coincides with the peak of the storm (and the highest total dissipation of wave energy found at the four output locations).

Table 5.4 Wave energy dissipation at the four considered output locations computed by SWAN.

Loc. ID + *Time*	Total dissipation [W/m^2]	Dissipation by white-capping [W/m^2] (steepness-induced breaking)	Dissipation by bottom friction [W/m^2]	Dissipation by depth-induced breaking [W/m^2]
1: *1-1-19 20:10*	3.4 (100%)	1.9 (55.27%)	1.5 (44.65%)	0.0 (0.08%)
2: *1-1-19 22:01*	3.2 (100%)	1.9 (61.51%)	1.2 (38.49%)	0.0 (0.00%)
3: *2-1-19 00:30*	5.6 (100%)	2.8 (51.09%)	2.4 (43.29%)	0.3 (5.62%)
4: *2-1-19 00:00*	3.3 (100%)	2.5 (76.71%)	0.8 (23.29%)	0.0 (0.00%)

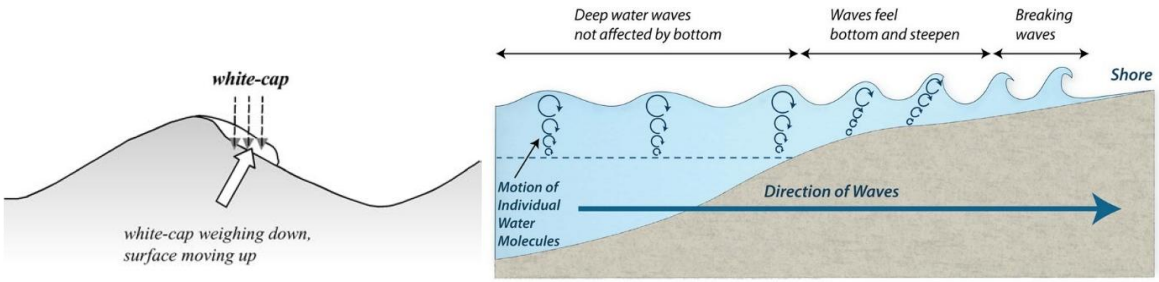

Figure 5.5 Visualisation of three dissipation mechanisms for waves. Left panel: White-cap at the lee-wind side of the crest of a steepness-induced breaking wave (source: Figure 6.25 of Holthuijsen, 2007). Right panel: bottom friction and depth-induced breaking of waves nearshore.

Figure 5.6 shows the time series of the total wave energy dissipation in the wave field experienced by the MSC Zoe and of the three dissipation mechanisms separately. The total level of energy dissipation increases up to the moment of the peak of the storm, as can be generally expected. For the most part white-capping occurs and energy dissipation by bottom friction. Very limited dissipation due to depth-induced wave breaking occurs, and only around the peak of the storm. That type of breaking would manifest itself as spilling, overtopping wave crests, similar to what is observed (on a smaller scale) at the beach. However, please note that the absolute and relative levels of this dissipation process are rather low, so this may correspond to only a few individual wave crests, and possible very intermittently.

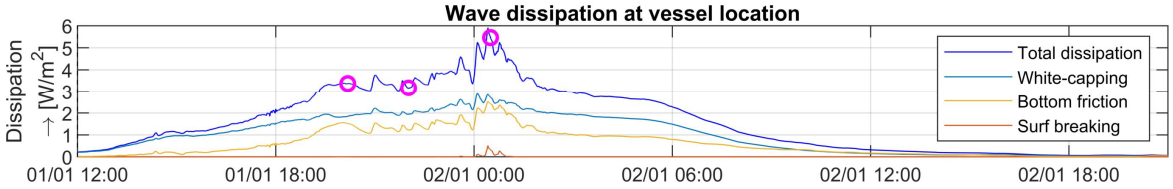

Figure 5.6 Timeseries of wave energy dissipation experienced by the MSC Zoe.

Because of the spectral description of the numerical wave model this overall (spectrally-lumped) ratio of dissipation mechanisms can be determined efficiently. When translated back to wave signals in time (individual waves experienced by the vessel) it may be that some of the modest dissipation effects found may be linked to only a few wave crests in a sea state. Therefore, these results do not necessarily imply that a dissipation mechanism will have been present continuously and with equal strength as part of that sea state.

Spatial variations in wave conditions in the area

Appendix B.3 provides spatial plots of H_s and T_p for the moments in time that the vessel was at the main output locations. These plots indicate that the wave heights and wave periods in the area were quite uniform and that changes in these parameters were mainly caused by the progression of the storm in time and to a much smaller extent the progression of the vessel along its track.

5.1.4 Bed level and under keel clearance

The top panel of Figure 5.7 presents the bed levels along the sailed route of the MSC Zoe, relative to MSL. As discussed in Sections 3.2 and 3.3, this route (Figure 3.1) includes two shallow parts: north of Terschelling and north of Borkum (Germany). Main output Locations 1 and 3 correspond to these shallow sections. The bottom panel of Figure 5.7 presents the under-keel clearance as registered by the vessel averaged over 1 minute (in red) together with an approximated under-keel clearance as derived from post-processing the model data (in blue). The latter is determined by subtracting the reported mean vessel draft of 12.41 m (as registered at departure) from the modelled water depth (see Figure 5.1). The agreement between the two lines is generally excellent, even though this comparison only considers the average vessel draft (measured close to the centre line of the vessel) and does not account for:

- squat (i.e. the effect that the vessel sinks deeper in the water than its static draft due to its forward speed),
- the exact location of the depth sensor on the vessel,
- eventual changes in draft (loss of containers) and
- motions of the vessel in waves[29].

[29] *The 1-minute average filter applied to the measurement data for plotting visibility purposes is expected to have removed most of the effects of motions of the vessel in waves.*

Based on the comparison of the measured and modelled under-keel clearances, it is concluded that the bathymetry data used to set up the numerical models is still up-to-date and of high accuracy. Furthermore, the comparison supports the validation of the modelled water levels as presented in Section 4.1.2.

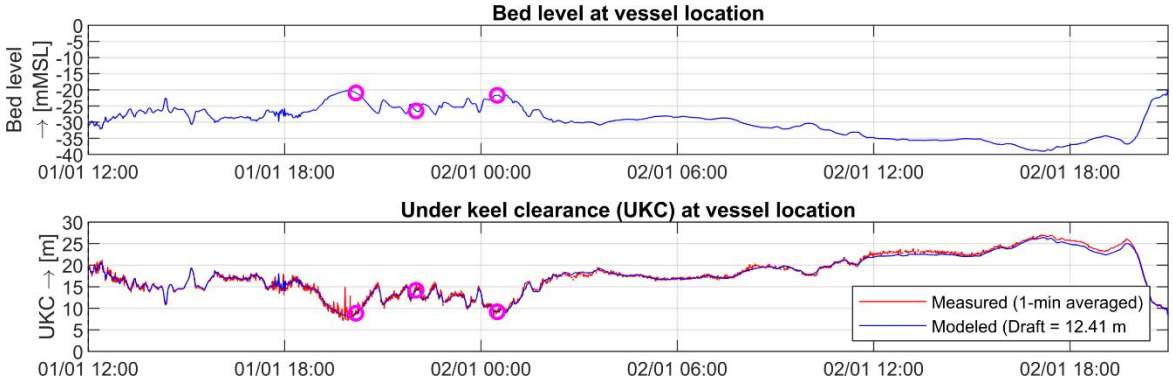

Figure 5.7 Timeseries of the bed level at the location of the MSC Zoe (top panel) and measured and modelled under keel clearance (UKC, bottom panel).

We expect that the large-scale morpho-dynamics of the bed in the area of interest are rather small, given that the bathymetric data available consists of a mix of recent and older sources, while still giving a good agreement with measurements. This hypothesis is supported by Deltares (2011), which included an evaluation of the hydrographic survey policy of the Netherlands Hydrographic Office. Information on bed levels of different years were inter-compared to assess the variability of the sea bed level over time. From this it was concluded that the temporal variability of the bathymetry along the Dutch northern sailing routes was small.

The smallest registered and modelled under-keel clearances are occurred around Location 1, north of Terschelling. The smaller water depth available at that location and on that moment in time is mainly the result of the high bed level at that location, and to a lesser extent the water level at that time. It should be noted that the available water depth could have been even lower if the vessel would have arrived at this location four hours later, considering that the water level was still falling (ebb phase, see Figure 5.1).

The tidal water level reached its lowest point around the time that the vessel arrived at Location 3 (north of Borkum, Germany), resulting in again an area with relatively small water depths. In this case this was largely the result of the lower water level present at that time and to a smaller extent the local bed level.

5.2 Return periods of metocean conditions

The metocean conditions experienced by the MSC Zoe have been assessed and discussed in Section 5.1 as part of Tasks 1.1 and 1.3 (from the Scope of Work described in Chapter 2). In this section we cover Task 1.2 and we assess how unique those conditions were and how often one can expect such conditions to occur in this area. As introduced in Section 2.2.2, first statistical descriptions of the local conditions will be are derived, which will serve as a statistical reference to which the results during 1-2 January 2019 will be compared. The outcome will indicate the probability of those conditions occurring again.

5.2.1 Approach

This section summarises the approach to derive the reference statistical descriptions of metocean conditions in the studied area. For a detailed general description of how such analyses are generally performed the reader is referred to Van Os and Caires (2011).

Local statistical descriptions of the wind and wave conditions in the area were derived via an Extreme Value Analysis (EVA, described in more detail below), which requires a high-quality long-term data source for accurate results. Generally, two options are available for selecting input data for this type of analysis: 1) measured data or 2) numerically generated data. In the area of interest, several measurement locations are available for which 10 year of measurement data is available (see Chapter 3). ECMWF's ERA5 reanalysis database provides 40 years of high-quality numerical data for the complete area of interest. As the smallest uncertainty in return values are found when the longest available data source is used for an EVA, the ERA5 database was selected as input for the analyses. Given that the spatial variation of the metocean conditions in the area of the critical section of the shipping route proved limited (Section 5.1), it was decided to perform the EVAs for one location, considered representative for the area studied. The location of Platform L91 has been selected for the analysis, since it is quite centrally located in the area, in between the southern and northern sailing routes north of the Wadden Islands (see e.g. Figure 3.6). Selecting one of the measurement stations as reference location for this statistical analysis also allows for a validation of the long-term numerical dataset, prior to that being used as input to the EVAs, by comparing it to the shorter measurement dataset at that observation location.

EVAs have been made for the wind and wave conditions. These parameters are expected to have influenced the vertical motions of the MSC Zoe predominantly. EVAs were not made for the water level and of the flow velocities as experienced by the vessel. This is because those were not extreme, with a water level at around MSL and depth-averaged current velocities of approximately 0.5 m/s (1 knot). They are quite common, occurring even daily. Furthermore, they may have had only little event-specific influence on the MSC Zoe.

To validate the accuracy of the ERA5 numerical database the values from that dataset were compared to the measured values at LP91. The modelled interval of 40 years encompasses the 10-year interval of measurement data, so the corresponding interval was selected from the numerical database to make the comparison. The results of these comparisons and the outcomes of the EVAs are presented in Section 5.2.2 (wind conditions) and 5.2.3 (wave conditions).

The statistical EVAs performed were all made using the metOcean data tRansformation, Classification and Analysis tool ORCA[30] of Deltares (Van Os and Caires, 2011). In all cases, the POT-GPD method was applied for performing the EVAs. This means that the Peaks-Over-Threshold (POT) approach was applied to select the events above a certain threshold value as input to further analysis. To ensure that independent high events are selected, values above the applied threshold less than 48 hours apart are considered to belong to the same storm and only the maximum value within that time frame is selected. A Generalised Pareto probability Distribution (GPD) was fitted to the values selected via POT. The GPD is a statistical probability distribution that is particularly suitable to describe extreme conditions such as studied here (Van Os and Caires, 2011). Using the longest dataset available (40 years) means that this fit can be made as reliably as possible. The resulting fitted distribution is then applied to derive

[30] https://www.deltares.nl/en/software/orca/

extreme values for different return periods, or conversely look up return periods corresponding to a given condition that has occurred (the latter is the application used here)[31].

5.2.2 Wind conditions

Validation of the ERA5 dataset for wind

Figure 5.8 presents scatter plots with the comparison of measured wind conditions (speed and directions) at the location of platform L91 to the corresponding modelled wind parameters from ERA5 for that location. The data in the plot covers approximately ten years (2010 – time of reporting in 2019). From these scatter plots it is observed that the modelled wind is highly correlated with the measured wind and shows relatively little scatter in the data. Please note that the wider spread of yellow squares represents very limited data occurrences relative to the warmer colours. The fact that the fitted relation almost follows a 1:1 relation (the diagonal dashed black line in each panel) is a confirmation of this. Based on these plots, it is concluded that the ERA5 timeseries of wind conditions are accurate and that they are suitable as reliable input to the EVA of wind conditions.

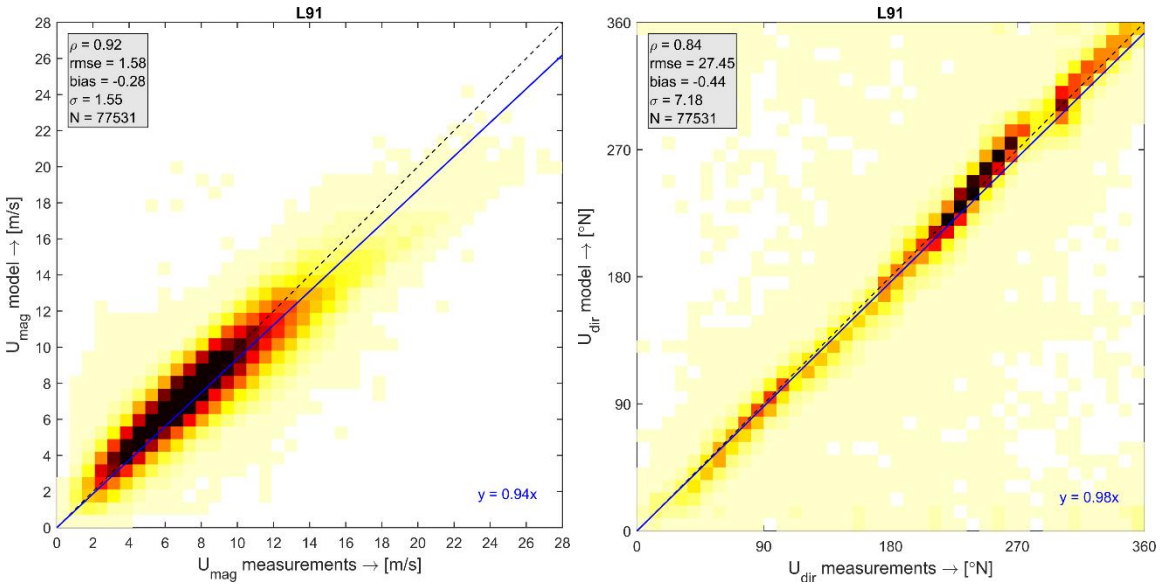

Figure 5.8 Scatter plots of wind speed (left panel) and direction (right panel) measurements against numerical model data (ERA5) for platform L91 for the period of 2010-2019. The coloured squares, ranging from yellow (low density) to black (high density), indicate the data density (i.e. how many instances) at each point in the scatter plot. Both panels include information on error statistics (grey box in top left corner) and an origin-crossing linear fit (blue line + the relation given in the bottom right corner).

Maximum wind condition during the event

Table 5.5 presents the maximum wind speed (and corresponding wind direction) that occurred during 1-2 January 2019 at Location L91, as calculated by the atmospheric model of ERA5. The timestamp of this value in the dataset is 02-01-2019 00:00, which corresponds to the timestamp of maximum wind as experienced by the MSC Zoe along its track (see Section 5.1.2). This further supports that Location L91 is a representative location to consider

[31] *Note that the return values presented here are solely intended to determine the probability of occurrence of the conditions as experienced by the vessel. The values are not intended and should not be used as (design) values for any other purposes.*

for this analysis, whereby comparing observations to statistical information for the same location.

Table 5.5 Maximum wind speed value during 1-2 January 2019 at platform L91 from ERA5.

Timestamp	U_{mag} [m/s]	U_{dir} [°N] (coming from)
02-01-2019 00:00	17.40	345

Extreme statistics and return period of the wind condition of 1-2 January 2019

Figure 5.9 presents the return value plot for wind speeds resulting from the EVA. The stars in this type of figure indicate the set of values selected from the input data series using the POT approach. The solid black line is the statistical distribution fitted through those data points. The top left box shows the main estimated return values according to the solid black line (commonly referred to as 'point values') for 1, 2, 5, 10, 20, 50 and 100 years. The box insert includes between brackets the values that define the 95% uncertainty bands around the main (or point) extreme value estimates. Note that with longer return periods the uncertainty bands become wider as those values are more difficult to derive reliably from the given duration of the input data series.

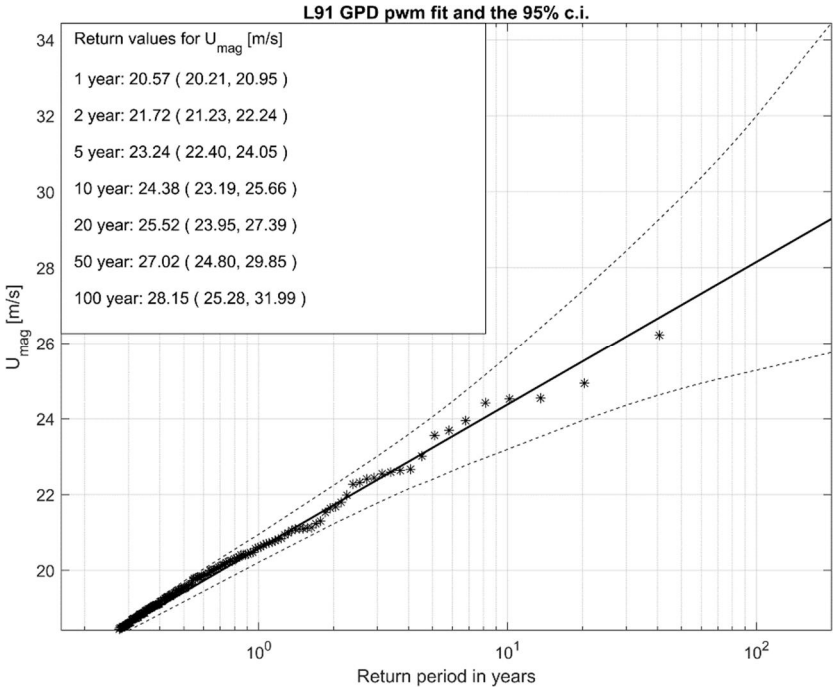

Figure 5.9 Return value plot for the wind speed at 10 m height, U_{mag}, at the location of platform L91.

Comparing the wind speed value of Table 5.5 with the return values of Figure 5.9 shows that that the return period of the highest wind speed as observed during the 1-2 January 2019 event is less than 1 year. This means that stormy conditions such as this are quite common and on average they can occur in any given year. Considering that the highest wind condition of 1-2 January 2019 is smaller than the lower edge of the uncertainty band for the 1-year return period, this outcome (return period for the wind conditions <1 year) has a high level of certainty. Wind speeds lower than the maximum that occurred on these days will occur even more often.

The considered 40-year dataset also provides information on wind directions in typical storm conditions and seasonal variation of wind speeds throughout the year. During most severe wind conditions, wind directions are typically coming from southwest to northwest. But also, when

only considering north-westerly wind directions, the wind conditions as experienced by the vessel during the 1-2 January 2019 event still corresponds to a return period of less than 1 year. Figure 5.10 shows the seasonal variation of wind speed values corresponding to a 1-year return period. As can be expected, the highest wind speeds typically occur during the autumn and winter.

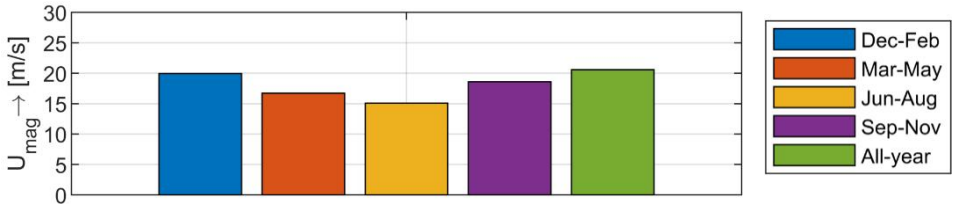

Figure 5.10 Seasonal variation of the 1-year return period value for wind speed at 10 m height, U_{mag}, at the location of platform L91.

5.2.3 Wave conditions

Validation of the ERA5 dataset for waves (H_s and T_p)

For analysis of T_p the first 5 years of measurements (2010-2014) were discarded from the comparison as the measurements from that period showed large deviations and clear data errors. Measured values of T_p from 2015 onwards were considered reliable (Figure 5.11) and were considered in the validation. For H_s the full period of available wave measurements (2010-2019) was used for the validation of the ERA5 data.

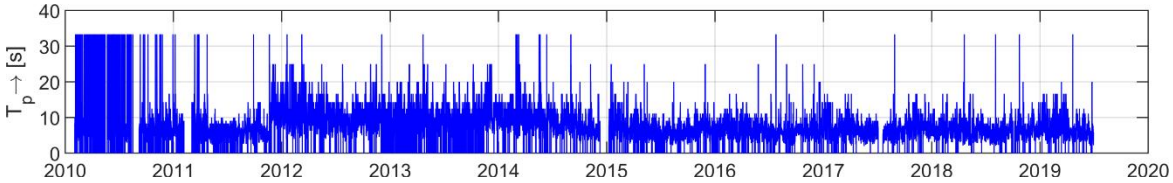

Figure 5.11 Measured timeseries of T_p at platform L91.

Figure 5.12 presents scatter plots of wave measurements (H_s and T_p) at the location of platform L91 compared to the modelled wave parameters of the ERA5 dataset at that location for the corresponding moments in time. Note the smaller number of samples (N) available for the validation of T_p, which is the result of the shorter time series with reliable measurement data of that parameter. This figure shows that the modelled values of both these parameters are highly correlated to the measured values and that they show relatively little scatter (highest densities of data points observed along the line for which the measurements are equal to the modelled values). Please note that the wider spread of yellow squares represents very limited data occurrences relative to the warmer colours. Based on these plots, it is concluded that the ERA5 timeseries of H_s and T_p are accurate and that they are therewith suitable as reliable and accurate input to the EVAs of those parameters.

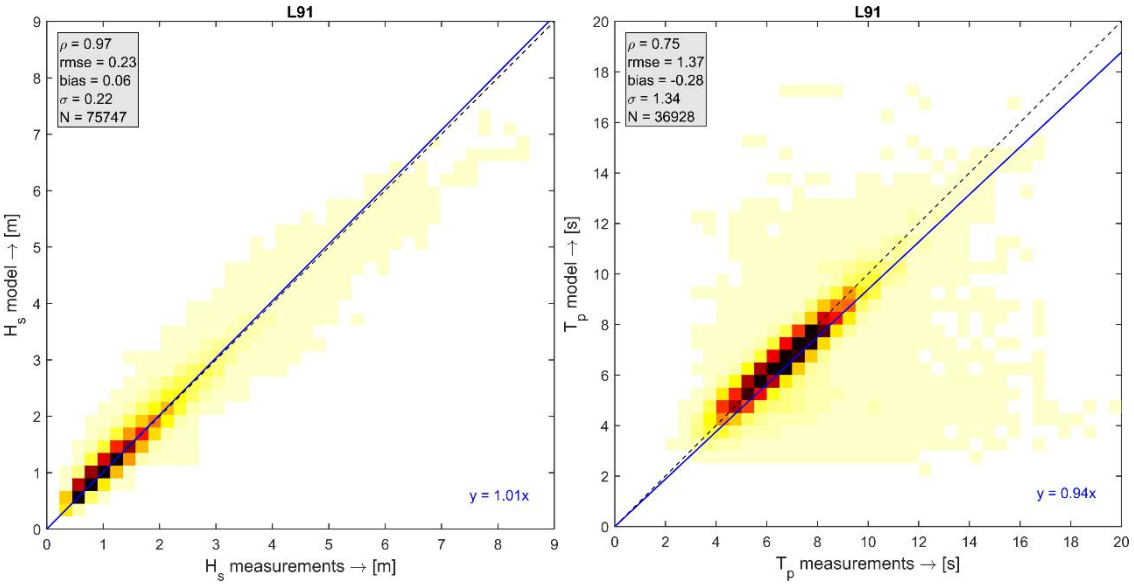

Figure 5.12 Scatter plot of measured and modelled (ERA5) H_s and T_p for the periods of respectively 2010-2019 (N=75747) and 2015-2019 (N=36928). The coloured squares, ranging from yellow (low density) to black (high density), indicate the data density in the scatter plot. All panels include information on error statistics (grey box in top left corner) and an origin-crossing linear fit (blue line + the relation given in the bottom right corner).

Maximum wave conditions during the event

Table 5.6 presents from the output of the wave model of ERA5 the maximum H_s and corresponding T_p (which is also the highest T_p that occurred during these days) for Platform L91 of 1-2 January 2019. The timestamp of this value is 02-01-2019 00:00, which corresponds to the timestamp of maximum waves along the sailed track of the MSC Zoe (see Section 5.1.3), as was the case for the wind conditions. Values from the ERA5 dataset for the event of 1-2 January 2019 are considered here to ensure a consistent comparison of the wave conditions on those days with the reference statistics derived using the same data source. The good agreement between measured data and the ERA5 data further supports this approach.

Table 5.6 Maximum H_s and T_p values during 1-2 January 2019 at platform L91.

Timestamp	H_s [m]	T_p [s]
02-01-2019 00:00	5.37	11.55

Extreme statistics and return period of the wave conditions of 1-2 January 2019

Figure 5.13 and Figure 5.14 present the return value plots for respectively H_s and T_p resulting from the EVAs. The top left boxes show the return values of the wave parameters for 1, 2, 5, 10, 20, 50 and 100 years (point values). The values between brackets indicate the 95% uncertainty bands around those main estimates. Comparing the values of Table 5.6 with the return values of Figure 5.13 and Figure 5.14, it is concluded that the return periods of the wave conditions that occurred on 1-2 January 2019 are smaller than 1 year. This means that they correspond to quite common storm conditions, considering that on average they can occur yearly. Since the local (storm) wave conditions will be highly correlated to the local wind conditions, it is logical that a similar return period is found for the wave conditions as was found for the wind conditions (Section 5.2.2).

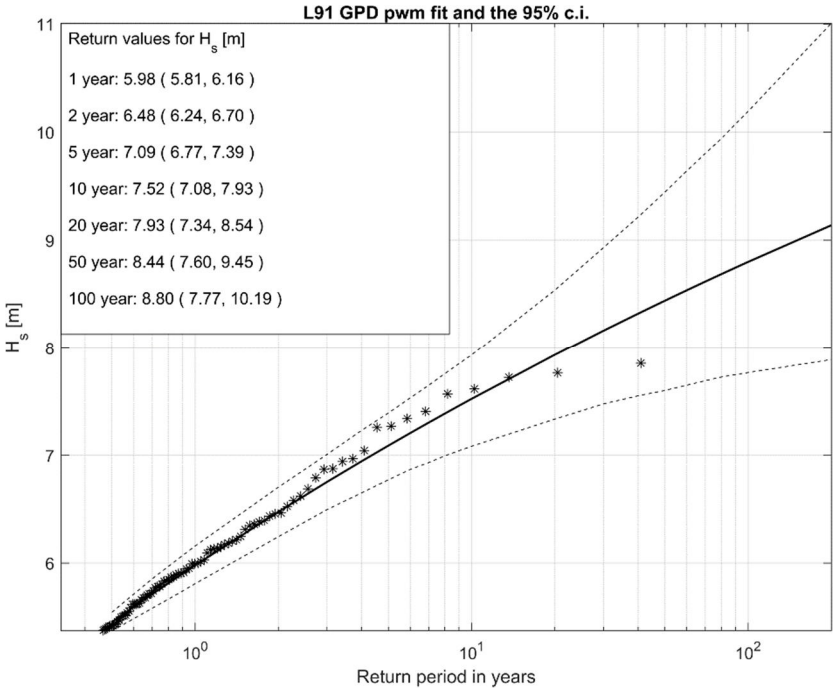

Figure 5.13 Return value plot for significant wave height, H_s, at the location of platform L91.

Considering that the highest wave conditions of 1-2 January 2019 (H_s and T_p) are smaller than the lower edge of the uncertainty band for the 1-year return period, this outcome (return period for H_s and T_p <1 year) has a high level of certainty. Note also that the underestimation in wind conditions (Section 4.2.2) will not influence these statistical outcomes, since a relative interpretation is made and the discrepancies in wind information will have affected all considered locations.

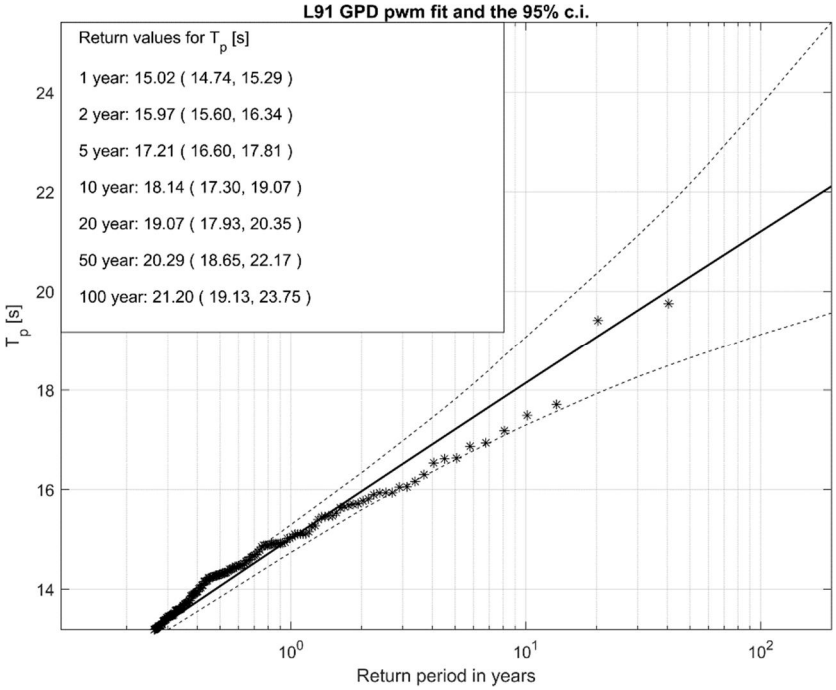

Figure 5.14 Return value plot for peak wave period, T_p, at the location of platform L91.

When considering the directional dependency of the wave conditions at the location of platform L91, analysis shows that the highest waves typically come from W to NW direction. Although also south-westerly storms may have similar wind speeds and frequency of occurrence as the north-westerly storms occurring at that location, these storms with a south-west wind direction do not lead to the highest wave conditions. This is because for wind directions coming from the north-west a much longer fetch (area over which wind the wind blows) is available for the waves to build up.

Figure 5.15 shows the seasonal variation of wave height and wave period values corresponding to a 1-year return period. In agreement with the trend as found for wind speed, the highest wave conditions, with the highest wave periods, typically occur during the autumn and winter.

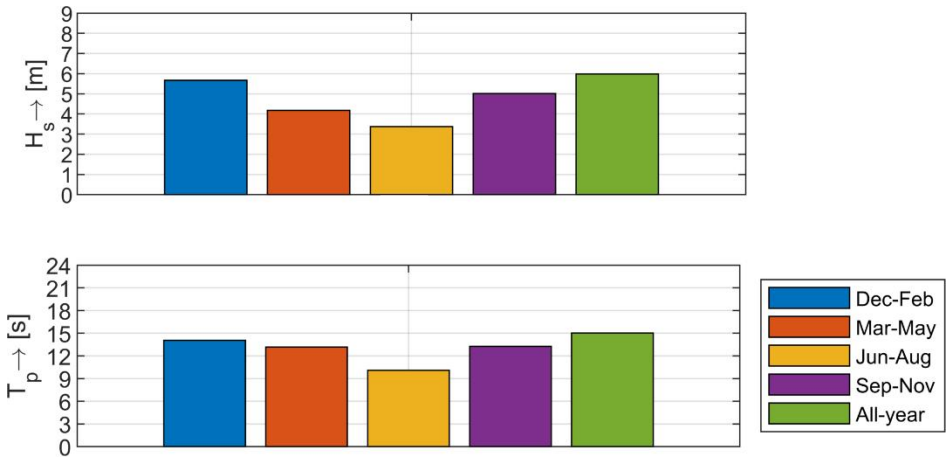

Figure 5.15 Seasonal variation of the 1-year return period value for significant wave height H_s and peak wave period T_p at the location of platform L91.

5.3 Discussion

The analyses presented in this chapter show that the storm conditions that occurred on the North Sea on 1-2 January 2019 north of the Dutch Wadden Sea Islands were not very extreme or exceptional. Table 5.7 summarises these conditions and their expected return periods, collected from the previous sections. These results indicate that conditions such as those during 1-2 January 2019 will occur in this area quite frequently and that the probability of similar conditions occurring there again is rather high. These conditions are most likely to occur during the storm season in the Netherlands, which generally runs from October to April.

Table 5.7 Overview of most severe metocean conditions experienced by MSC Zoe on 1-2 January 2019 (numerical model outcomes).

Parameter	Representative value (range) along the track of the ship on 1-2 January 2019	Frequency of occurrence, exceptionality
Current speed	up to 0.5 m/s (1 kn)	Very common, occur daily
Water level	MSL + 0 m – MSL + 1 m	
Wind speed	16 – 18 m/s	Are exceeded on average one to two times in a year
Spectral wave height (H_s)	5 – 6.5 m	
Spectral wave period (T_p)	11 – 13 s	

Depth-averaged flow velocities in the critical track section were in the order of 0.5 m/s (1 kn), which is a typical tidal flow magnitude that generally occurs daily. The flow was directed approximately to the west, corresponding to a counter current for the eastward-bound vessel.

Given that the wave direction was approximately perpendicular to the flow direction, no strong wave-current interactions will have occurred. And seeing that the incoming wave directions were approximately perpendicular to the vessel heading, wave encounter frequencies for the vessel will not have been influenced by the forward speed of the vessel. If those interactions would have occurred, then they otherwise may have complicated the influence of the waves on the vessel. The absence of these types of interactions is expected to be generally the case in this area, given typical (north)western storm conditions influencing this area most and the east-west orientations of the main shipping routes there.

The conditions derived in previous sections indicate that the vessel will have experienced waves that exhibit steepened wave crests and flattened troughs. This could be consistent with what mariners call ground seas (‘grondzee’, Section 3.2). The influence of the shallower depths has not been large enough to result in strong depth-induced wave breaking, but the steepened crests will have shown significant white-capping. Only at Location 3 a small amount of depth-induced wave-breaking dissipation was present around the peak of the storm, indicating that in that situation the highest waves present in the sea-state will likely have shown a more complicated breaking behaviour compared to the other considered locations. Similar wave conditions will also occur elsewhere on the North Sea, but north of the Wadden Islands they happen to occur together with unfavourable wave directions relative to the heading of the vessel (beam-on waves) and with a larger vessel traffic intensity. This potentially leads to hindrance.

The metocean conditions in the area were found to be quite uniform. As a result, the highest conditions at Location 4 do not differ strongly from those that occurred at the three main output locations along the southern sailing route (cf. Figure 5.16). At Location 4, at the northern sailing route, the difference between the crest height and trough depth of H_{max} is smaller than at the other 3 locations, but still also there h_{cr} is larger than h_{tr}, indicating that shallow-water effects are also present there, but less strong. In principle this may indicate that the wave conditions along the northern route would have been less disadvantageous for the vessel, but at Location 4 the intensity of white-capping is larger than at Location 1 and 2. It is relatively large because due to the larger water depth bed friction has a smaller influence, but it is also larger in absolute sense compared to the white-capping dissipation levels at the other two locations. This shows that further analyses are required to reach definitive conclusions on recommendations or preferences for sailing routes related to specific wave conditions. An important factor in such an assessment will be the larger water depths available along the northern route, which could mean around 10-15 m more under-keel clearance compared to the shallowest sections of the southern sailing route.

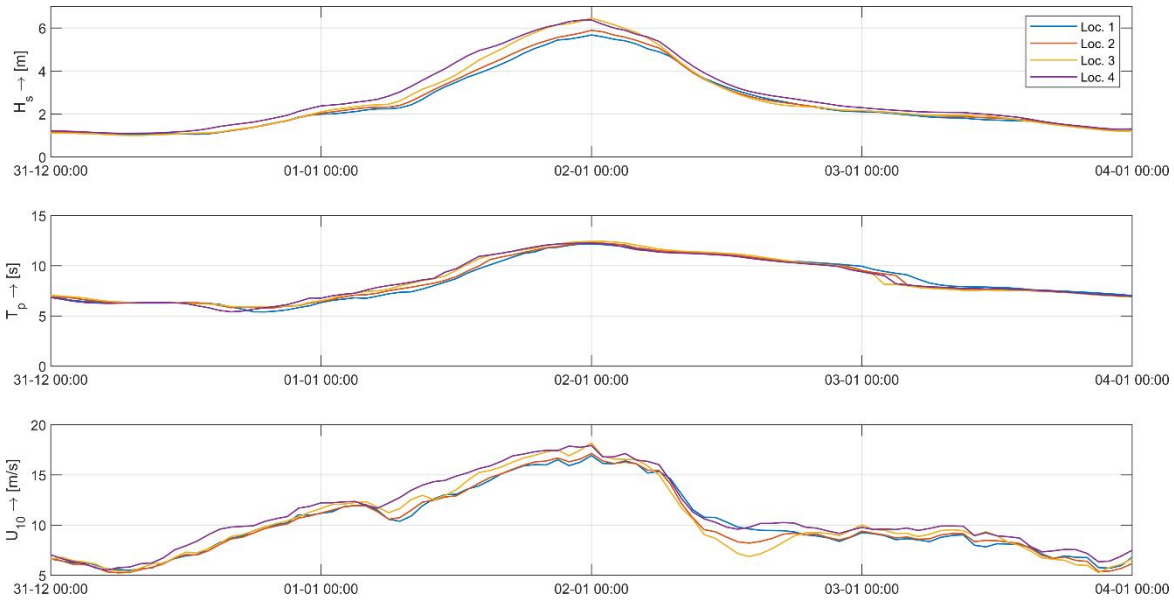

Figure 5.16 Timeseries of significant wave height (H_s, top), peak wave period (T_p, middle) and wind speed at 10 meter height (U_{mag}, bottom) at the four considered output locations.

It will be important in the scale model of MARIN to represent the different available water depths, and resulting under-keel clearance values, particularly considering that a vessel can encounter higher waves in a sea state than the value of H_s (see the H_{max} values in Table 5.3).

6 Translating metocean conditions to test conditions

6.1 Recommended metocean conditions for use in scale model tests by MARIN

Relevant water depths were provided to MARIN in the form of Table 5.1, on Page 36 of this report. Information on current magnitudes and directions included in that table was also shared. This current information was applied by Deltares in the numerical wave modelling performed (Chapter 4). Results from those calculations indicated that little wave-current interactions will have occurred, given that the flow directions were mostly perpendicular to the main directions of the waves (Section 5.1.1). This is one of the reasons why currents were not generated directly in the scale model tests but considered in another way. The effect of the (fairly constant) counter current on the vessel moving through the water was mimicked in the scale model basin by increasing the targeted speed of the vessel with the current magnitude (+ 1 kn), leading to the same vessel speed relative to the water.

Table 5.2 (see Page 37) summarizes the wind conditions that occurred at the focus locations at the time that the vessel passed there (or at the time of the peak of the storm for Location 4). Although this information was used in the study tasks by Deltares, wind conditions were not part of the scale model tests performed by MARIN.

The basis for the information on wave conditions provided by Deltares to MARIN is Table 5.3, included on Page 38 of this report. For those locations and time stamps Deltares generated 2D wave spectra from the SWAN model as one of their main project deliverables. The top left panels of the figures included in Appendix C depict these spectra, showing at which frequencies (wave periods) and from which directions wave energy reaches a considered location.

At the request of MARIN, the 2D wave spectra from SWAN have been approximated using standard formulations in frequency (JONSWAP) and direction, whereby applying scaling (fitting) parameters to match the targeted 2D spectrum. To meet this request, parameterised spectra have been fitted by Deltares using a least-squares estimate, which seeks to minimise the difference between the targeted shape and the approximation, whereby putting more weight on larger deviations. The top right panels of Appendix C show the outcomes of such an approximation in 2D (i.e. a parametrized 2D JONSWAP spectrum), for comparison to the original spectra in the top left panels of these figures. The bottom panels in that appendix show for each location the same spectra as in the two top panels, only now projected onto 1 dimension, either frequency or direction (with information in the other dimension of the 2D spectrum lumped). These two lower panels show that at some of the considered locations deviations are present in the parameterised spectra compared to the original spectra from SWAN, particularly within the directional distribution. However, for practical applications these deviations are expected to be sufficiently small, especially considering that typical, representative wave conditions will be considered in the scale model tests (Section 2.3.1). MARIN is recommended to use the original full 2D spectra from SWAN for defining the wave conditions in their scale model basin, or otherwise the fitted parameterised spectral descriptions that were provided to them by Deltares on their request as an additional service.

In a meeting on 19 August 2019 experts of Deltares and MARIN discussed the information on metocean conditions as determined by Deltares from their computations and analyses. Deltares contributed to the discussion on selecting the conditions to be modelled in the scale model basin. To cover the uncertainties in the numerical modelling, Deltares recommended to

include in the test series also tests with 10% enhanced values for H_s and T_p values increased by 2 s (Section 4.4).

Following the meeting of 19 August 2019, the experts of the physical test facilities at MARIN have used the information provided by Deltares to set up their tests within the basin following their selected approach. This included translating the (parameterized) spectral wave information from the numerical model into time series and selecting the most relevant section from that time series to be considered for the tests with a forward moving vessel in the basin (described in a separate research report). Additional information on non-linear effects in the wave fields present during storm conditions in the area were also considered.

6.2 Wave field complexities

The interpretation of complex wave phenomena that may have occurred in the wave fields during the event of 1-2 January 2019 have been discussed as part of Chapter 4, describing the numerical wave modelling, and Chapter 5, considering the conditions as encountered by the MSC Zoe and the spatial and temporal variations in conditions.

Multiple wave phenomena typically occur in the area north of the Wadden Islands during storms that will enhance the complexity of wave fields. Examples of these are shallow-water effects and breaking of waves. Such phenomena lead to non-linear wave behaviour, including enlarged crest heights and flattened troughs, which can have a different impact on a vessel than linear waves (with crests and troughs of equal size, each half of the total height of a wave). To some extent these phenomena will be present during every (significant) storm event, but the severity of the resulting wave conditions will depend on the strength of the storm and on the heights and periods of the waves generated. The resulting wave fields can be well described by often-applied and proven spectral numerical wave models such as applied in this study (SWAN).

The storm conditions on 1-2 January 2019 resulted in one main wave system approaching the Dutch coastline. The conditions included saturated (almost) fully-grown sea states without additional complexities such as multiple wave systems, that may have otherwise led to double-peaked wave spectra. The single-peaked wave spectra as occurred during the considered storm can be approximated accurately by standard spectral shapes in frequency and direction, which could then be used to steer the wave machines in the laboratory basin, as an alternative to considering the full 2D spectra from SWAN.

If the wave conditions generated by the wave makers in the basin of MARIN will match adequately the wave parameters as they occurred in the field, combined with representative shallow water depths, then the natural behaviour of the waves in the model basin should show the same (complex) wave phenomena. This behaviour will then 'automatically' lead to similar complexities occurring in the wave field as generated in the laboratory wave basin as they did in the field. Verifications of this expected result may include assessing whether spurious scale model effects remain sufficiently small relative to the natural wave behaviour modelled. Such spurious model effects can for example be related to the finite dimensions of the scale model basin compared to the large open sea area in reality, for example effects related to unintended reflections of waves from the scale model basin walls.

6.3 Verification of wave conditions as created in the scale model basin of MARIN

The time signals of waves measured by MARIN during the wave calibration tests performed in their basin (MARIN, 2019) have been delivered to and assessed by Deltares as part of Task 2.3 (from the Scope of Work described in Chapter 2). In this section the representativeness of the

wave conditions as generated in the basin of MARIN is verified by first processing the measured wave signals from a selection (subset) of the tests and comparing the outcomes to the targeted wave parameter values and spectra as prescribed at their wave maker (Section 6.3.1). Second, wave conditions as generated in the basin are compared to the SWAN spectra as presented in Appendix C for a smaller selection of conditions that are a direct representation of the conditions at two of the main output locations considered in earlier chapters.

6.3.1 Verification of wave conditions generated vs. prescribed

Based on the wave conditions provided by Deltares to MARIN and on the meeting of 19 August 2019, four main combinations of significant wave height (H_s) and peak wave period (T_p) were selected for which MARIN performed wave calibration tests with a duration of at least 3 hours. All combinations of H_s and T_p included the same JONSWAP peak enhancement factor ($\gamma = 1.5$). Three different ambient water depths (cf. Table 5.1) were considered in the tests by MARIN (d =21.3, 26.6 and 37.5 m). These depths were based on the water depths represented in the SWAN model at the main output locations during the 1-2 January 2019 event. For the most severe combination of wave parameters considered in the laboratory basin (H_s = 7.5 m and T_p = 14.5 s, in line with the recommendations in the last-but-one paragraph of Section 6.1), only the shallowest specific depth situation (d = 21.3 m) was included in the laboratory tests. In addition, MARIN considered deep-water conditions[32] for all combinations of H_s and T_p to serve as general analysis reference with all bed level influences removed. The different combinations resulted in a total of fourteen sets of H_s, T_p and ambient depth (see Table 6.1). Last, a long-crested (not including directional spreading) and a short-crested (including directional spreading, $\sigma = 21.2°/m = 6$) case was considered for each of the fourteen combinations, resulting in a total of 28 test conditions.

Table 6.1 Wave parameter combinations generated by MARIN for their scale model wave calibration tests. The combinations indicated with bold characters are analysed in this report. The tests indicated with bold red characters are a direct representation of the ambient conditions at two of the main output locations considered with SWAN (see Section 6.3.2).

T_p [s] / **H_s [m]**	**11.8**	**12.4**	**14.5**
5.2	X (***d = 21.3***, *26.6 and 37.5 m + deep*)		
6.5		X (***d = 21.3***, *26.6 and 37.5 m + deep*)	X (***d = 21.3***, *26.6 and 37.5 m + deep*)
7.5			X (***d = 21.3 m*** + *deep*)

Based on the available calibrated wave conditions, MARIN eventually selected a set of test conditions to perform the actual vessel motion tests with. Please refer to MARIN (2019) for the complete overview of tests performed and which test conditions have been selected for tests including the vessel.

[32] *Deep water means that the wave propagation and evolution is not influenced by the bathymetry. As a rule of thumb, this is the case when the water depth is more than half the wave length: d>0.5L.*

For the verification of the representativeness of the wave conditions as measured by MARIN, four test conditions are considered here, describing the most complex realistic cases (e.g. including shallow depths and directional spreading). This selection has been made since only those allow for a more direct comparison to the conditions as determined by Deltares. Other conditions have been added to the test program to cover a wider range of conditions or to analyse specific isolated vessel behaviour (such as under unidirectional waves). The analysed wave conditions include short-crested waves and the shallowest water depth (printed bold in Table 6.1 and summarized in Table 6.2). The verification made for this set of reference conditions is seen as an indirect verification of the other conditions generated by MARIN, which are considered variations of these reference conditions.

Table 6.2 Test input of considered scale model tests for verification analyses by Deltares.

MARIN run-ID	d [m]	H_s [m]	T_p [s]	MWD [°] (cartesian)	σ [°] (m [-])	γ [-]
007	21.3 m	5.2	11.8	270	21.2 (6.0)	1.5
008		6.5	12.4			
009		6.5	14.5			
010		7.5	14.5			

To verify the wave conditions throughout the basin, for each test the wave signals of four measurement probes spread out over a large extent of the basin area were considered: WAVE.CL, WAVE.9, W.SC2.CL and WAVE.7. Refer to Appendix D for the coordinates of the wave height probes as applied in the physical scale model tests by MARIN. Probes WAVE.9 and W.SC2.CL are situated along the sailing line over which the vessel was moving (parallel to the wave machine) in tests that included the vessel and therewith describe the spatial uniformity of the waves over the width of the basin[33]. Probes WAVE.CL and WAVE.7 do the same for the direction perpendicular to the wave machine. Note that the wave signal of WAVE.CL was used by MARIN to calibrate their wave conditions. That location is the focus point in the tests, it was where the vessel was positioned in the tests without forward vessel speed. Some deviations at the other locations in the basin generally may not be critical; here we consider the data from those other locations merely as a general check of (a proxy for) unexpected or unintended overall wave behaviour to the extent that such effects may influence the main central measurement locations.

The directional distribution was verified using the set of wave probes located at WAVE.SC1 (close to WAVE.CL). By considering wave height measurements from an array of specifically positioned probes the resulting set of time series can be used in a combined analysis to derive the directional spreading of the wave field[34].

For each of the tests of Table 6.2, a three-hour period was selected to be analysed as part of this assessment. Each signal was subsequently processed into a 1D frequency wave spectrum using the fast Fourier Transformation (FFT) technique. Based on these spectra a number of spectral wave parameters were determined (H_{m0}, $H_{m0,low}$, T_p, $T_{m0,1}$, $T_{m0,2}$ and $T_{m-1,0}$)[35] to establish and analyse the characteristics of the wave fields, just as has been done with the values for the same parameters from the SWAN wave model output in earlier chapters. The

[33] *In tests including the (moving) vessel, after the wave calibration, those probes were not present.*

[34] *Such a technique uses the phase lags between the different probes to identify the directions of the different wave components.*

[35] *H_{m0}, T_p, $T_{m0,1}$, $T_{m0,2}$ and $T_{m-1,0}$ were determined over the same frequency range as used for SWAN: 0.03-0.6 Hz. The spectral low-frequency wave height, $H_{m0,low}$, was determined based on all wave energy at frequencies <0.03 Hz.*

maximum wave height (H_{max}) was also derived from the data as the individual wave included in the timeseries with the largest wave height (crest + trough). As the three-hour timeseries contain approximately 900-1200 individual waves, this is considered a good approximation of the 1 in 1000 highest wave, which is generally used as the definition of H_{max}. For the highest wave the crest height, h_{cr}, trough height, h_{tr}, and the ratio h_{cr}/h_{tr} were also determined. The latter ratio gives an indication of the non-linearity of the waves. Having these parameter values available allows for a similar interpretation of the wave field as described in previous chapters on the SWAN model output, including assessing non-linear shallow-water effects.

For each of the considered tests, a 2D wave spectrum was derived using the wave timeseries of the 6 probes at location WAVE.SC1 using the Extended Maximum Entropy Method (EMEP, Hashimoto et al. 1983) available from the DIWASP (Directional Wave Spectra Toolbox) MATLAB toolbox[36].

Below, the results of the data analyses for each of the tests are presented in the form of 1) a table containing the derived wave parameters described above combined with the percentual deviations of H_s and T_p relative to the target values at the wave maker (ΔH_s and ΔT_p) and 2) two plots of respectively the measured and target 1D *frequency* wave spectra and the measured and target 1D *directional* wave spectra at the location of the probe array WAVE.SC1 (see also Section 6.1). Because of its proximity to WAVE.CL results for this array are considered also representative of the directions at the main test location WAVE.CL.

Table 6.3 Parameter values derived from the measured wave signals of Run 007

Wave probe	H_{m0} [m]	ΔH_{m0} [-]	T_p [s]	ΔT_p [-]	$T_{m0,1}$ [s]	$T_{m0,2}$ [s]	$T_{m-1,0}$ [s]	H_{max} [m]	h_{cr} [m]	h_{tr} [m]	h_{cr}/h_{tr} [-]	$H_{m0,low}$ [m]
WAVE.CL	5.3	1%	12.0	2%	9.5	8.9	10.4	9.3	6.2	3.0	2.1	0.4
WAVE.9	5.7	10%	11.7	-1%	9.5	8.9	10.5	10.3	8.1	2.2	3.6	0.4
W.SC2.CL	5.4	3%	11.5	-3%	9.5	8.9	10.4	11.4	7.8	3.5	2.2	0.4
WAVE.7	5.7	9%	12.0	2%	9.7	9.1	10.6	9.3	5.5	3.8	1.4	0.4

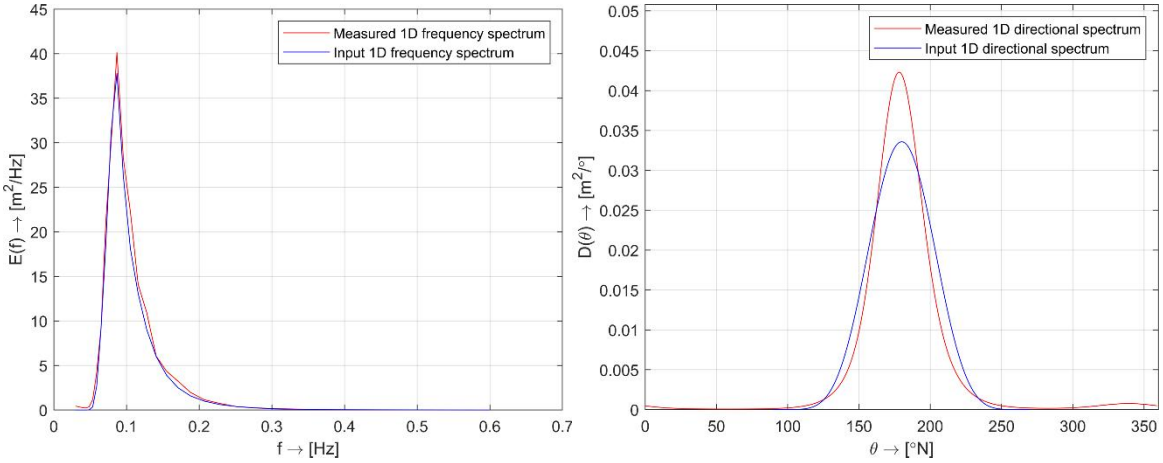

Figure 6.1 Comparison of measured and input 1D wave spectra for Run 007 at location WAVE.SC1.

[36] *Available from https://github.com/metocean/diwasp.*

Table 6.4 As Table 6.3, now for Run 008.

Wave probe	H_{m0} [m]	ΔH_{m0} [-]	T_p [s]	ΔT_p [-]	$T_{m0,1}$ [s]	$T_{m0,2}$ [s]	$T_{m-1,0}$ [s]	H_{max} [m]	h_{cr} [m]	h_{tr} [m]	h_{cr}/h_{tr} [-]	$H_{m0,low}$ [m]
WAVE.CL	6.6	1%	12.2	-1%	9.9	9.2	10.9	12.9	7.5	5.4	1.4	0.6
WAVE.9	7.0	8%	12.2	-2%	9.9	9.2	10.9	12.4	8.9	3.5	2.6	0.6
W.SC2.CL	6.7	3%	12.2	-1%	10.0	9.3	11.0	10.2	5.6	4.6	1.2	0.6
WAVE.7	7.3	12%	12.5	1%	10.1	9.5	11.2	12.1	7.5	4.6	1.6	0.6

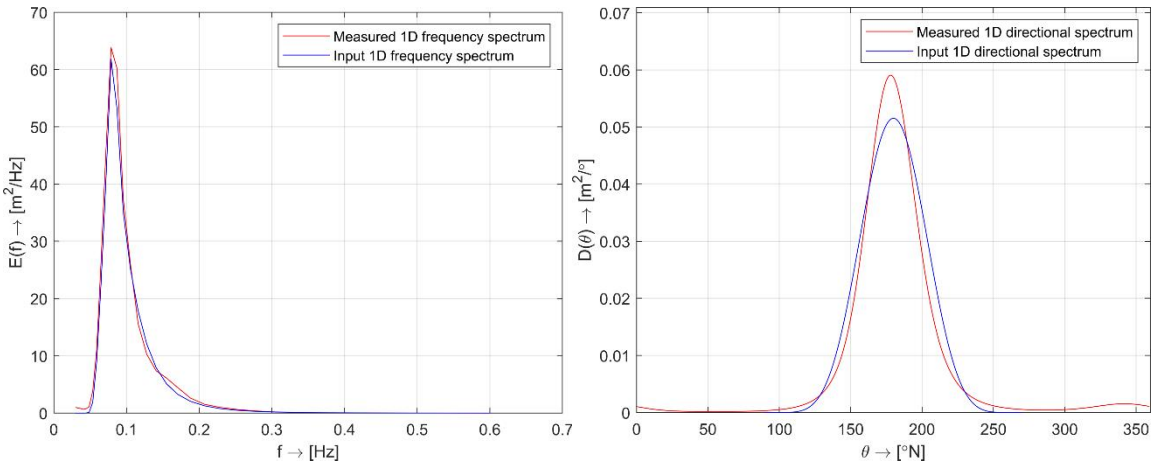

Figure 6.2 As Figure 6.1, now for Run 008.

Table 6.5 As Table 6.3, now for Run 009.

Wave probe	H_{m0} [m]	ΔH_{m0} [-]	T_p [s]	ΔT_p [-]	$T_{m0,1}$ [s]	$T_{m0,2}$ [s]	$T_{m-1,0}$ [s]	H_{max} [m]	h_{cr} [m]	h_{tr} [m]	h_{cr}/h_{tr} [-]	$H_{m0,low}$ [m]
WAVE.CL	6.6	2%	14.2	-2%	11.2	10.4	12.6	11.0	6.8	4.3	1.6	0.9
WAVE.9	7.3	12%	13.9	-4%	11.3	10.5	12.6	15.0	9.1	5.9	1.5	0.8
W.SC2.CL	6.9	5%	14.1	-3%	11.7	10.8	13.0	11.7	7.9	3.8	2.1	0.8
WAVE.7	7.4	14%	14.2	-2%	11.5	10.6	12.8	15.0	11.0	4.0	2.8	0.9

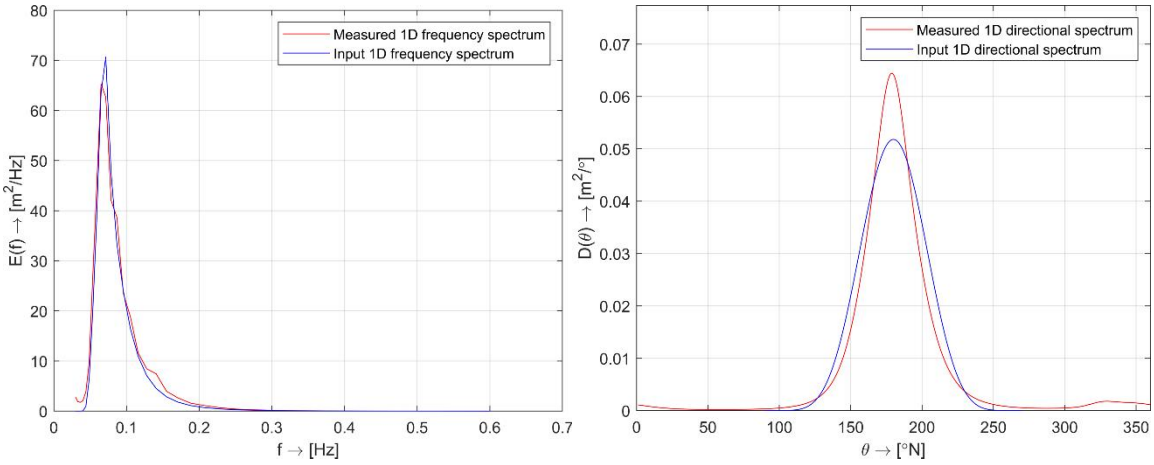

Figure 6.3 As Figure 6.1, now for Run 009.

Table 6.6 As Table 6.3, now for Run 010.

Wave probe	H_{m0} [m]	ΔH_{m0} [-]	T_p [s]	ΔT_p [-]	$T_{m0,1}$ [s]	$T_{m0,2}$ [s]	$T_{m-1,0}$ [s]	H_{max} [m]	h_{cr} [m]	h_{tr} [m]	h_{cr}/h_{tr} [-]	$H_{m0,low}$ [m]
WAVE.CL	7.8	4%	14.4	-1%	11.1	10.2	12.6	13.5	8.9	4.7	1.9	1.0
WAVE.9	8.1	8%	14.2	-2%	11.2	10.2	12.6	14.7	10.4	4.4	2.4	1.0
W.SC2.CL	7.9	6%	14.5	0%	11.3	10.4	12.7	13.9	9.8	4.2	2.3	1.0
WAVE.7	8.4	11%	14.2	-2%	11.3	10.4	12.7	14.2	8.2	6.0	1.4	1.1

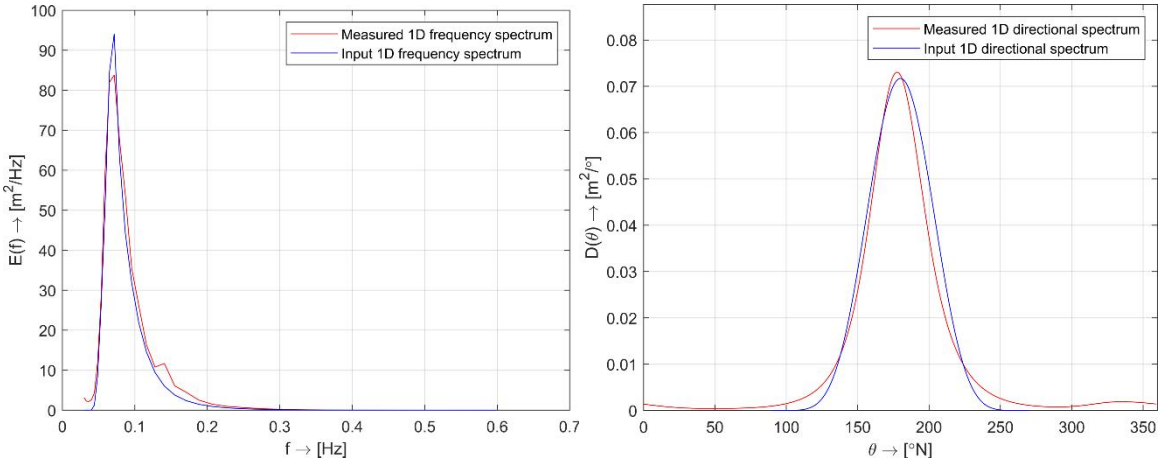

Figure 6.4 As Figure 6.1, now for Run 010.

From the tables and figures above it follows that at location WAVE.CL and at the nearby location WAVE.SC1, the parameters H_s and T_p have all been reached within 5% of their target values (see Table 6.2). This is also represented in the excellent fits of the measured 1D wave frequency spectra compared to the target spectral shapes (shown in the left panels of the figures). The small deviations between the measured 1D directional spectra and the target spectra are not expected to have a significant influence on the tests. This is because the overall widths of the directional spectra still match quite well and because a slightly more peaked directional spectrum is considered conservative for vessel response studies (for focussed wave energy reaching the ship)[37]. At the other three wave probe locations (plots not reproduced here), the deviations in H_s and T_p compared to the target values are somewhat larger. However, the deviations in wave height at those other locations are structurally higher than the target values for all test conditions, and therefore maybe simply a general basin characteristic. Also, the ratios between the deviations at the different probes are practically constant. This indicates that the distribution of wave energy over the basin has been relatively constant for all considered test, thus no signs of unexpected or unexplained effects due to non-uniformity of wave conditions have been found.

The parameter values in the tables above express that in all tests the waves show a strong non-linear shape, with high steep crests and relatively flattened troughs. This is the direct result of shallow-water influences, as would be the case in reality. This also corresponds with the general results and observations found based on the SWAN output, which is discussed in more detail in Section 6.3.2.

Last, it is noted that some low-frequency wave energy has been present during the tests. These are very long waves, longer than swell waves, that typically have wave periods in the order of

[37] *Any significant deviation in the frequency distribution – not found here – would have been a much more critical potential mismatch.*

one minute. In the field they particularly arise in sea areas of shallow depth. When such shallow regions are modelled to scale, such as considered as part of the laboratory tests by MARIN for this study, these very long waves will also occur. Especially moored vessels can be sensitive to such waves and show large motions. Sailing vessels are not significantly impacted by such waves. As most of the tests including the vessel have been performed as “Forward Speed” tests, this will not have had a significant influence on the results. For the “Zero Speed” tests, with the vessel moored at location WAVE.CL, the possible influence of the low frequency energy on the vessel motions should be checked. If low-frequency motions of the vessel have not been amplified, and if eigenfrequencies of the mooring configuration are far from the frequency range of these long waves, then no significant impact of these waves on the tests is to be expected.

Considering all information above, it is concluded that the wave conditions as prescribed at the wave maker have been created in the basin correctly, including non-linear shallow-water effects. This also means that the wave breaking phenomena that are triggered or intensified within such wave fields should have occurred in the scale model basin representative of such wave conditions in the field.

6.3.2 Verification of representativeness of basin conditions

As described previously, the wave conditions considered by MARIN describe typical field conditions that cover a larger range of parameter values to allow for analyses beyond the conditions that occurred during the 1-2 January 2019 event, which will allow reaching overarching conclusions. A larger range (H_s and T_p) was also recommended to MARIN by Deltares to cover for the uncertainty in the available wind input fields. However, this means that not all considered test conditions can directly be compared to the numerical SWAN results of Chapter 5 for the main output locations. Two of the four test conditions considered in Section 6.3.1 can be directly compared with the SWAN output at the main output locations: Condition 007 from the laboratory tests with Location 1 from SWAN and Condition 008 from the tests with Location 3 from SWAN (bold red in Table 6.1).

Table 6.7 presents a direct comparison of the numerical SWAN results at Locations 1 (top 2 rows) and Location 3 (lower two rows) with the values measured in the basin at (calibration) probe WAVE.CL for the corresponding test conditions.

Table 6.7 Comparison of numerical SWAN results (Locations 1 and 3) with the values measured in the basin at wave probe WAVE.CL for the corresponding test conditions.

	d [m]	H_{m0} [m]	T_p [s]	$T_{m0,1}$ [s]	$T_{m0,2}$ [s]	$T_{m-1,0}$ [s]	H_{max} [m]	h_{cr} [m]	h_{tr} [m]	h_{cr}/h_{tr} [-]	$H_{m0,low}$ [m]	γ [-]
SWAN Loc. 1	21.30	5.23	11.77	9.07	8.36	10.20	9.59	6.48	3.11	2.08	0.16	1.15
Cond. 007 WAVE.CL	21.3	5.3	12.0	9.5	8.9	10.4	9.3	6.2	3.0	2.1	0.4	1.5
SWAN Loc. 3	21.61	6.46	12.43	10.03	9.33	11.08	11.53	8.25	3.28	2.52	0.27	1.67
Cond. 008 WAVE.CL	21.3	6.6	12.2	9.9	9.2	10.9	12.9	7.5	5.4	1.4	0.6	1.5

A cross-comparison of the spectral wave heights H_{m0} (which is a value for H_s derived from the spectrum) for both locations with the corresponding laboratory value at (calibration) probe WAVE.CL, shows that the values measured in the basin are only slightly higher (<2%), but for practical purposes the same. A cross comparison of the spectral periods T_p, $T_{m0,1}$, $T_{m0,2}$ and

$T_{m-1,0}$ shows that for SWAN Location 1 the different period parameters are slightly overestimated in the corresponding scale model test (Condition 007), while for Location 3 the different periods are slightly underestimated in the laboratory. This behaviour is also visible in the spectral shapes of the measured and computed 1D frequency spectra (Figure 6.5 for SWAN Location 1 and Figure 6.6 for SWAN Location 3). This is well within typical accuracy levels that generally can be demanded from physical scale model tests.

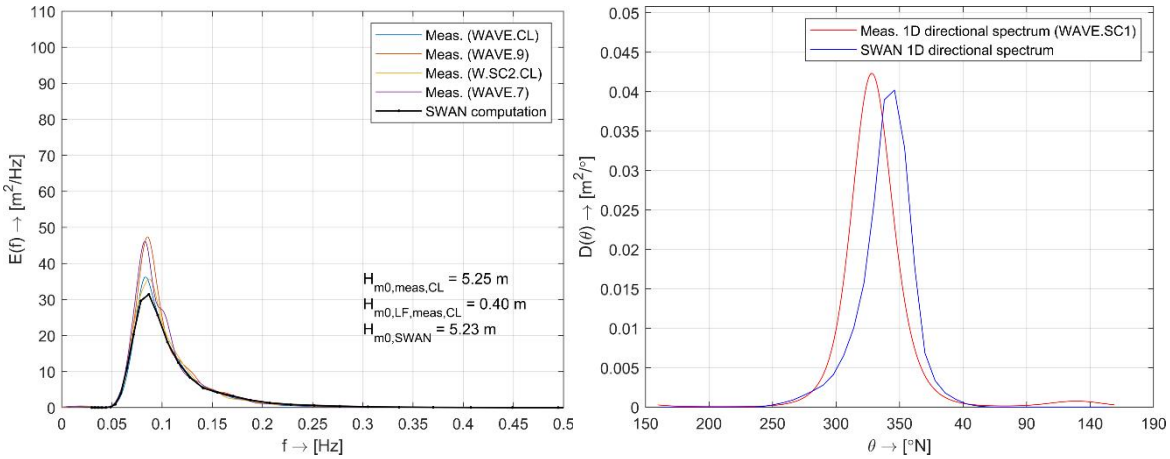

Figure 6.5 Comparison of measured and computed spectral shapes for SWAN Location 1 (MARIN test condition 007). Left panel: 1D frequency spectra. Right panel: 1D directional spectra.

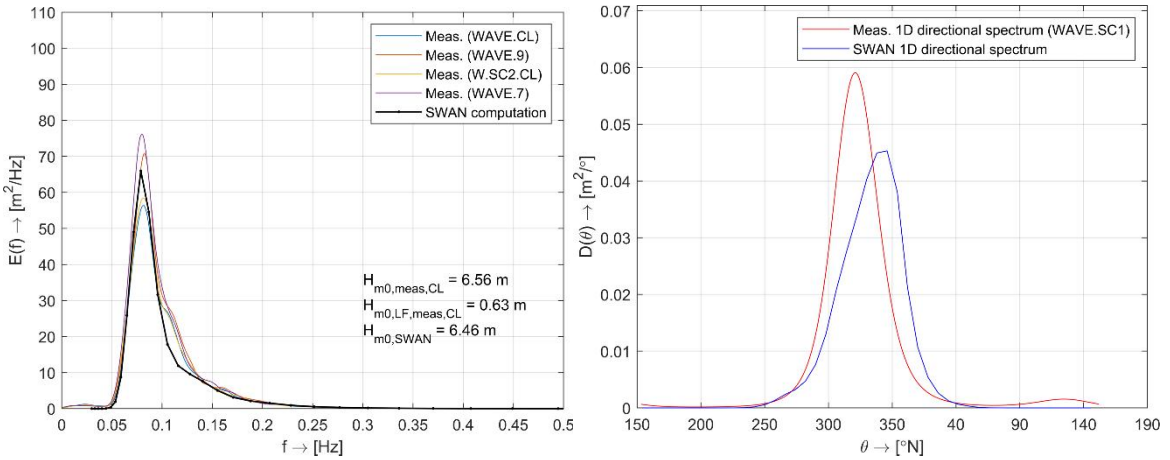

Figure 6.6 Comparison of measured and computed spectral shapes for SWAN Location 3 (MARIN test condition 008). Left panel: 1D frequency spectra. Right panel: 1D directional spectra.

A comparison of the 1D directional spectra[38] shows quite some deviations at both locations. However, the areas underneath the corresponding spectra are very much comparable as are the overall directional widths. Considering this and the fact that the exact directional shape is less critical here, the scale model tests are considered to represent the SWAN conditions sufficiently well in terms of directional distribution.

The values for the maximum wave height measured in the laboratory and the corresponding crest and trough heights (Table 6.7) fall within the expected order of magnitude. An exact match between the measured values and the theoretical values is not sought here, as the theory is

[38] *The mean wave directions of the measured spectra have been shifted to the computed mean wave directions to be able to make a consistent comparison.*

based on assumed statistical characteristics. The nature of the simulated physical processes will always show such variations, since only one specific realisation of a sea-state is considered in the scale model tests. In practice this an unavoidable characteristic of performing physical scale model tests and it is not critical.

Last the measured low-frequency wave energy (expressed in terms of $H_{m0,low}$, see Footnote 35) is compared to theoretically derived values for the SWAN output locations (third column from the right in Table 6.7) based on the theoretical formulation for such waves by Herbers et al. (1994). This comparison shows that the measured low-frequency wave heights are approximately twice as high as the theoretical values. This shows that the low-frequency wave energy has most likely been influenced by reflections within the basin. Given that the height values only show a doubling indicates that the long waves may reflect on the basin walls and propagate back towards the wave board, but that this behaviour apparently does not result in resonance and further increases in low-frequency wave heights. Even though this type of waves is not critical for sailing vessels, it is good to have verified that these very long waves were not unintentionally amplified by resonance in the basin.

From the results and observations above we conclude that the wave conditions as generated in the basin of MARIN are representative for typical conditions as those computed in SWAN for the storm of 1-2 January 2019 for the area north of the Wadden Islands (Chapter 5).

7 Conclusions

7.1 Metocean conditions during the event of MSC Zoe on 1-2 January 2019

The following conclusions are drawn from this study related to the metocean conditions as they occurred on 1-2 January 2019 and how they were experienced (encountered) by the MSC Zoe.

Conditions experienced by the vessel

- The MSC Zoe encountered the following maximum metocean conditions on 1-2 January 2019, along the most critical section of its sailing route north of the Wadden Islands:

Table 7.1 Overview of most severe metocean conditions experienced by MSC Zoe on 1-2 January 2019 (numerical model values). This table has been copied from Chapter 5 of this report.

Parameter	Representative value (range) along the track of the ship on 1-2 January 2019	Frequency of occurrence, exceptionality
Current speed	up to 0.5 m/s (1 kn)	Very common, occur daily
Water level	MSL + 0 m – MSL + 1 m	
Wind speed	16 – 18 m/s	Are exceeded on average one to two times in a year
Significant wave height (H_s)	5 – 6.5 m	
Peak wave period (T_p)	11 – 13 s	

The wave parameters listed above include a representative wave height and period, characterising the total irregular wave field consisting of a mixture of wave components with different lengths and heights (i.e. a spectrum of wave conditions). Conclusions related to the accuracy of these values obtained from numerical modelling are given further below.

- These metocean conditions are not very extreme or exceptional: these water levels and flow conditions occur daily, and these storm and resulting wave conditions on average are exceeded one to two times in a year. Such situations will most likely occur during the storm season in the Netherlands, which generally runs from October to April.
- Currents were directed towards the west, leading to a counter current for the vessel of moderate magnitude (≈0.5 m/s, 1 knot).
- The tide was falling (ebb tidal phase) and the vessel experienced slowly dropping water levels as it progressed along its track. However, the wind-induced storm surge present resulted in water levels not dropping below mean sea level.
- The timing of the water levels combined with the sea bed levels along the route resulted in two areas with relatively small water depths. Water depths experienced by the vessel could have been even smaller, if the lowest tidal water levels would have occurred while the vessel was at the shallowest location.
- The wave conditions present in the area were influenced by the shallower depths and particularly the highest and longest waves within the wave fields (H_{max}) showed steepened crests and flattened troughs, i.e. much higher crests and smaller troughs. Mariners have reported that such conditions (referred to by them as 'ground seas', or 'Grondzee' in Dutch) are known to occur along the southern sailing route north of the Wadden Islands. These wave shapes (non-linear waves) correspond to more complex wave conditions than deep-water waves with crests and troughs of the same size (linear waves).
- The steepening of the wave crests will have enhanced wave breaking by foamy, spilling wave crests (called 'white-capping'). Even though this wave energy dissipation effect is

very common out at the open sea, it may have contributed to the complexity of the wave conditions encountered by the vessel.
- Waves were directed beam-on to the vessel (i.e. approaching the ship from the side), which generally is an unfavourable direction for vessels. However, given typical directions of storms on the North Sea and the orientation of the sailing routes north of the Wadden Islands, this will be a common situation.
- Given that the waves were directed approximately perpendicular to the current, wave-current interactions will have been very small or absent.
- Given that the waves were directed approximately perpendicular to the vessel heading, the encounter frequency of the waves by the vessel will not have been influenced by the forward velocity of the vessel.

Spatial distribution of metocean conditions in the area
- The maximum individual wave heights (H_{max}) within the wave fields present on 1-2 January 2019 reached up to 10-12 m. It is therefore probable that along the route the vessel encountered higher individual waves than the H_s significant wave height value representative of the complete wave field (including lower and higher waves). However, since such individual higher waves can have occurred anywhere in the wave field, and at any time, it is not to say that the vessel has necessarily experienced the largest of wave heights within the wave field (H_{max}).
- The magnitude and direction of the currents in the area changed in space and time along with the tide. However, since the vessel progressed eastward, more-or-less along with the tidal motion, the vessel experienced quite constant flow conditions along the critical section of the route.
- The representative wave conditions (heights, periods) and wind conditions (magnitude, direction) were quite uniform in the area north of the Wadden Islands, including both the southern and northern sailing routes.
- Due to the larger water depth present, the waves showed less steepening of crests along the northern sailing route. In principle, this may correspond to somewhat less adverse wave conditions, even for the same representative significant wave height (H_s). However, white-capping breaking effects of waves were still quite intense at the location considered along the northern sailing route, even larger than at two of the locations considered along the southern route and of the same magnitude as for the third location. This indicates that a vessel along the northern route would have also experienced breaking waves, of at least the same intensity, impacting the vessel. This shows that further analyses are required to reach definitive conclusions on recommendations or preferences for sailing routes related to specific wave conditions.
- An important difference between the northern and southern sailing routes with respect to metocean conditions is the water depth available to the vessels, which corresponds to 10-15 m more under-keel clearance along the northern route compared to the smallest water depths available along the southern sailing route.

Validation of the numerical modelling approaches
- Numerical models were applied to derive the conditions along the track of the vessel and in the area, since measurements are only available at observation locations scattered throughout the area. Data retrieved from archived model outcomes and newly computed numerical results were validated as part of this study by comparing computed results with corresponding conditions measured at the observation locations included in the area covered by the numerical model. This comparison showed accuracy levels as summarised in Table 7.2.

Table 7.2 Overview of validation results (accuracy levels).

Type of data	Parameter	Typical deviation
Archived data used as modelling input	Water levels	<0.1 m
	Wind speeds	appr. 5% underestimation
Model output	All wave parameters	0.92-0.99 correlation
	Significant wave heights (H_s)	5-10% underestimation
	Peak wave periods (T_p)	2-3 s underestimation

- The high correlation factors between measured and computed results (0.92-0.99) show that the overall trends in the wave parameter values are reproduced accurately, indicating that the general physics of the natural system are captured well by the numerical models.
- Overall, the accuracy level found is typical for these kinds of computations, although unfortunately the largest deviations were found around the peak of the storm. This is a challenge typical for numerical wave modelling, but it may also be partly related to measurement challenges during intense conditions. Regardless, in the local wave model it is linked to the accuracy of the archived spatial wind fields available to force the numerical wave model. In this case the computed wave results have the same typical accuracy as those wind fields.
- Since an unambiguous calibration (tuning) of the wind fields was not possible, the available wind fields were used unchanged. As a practical solution to the resulting underestimation in wave parameters, Deltares recommended MARIN to cover this as part of the laboratory tests by considering a set of wave conditions that also included slightly elevated values of spectral wave parameters. By considering additional tests with somewhat higher values for H_s and T_p the laboratory tests show whether such adjusted conditions would lead to other results and conclusions than those that result from using the computed wave values.
- The observed underestimation of the winds does not affect the conclusions of this study regarding exceptionality of the conditions, given that it affected all considered locations and that the severity of the storm conditions (frequency of occurrence) was determined consistently, i.e. relative to reference information from the same dataset.

7.2 Translating metocean conditions to laboratory test conditions

- Deltares provided 2D wave spectra to MARIN as one of the main project deliverables. In addition, parameterised spectral descriptions were provided on request from MARIN to facilitate easy use of this information in the scale model tests.
- When suitable wave conditions are sent into the basin of MARIN, using the proper settings for the wave maker and combined with a properly represented shallow-water depth, an accurate wave field with similar complexity as occurred in the field will automatically be generated in the wave basin. This is because the waves in the basin will then show the same complex wave phenomena as in the field.
- From checks performed on the wave signals measured in the wave basin of MARIN it follows that the wave conditions considered in their basin:
    - have been created correctly, including the relevant non-linear shallow water effects, and
    - are representative for typical wave conditions as those computed for the area north of the Wadden Islands during the storm of 1-2 January 2019.

References

API, 2000: Recommended Practice for Planning, Designing and Constructing Fixed Offshore Platforms - Working Stress Design (RP 2A-WSD)

Battjes, J.A. and H.W. Groenendijk, 2000: Wave height distributions on shallow foreshores, Coastal Engineering. 40, 161-182.

Battjes, J.A. and J.P.F.M. Janssen, 1978: Energy loss and set-up due to breaking of random waves, Coastal Engineering. 16, 569-587.

Booij, N., R. C. Ris and L. H. Holthuijsen, 1999: A third generation wave model for coastal regions. Part 1. Model description and validation, J. Geophys. Res., 104(C4), 76497666.

Deltares, 2011: The scientific validation of the hydrographic survey policy of the Netherlands Hydrographic Office, Royal Netherlands navy, Deltares reference: 1201907-000-BGS-0008, authors: T.A.G.P. van Dijk, C. van der Tak, W.P. de Boer, M.H.P. Kleuskens, P.J. Doornenbal, R.P. Noorlandt and V.C. Marges.

Hashimoto, N., T. Nagai and T. Asai, 1993: Modification of the extended maximum entropy principle for estimating directional spectrum in incident and reflected wave field. Rept. Of P.H.R.I. 32(4) 25-47

Hasselmann, K., T.P. Barnett, E. Bouws, H. Carlson, D.E. Cartwright, K. Enke, J.A. Ewing, H. Gienapp, D.E. Hasselmann, P. Kruseman, A. Meerburg, P. Müller, D.J. Olbers, K. Richter, W. Sell and H. Walden, 1973: Measurements of wind-wave growth and swell decay during the Joint North Sea Wave Project (JONSWAP), Dtsch. Hydrogr. Z. Suppl., 12, A8

Herbers, T.H.C., S. Elgar, R.T. Guza, 1994: Infragravity-frequency (0.005-0.05 Hz) motions on the shelf. Part I: Forced Waves, J. Phys. Oceanogr., 24, 917-927.

Holthuijsen, L.H., 2007: Waves in oceanic and coastal waters, Cambridge University Press, ISBN-13 978-0-521-86028-4.

KNMI, 2009. HiRLAM version H7.2. Tech. Rep. http://projects.knmi.nl/datacentrum/catalogus/catalogus/content/history/HIRLAM72_eng__151009.pdf, KNMI.

MARIN, 2019, Report on scale model measurements related to the OVV research. Definitive title and reference to be added.

Rienecker, M.M. and J.D. Fenton, 1981: A Fourier approximation method for steady water waves. J. Fluid Mechanics, 104, 119–137.

Rogers, W.E., P.A. Hwang, and D.W. Wang. 2003: Investigation of wave growth and decay in the SWAN model: three regional-scale applications, J. Phys. Oceanogr., 33, 366-389.

Tiessen, M. en F. Zijl, 2015: Stromingsvalidatie DCSMv6 en DCSMv6-ZUNOv4, Deltares memo, reference: 1209448-003-ZKS-0004.

Van der Westhuysen, A. J., 2010: Modeling of depth-induced wave breaking under finite depth wave growth conditions. J. Geophys. Res, 115, C01008, 2010.

Van Os, J. and S. Caires, 2011. How to carry out metocean studies, Proc. 30th Int. Conf. On Offshore Mechanics and Arctic Eng. (OMAE2011-49066).

Wu, Y, D. Randell, M. Christou, K. Ewans and P. Jonathan, 2016: On the distribution of wave height in shallow water, Coastal Engineering, 111, 39–49.

Wu, J., 1982: Wind-stress coefficients over sea surface from breeze to hurricane, J. Geophys. Res., 87, C12, 9704-9706

Zijlema, M., 2010: Computation of wind-wave spectra in coastal waters with SWAN on unstructured grids. Coastal Engineering, 57, 267-277.

Zijlema, M., G.Ph. van Vledder and L.H. Holthuijsen, 2012: Bottom friction and wind drag for wave models. Coastal Engineering, 65, 19-26.

A Wave validation plots

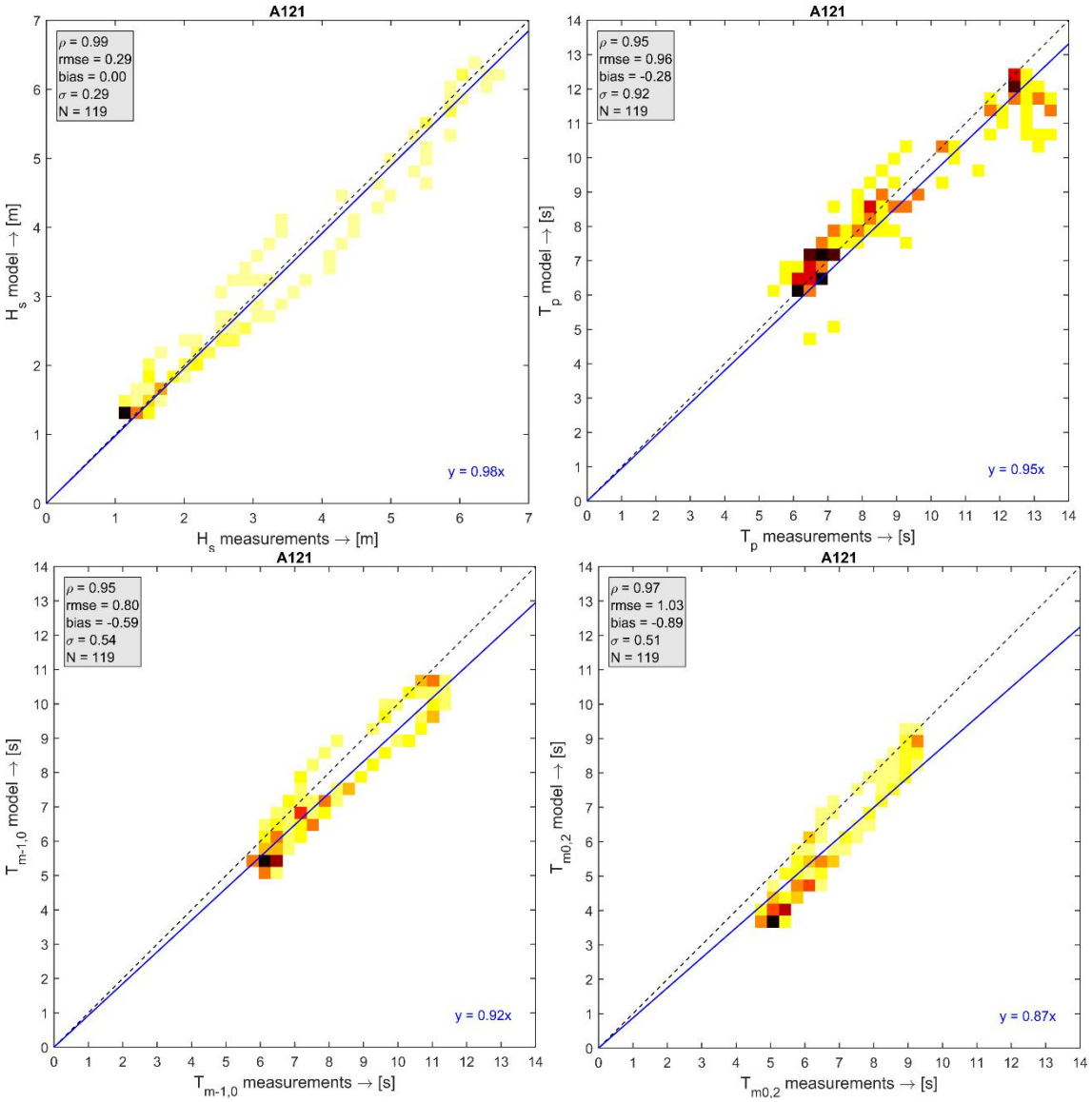

Figure A.1 Scatter plots of significant wave height (top left panel), peak wave period (top right panel), spectral wave period $T_{m-1,0}$ (lower left panel) and spectral wave period $T_{m0,2}$ (lower right panel) measurements against wave model data for platform A121. The coloured squares, ranging from yellow (low density) to black (high density), indicate the data density in the scatter plot. All panels include information on error statistics (grey box in top left corner) and an origin-crossing linear fit (blue line + the relation given in the bottom right corner). Units of the error parameters relate to that of the parameter considered.

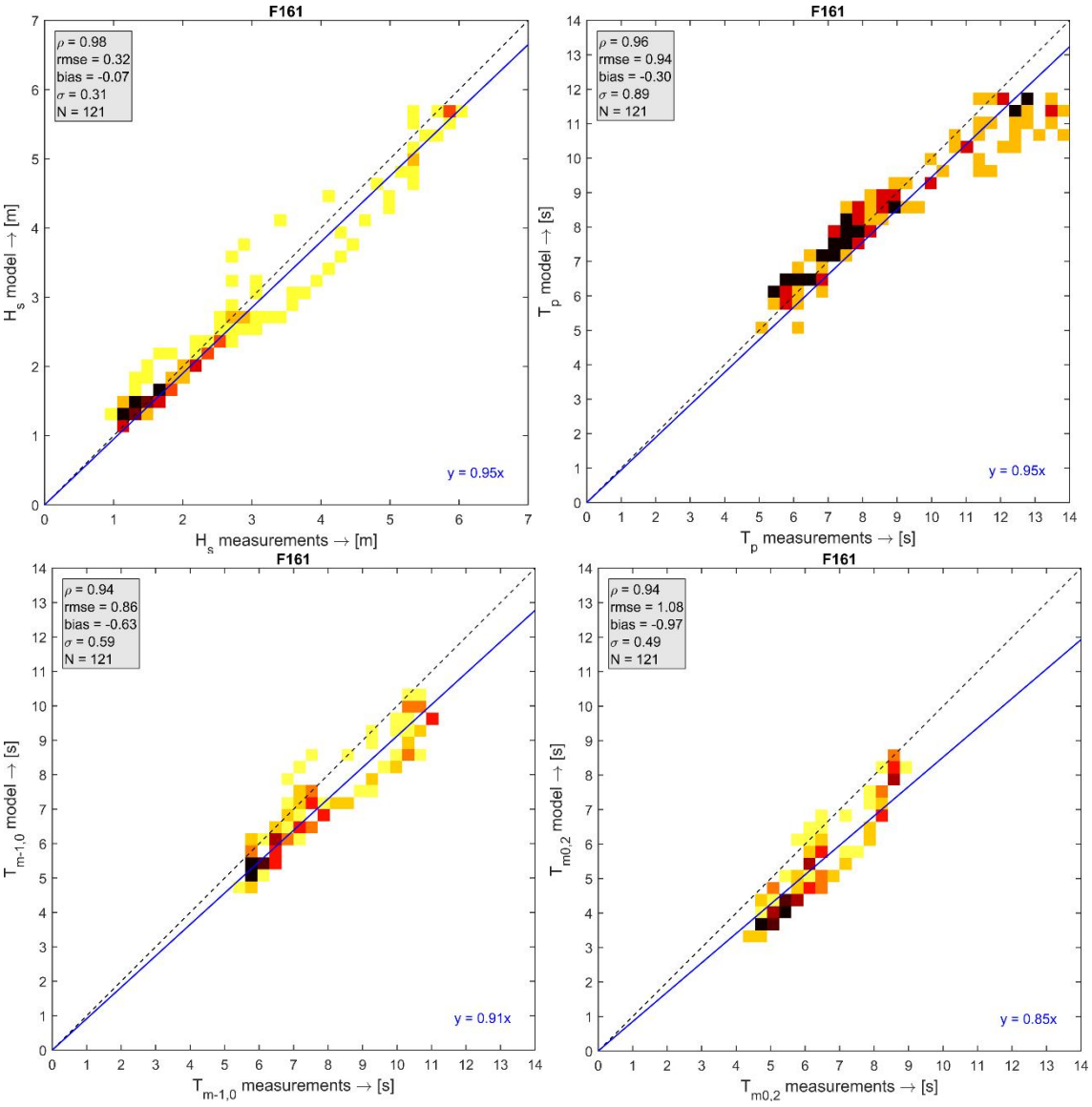

Figure A.2 As Figure A.1, now for platform F161.

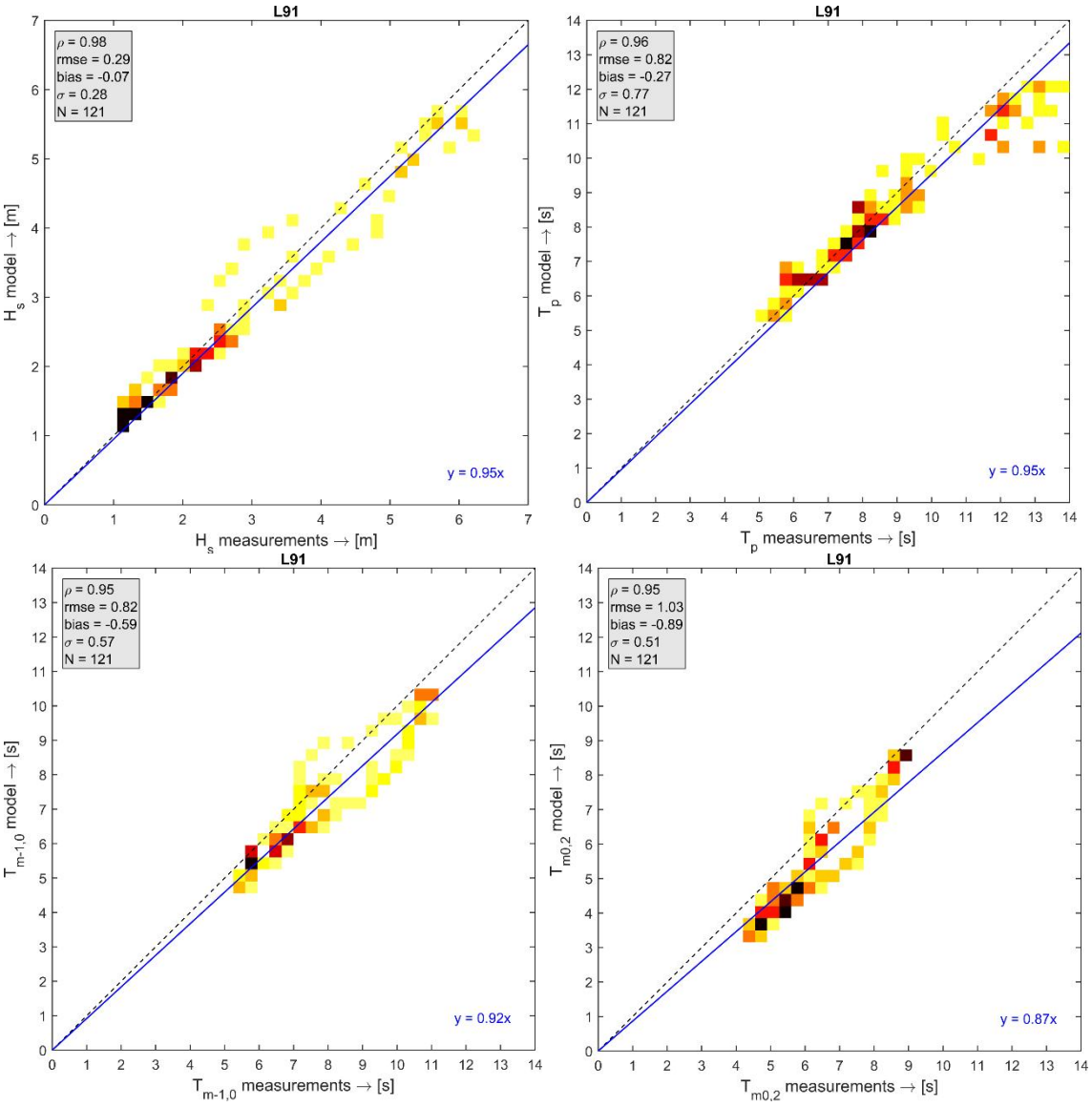

Figure A.3 As Figure A.1, now for platform L91.

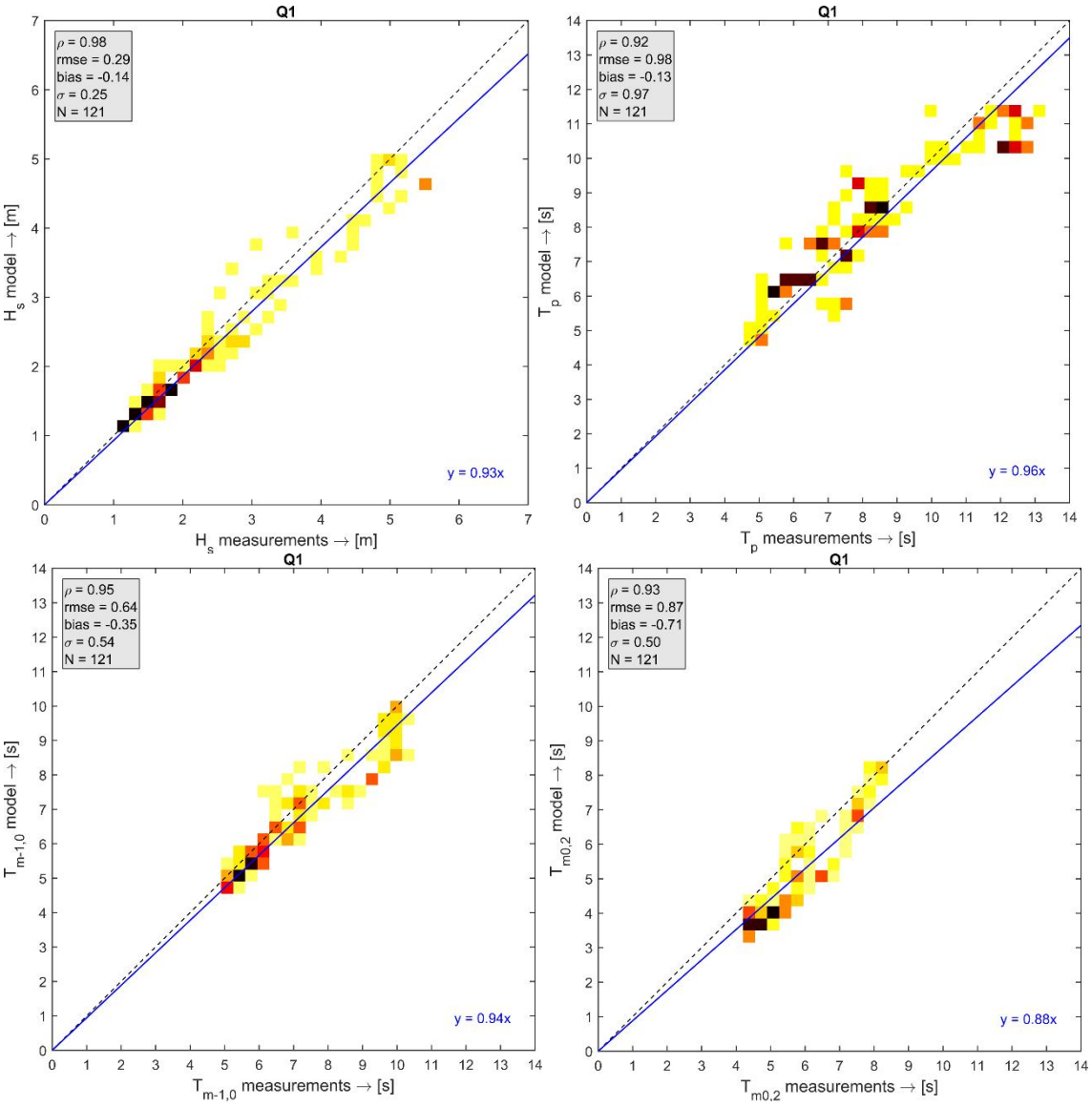

Figure A.4 As Figure A.1, now for platform Q1.

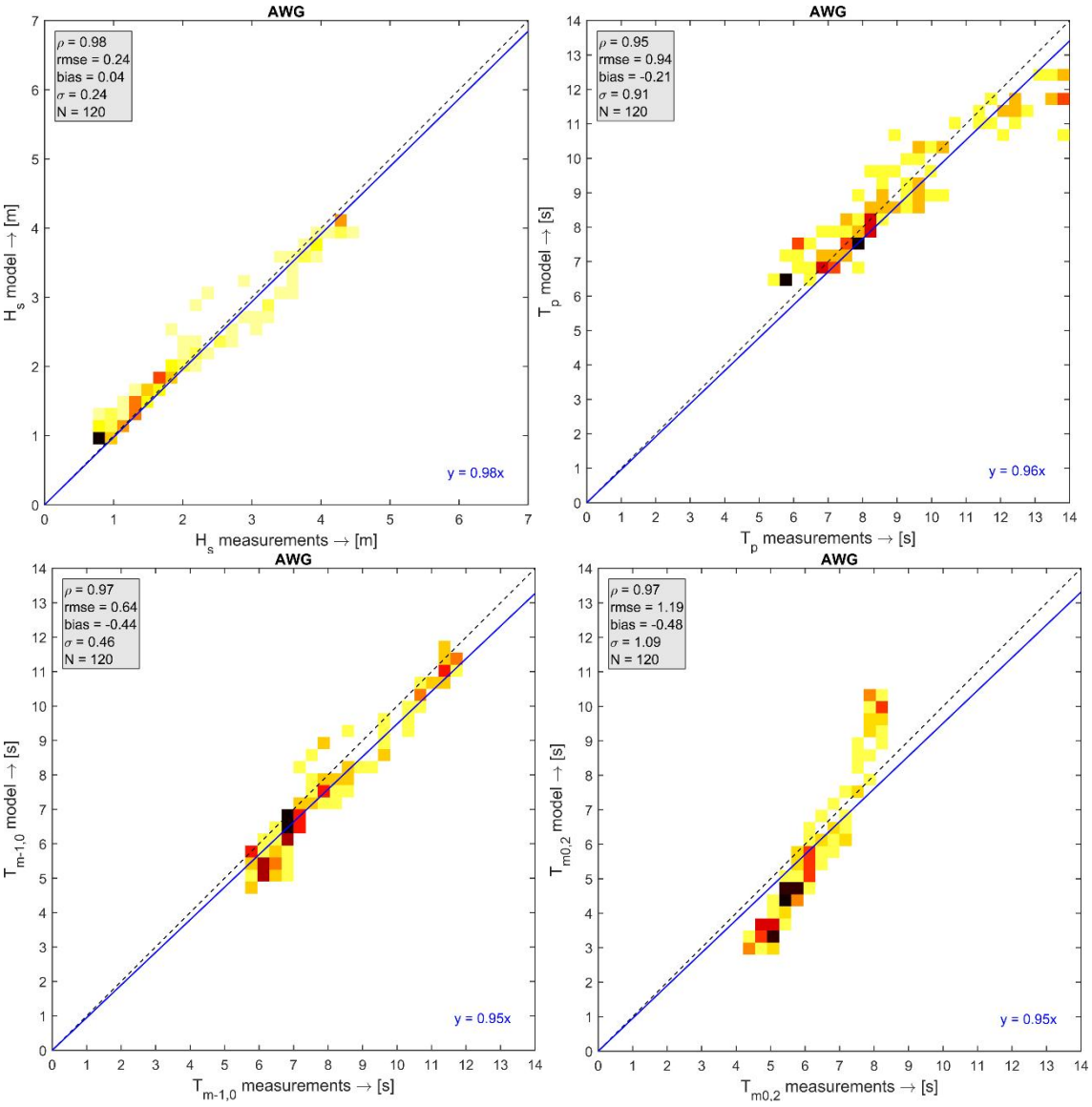

Figure A.5 As Figure A.1, now for platform AWG.

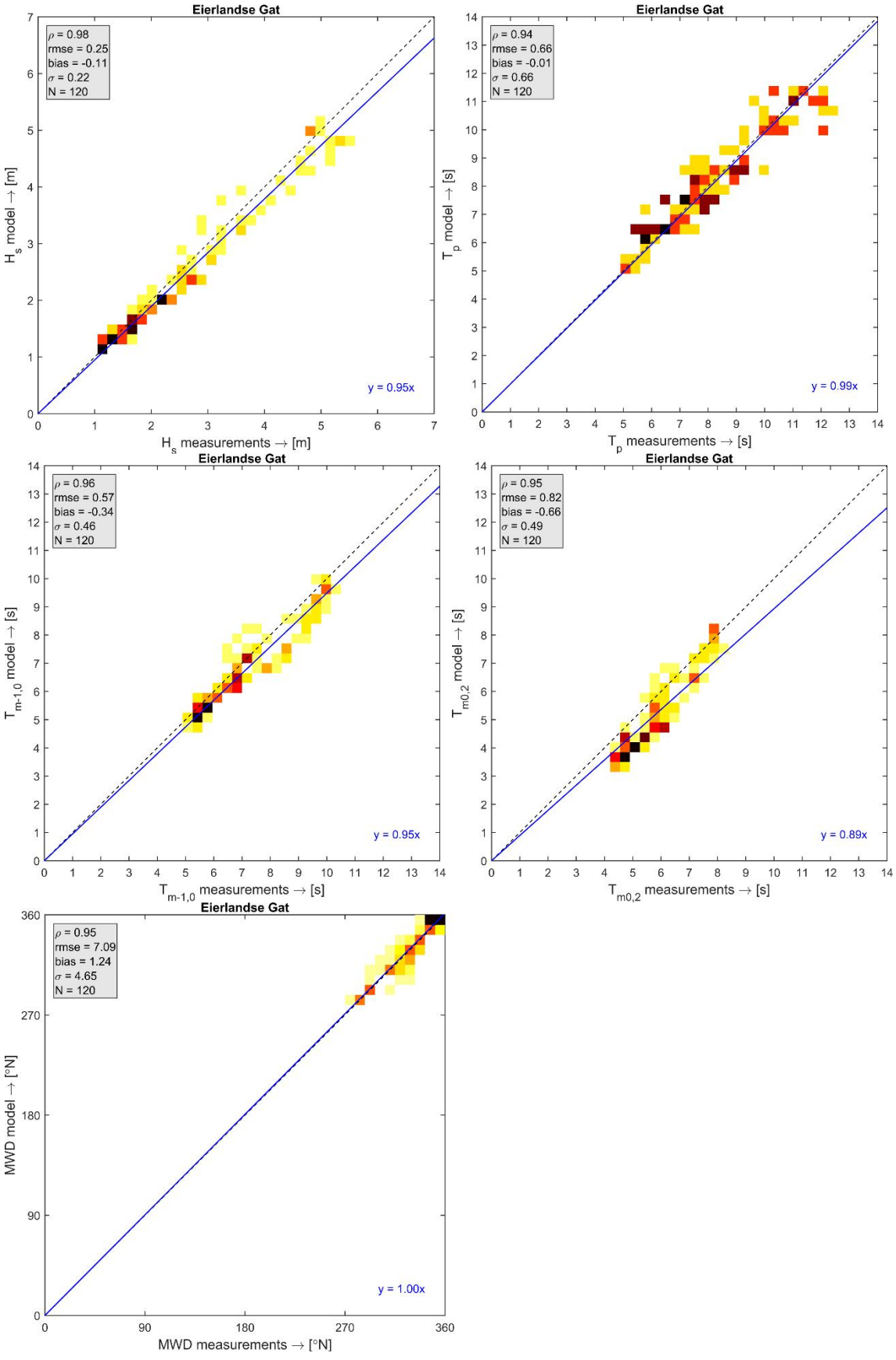

Figure A.6 As Figure A.1, now for buoy Eierlandse gat (EiG), incl. scatter plot for mean wave direction (last panel).

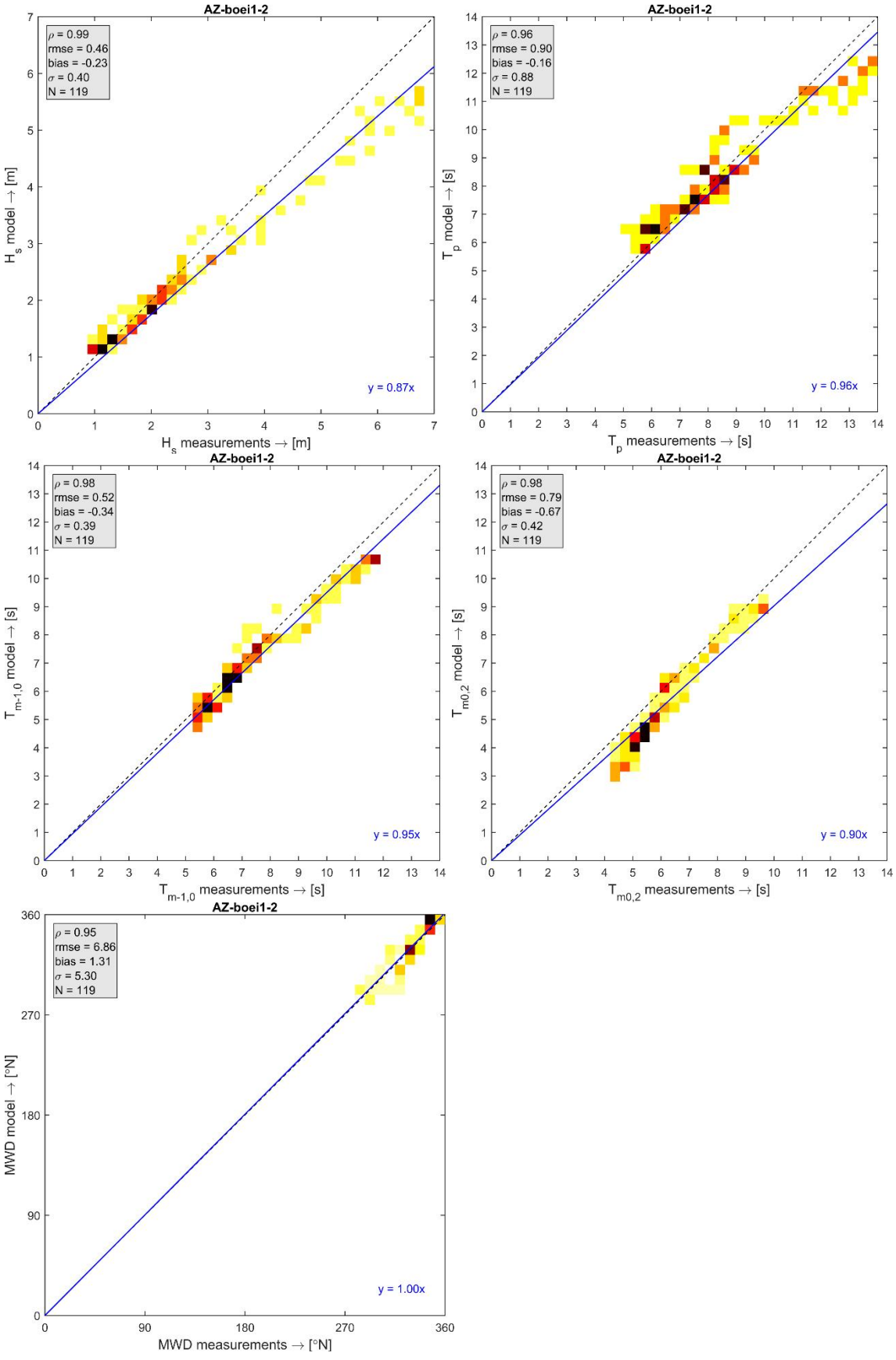

Figure A.7 As Figure A.6, now for Amelander Zeegat buoy 1-2 (AZ 1-2).

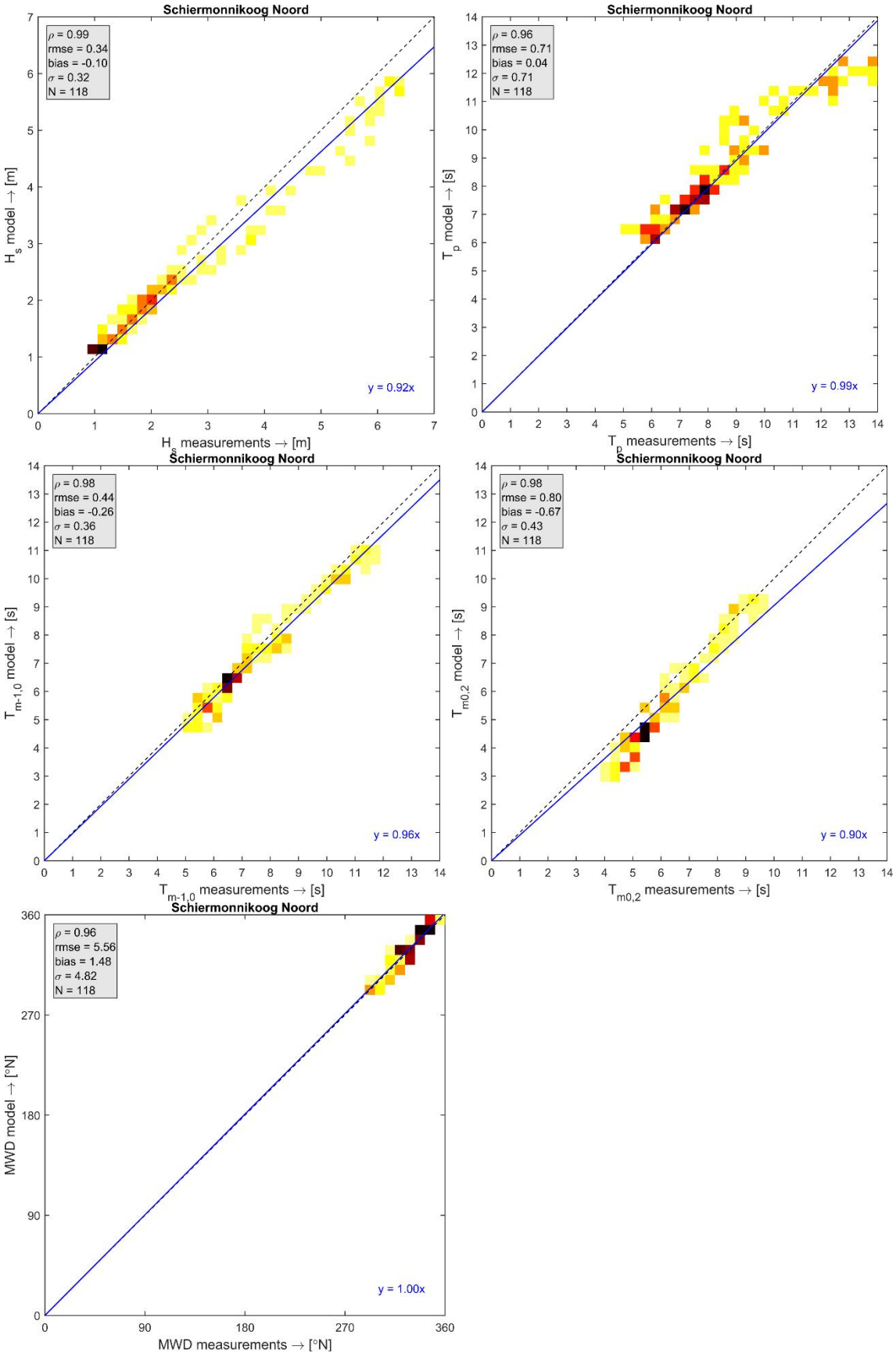

Figure A.8 As Figure A.6, now for buoy Schiermonnikoog Noord (SoN).

B Spatial numerical results

B.1 Flow conditions (water levels and currents)

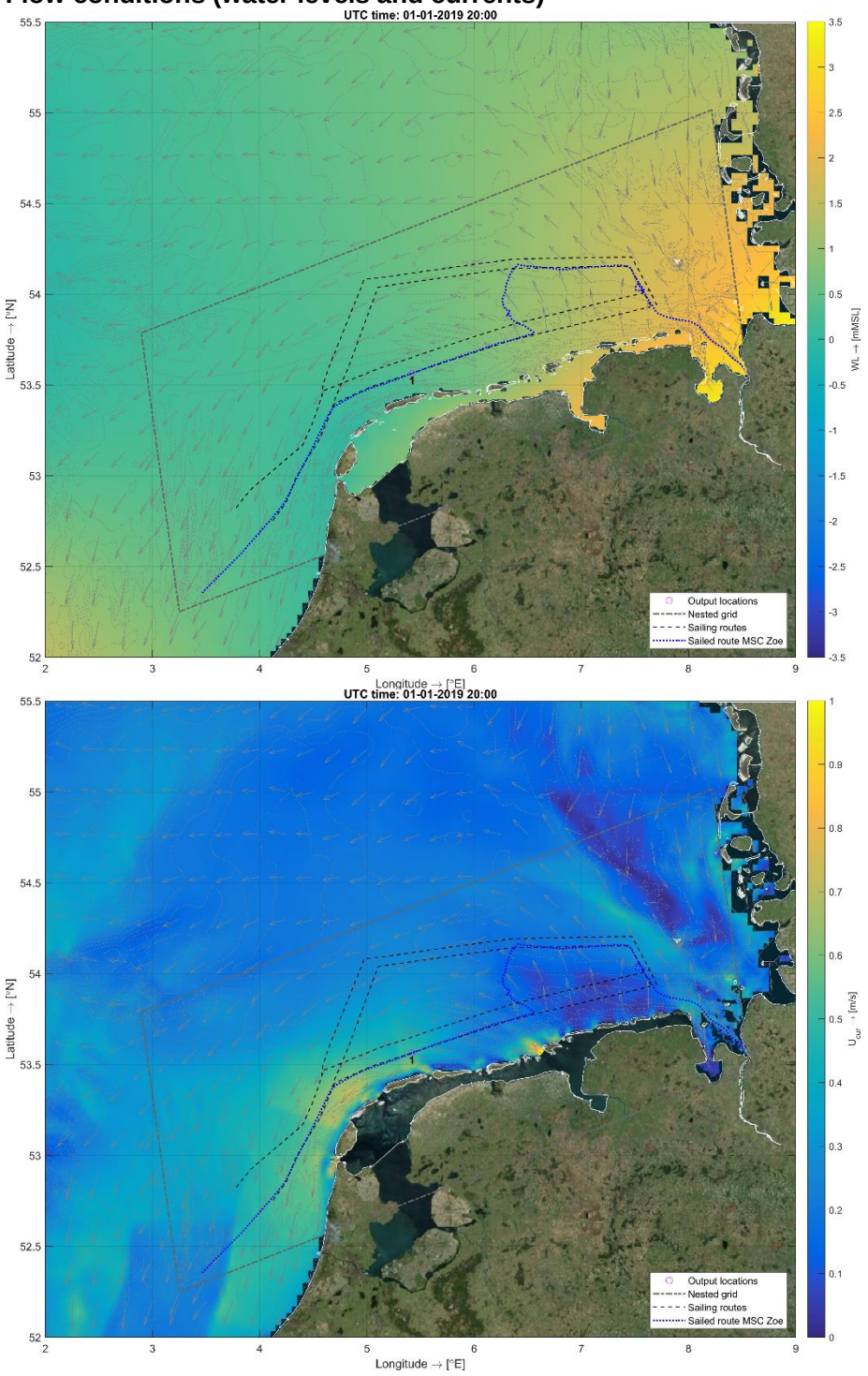

Figure B.1 Upper panel: spatial plot of water level at the timestamp corresponding to the vessel being at Location 1. The grey arrows indicate the depth-averaged current directions. The depth contours are indicated by grey dashed lines. Lower panel: same as upper panel, now for depth-averaged current speeds.

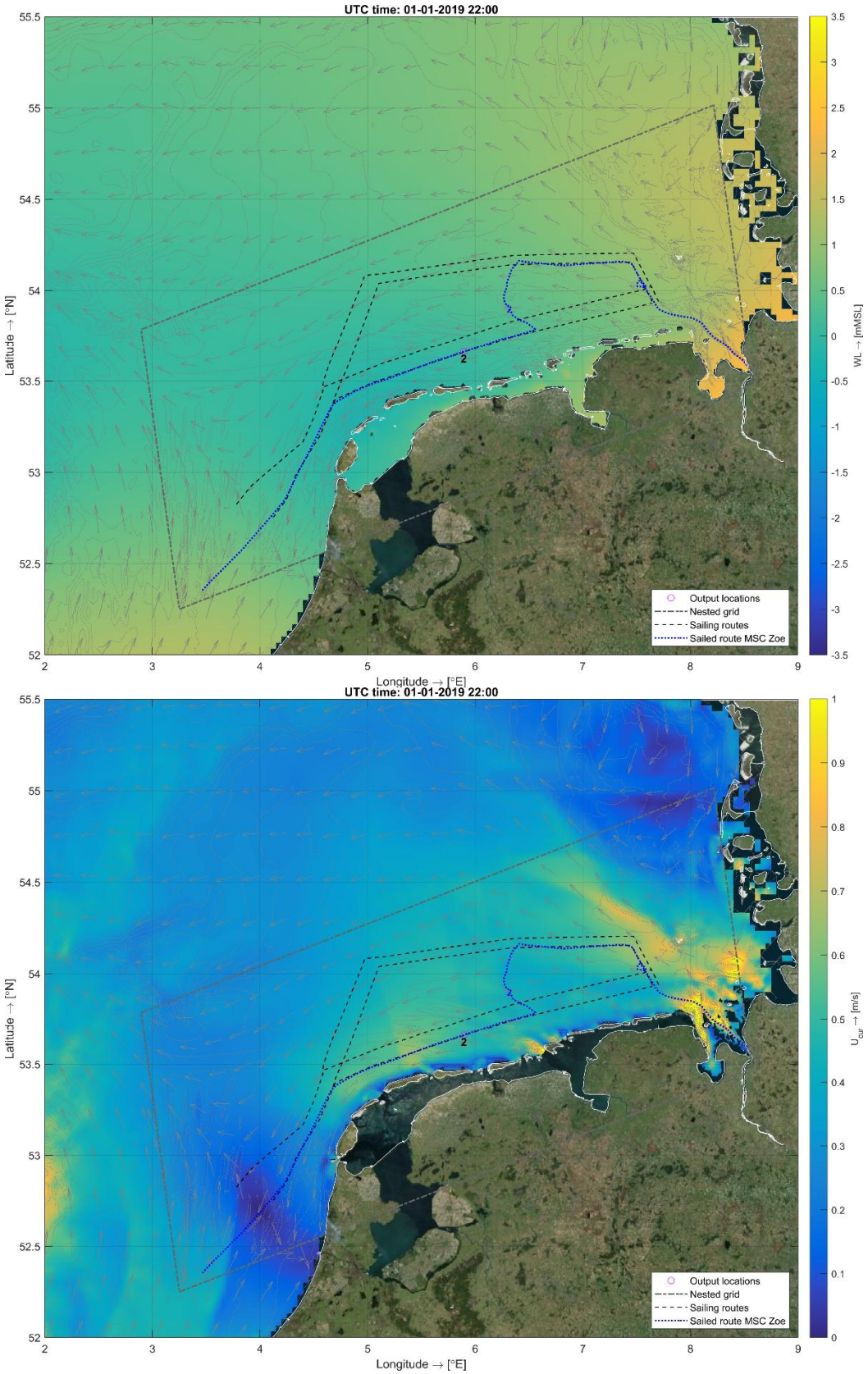

Figure B.2 As Figure B.1, now for Location 2.

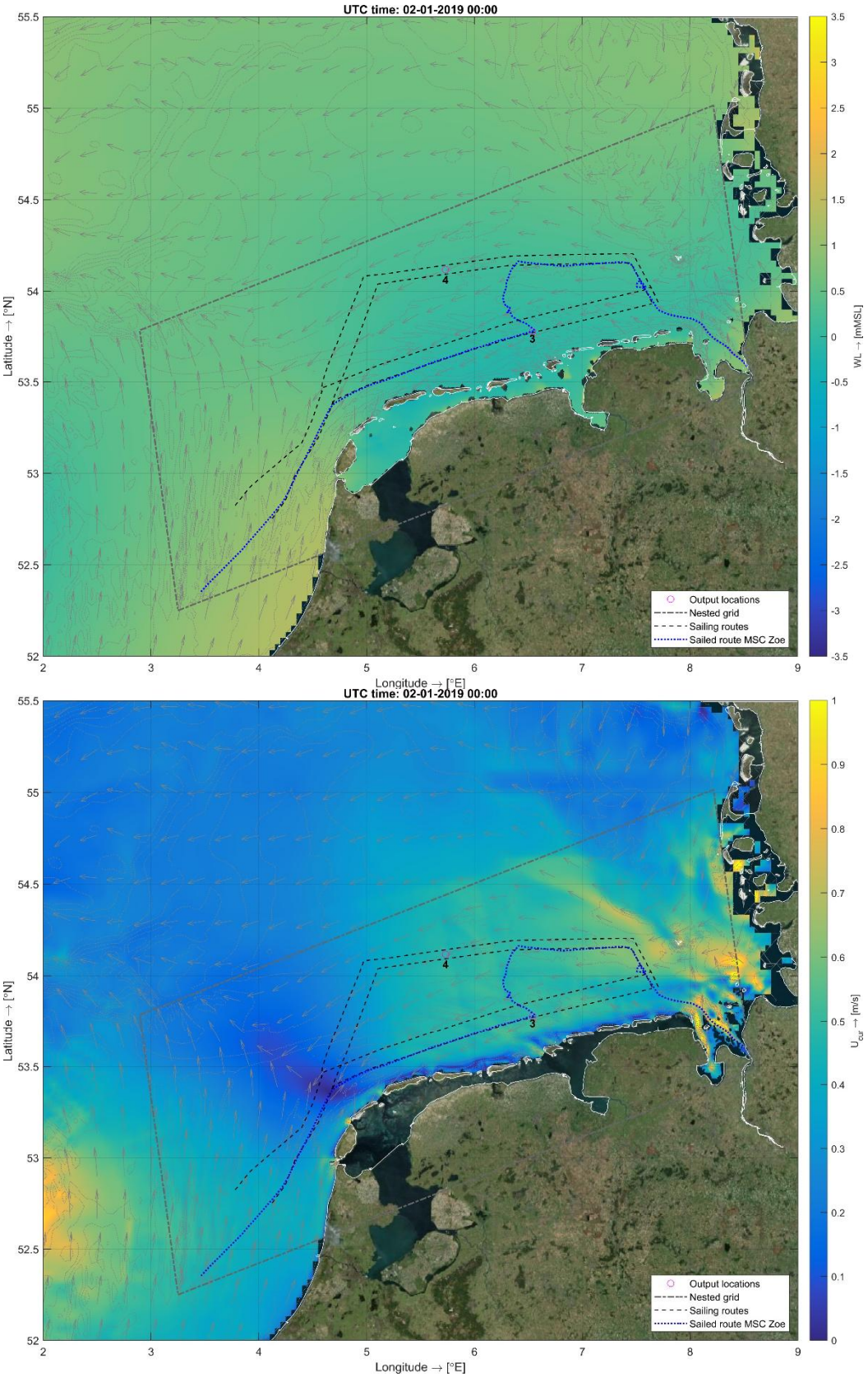

Figure B.3 As Figure B.1, now for Locations 3 and 4.

B.2 Wind

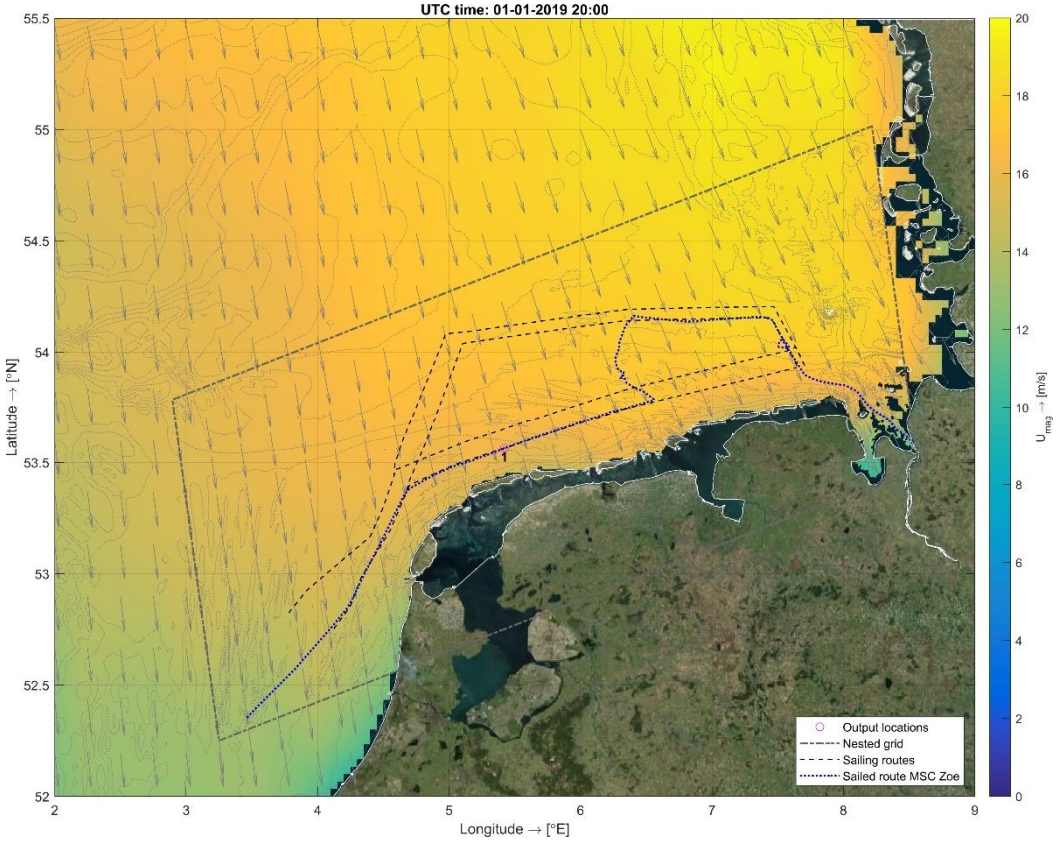

Figure B.4 Spatial plot of wind speed at 10 m height at the timestamp representative for Location 1. The grey arrows indicate the corresponding wind directions. The depth contours are indicated by grey dashed lines.

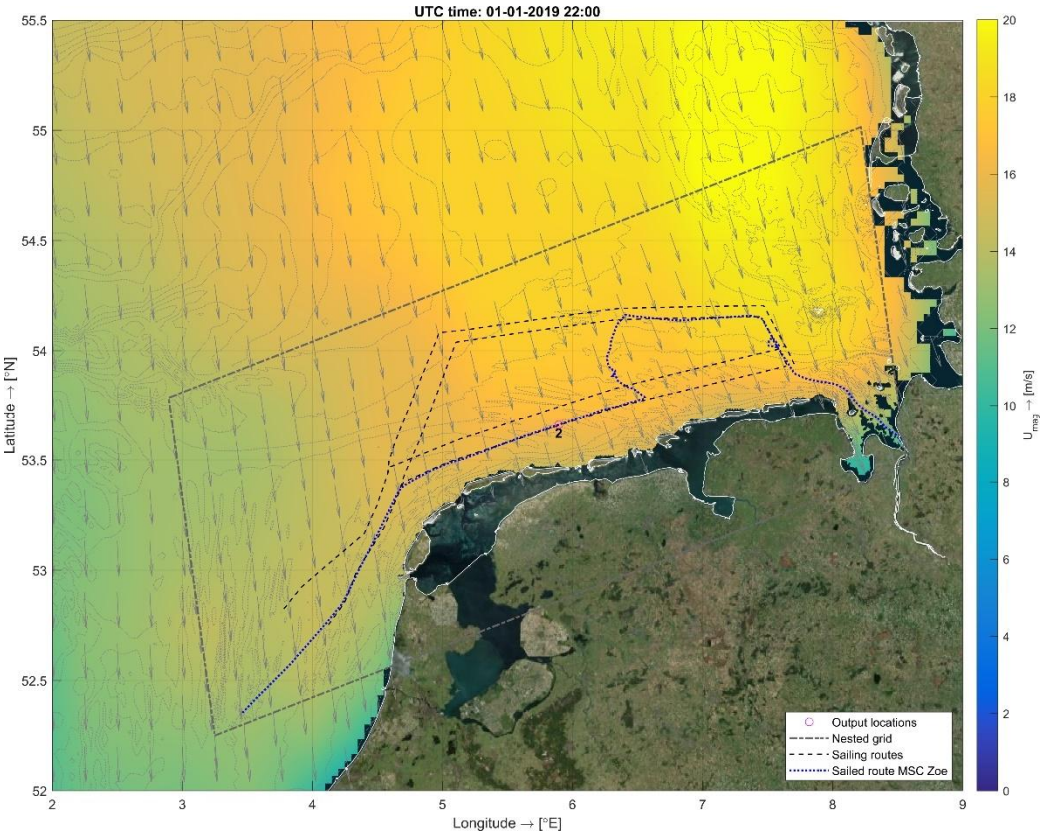

Figure B.5 As Figure B.4, now for Location 2.

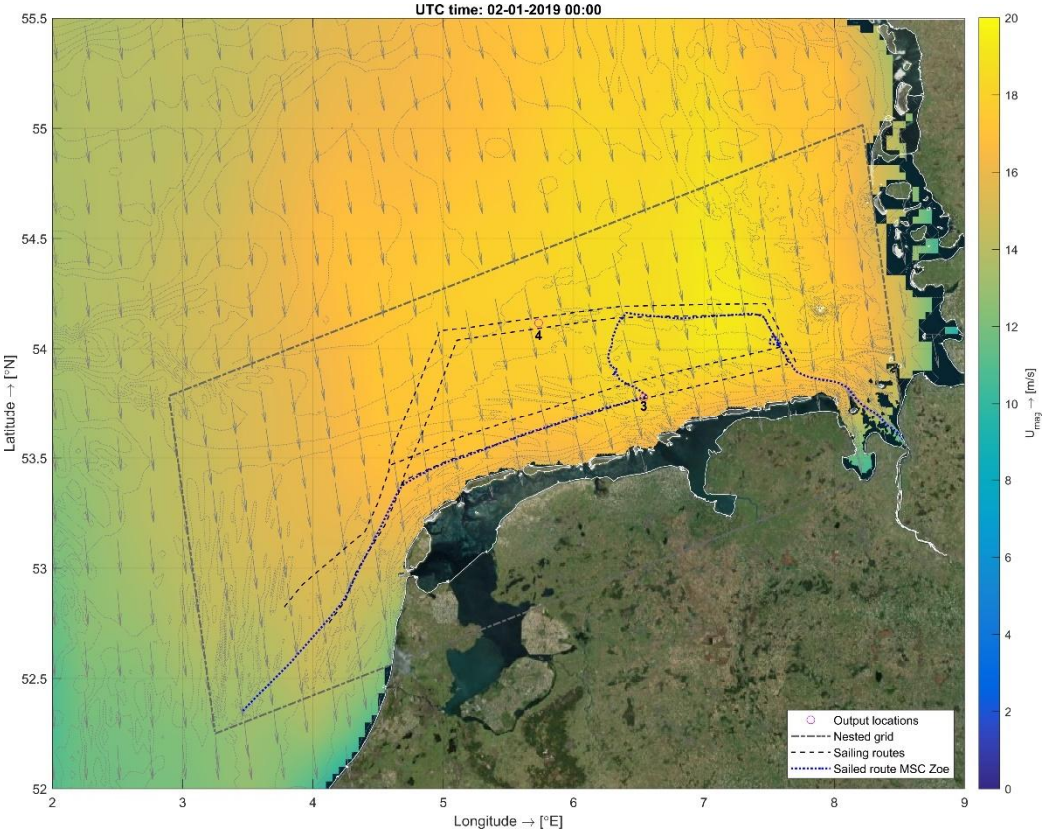

Figure B.6 As Figure B.4, now for Locations 3 and 4.

B.3 Waves

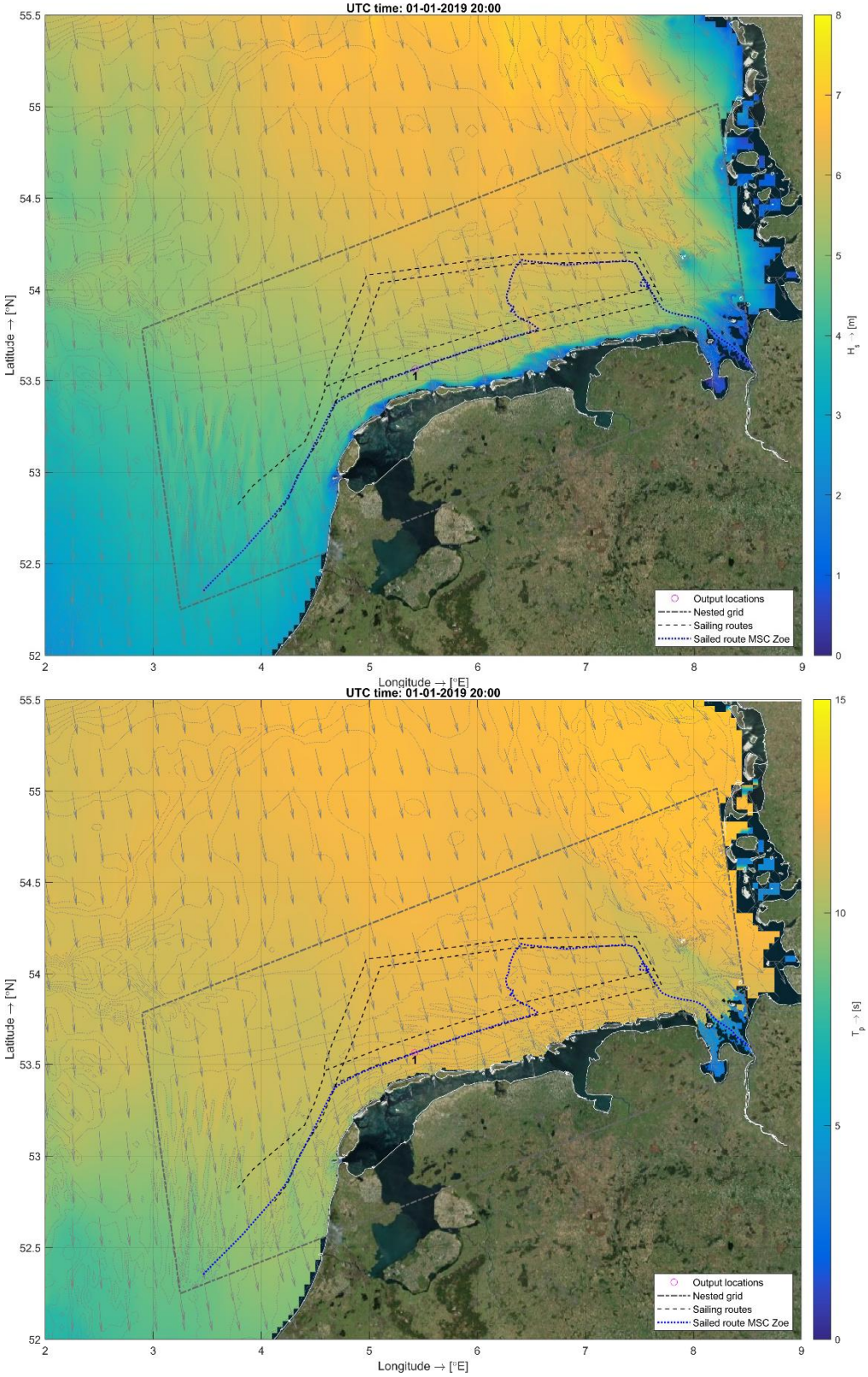

Figure B.7 Upper panel: spatial plot of H_s at the timestamp representative for Location 1. The grey arrows indicate the mean wave directions. The depth contours are indicated by grey dashed lines. Lower panel: same as upper panel, now for T_p.

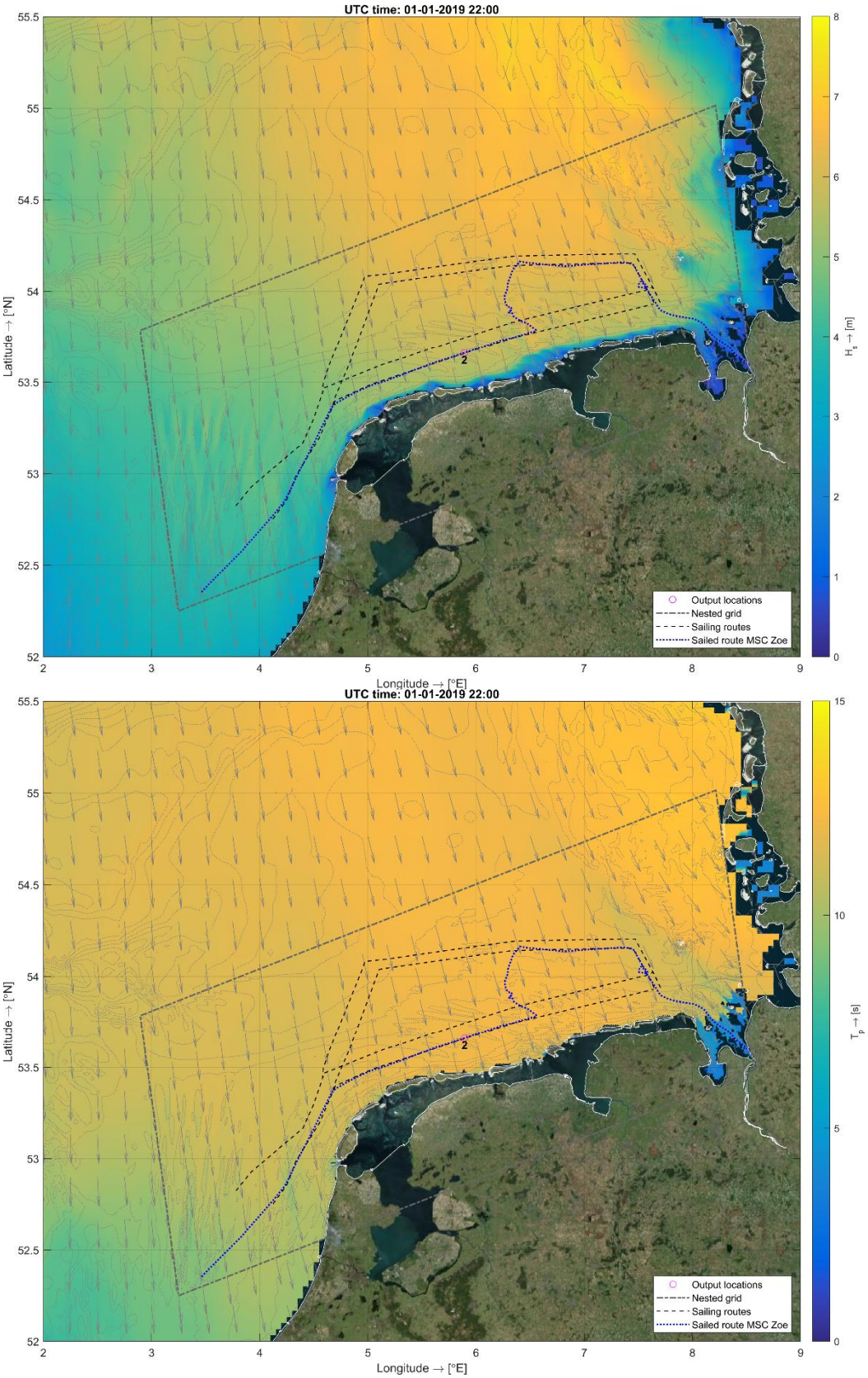

Figure B.8 As Figure B.7, now for Location 2.

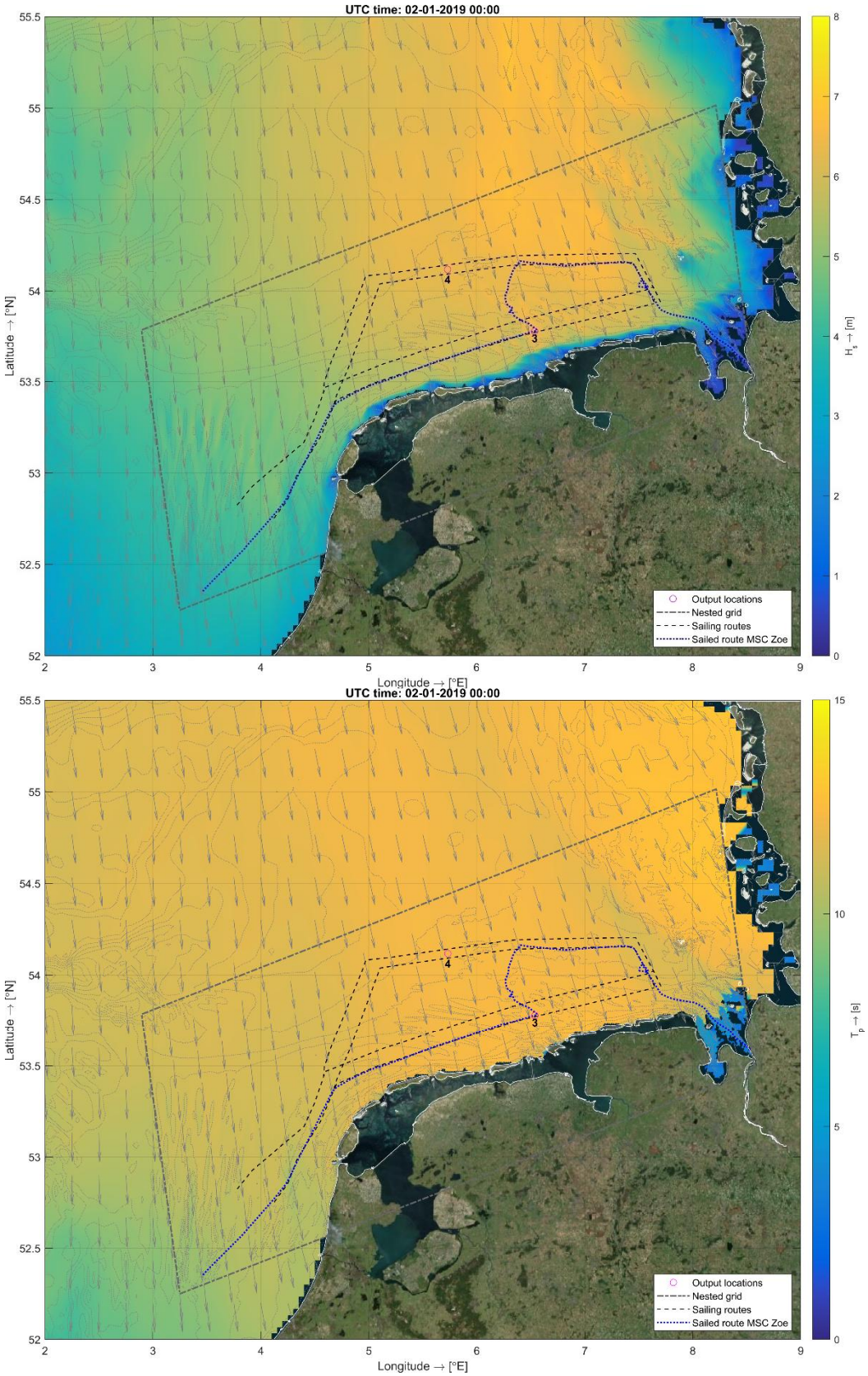

Figure B.9 As Figure B.7, now for Locations 3 and 4.

C Wave spectra

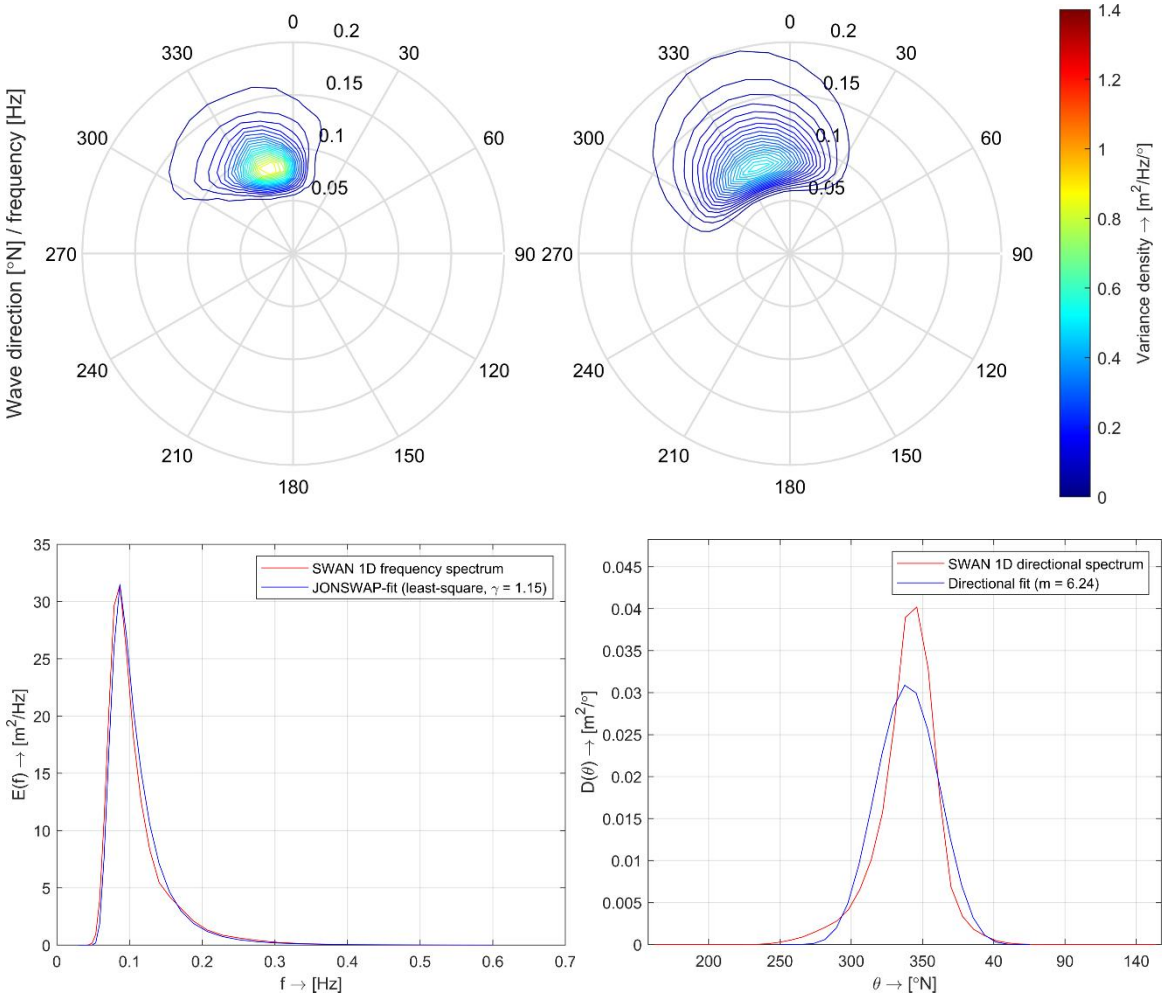

Figure C.1 Parametrisation of wave spectrum at Location 1. Top left: modelled 2D wave spectrum (SWAN). Top right: parametrized 2D JONSWAP wave spectrum. Bottom panels: representations of the same wave spectra, only now considered in 1D (in frequency, left, and direction, right).

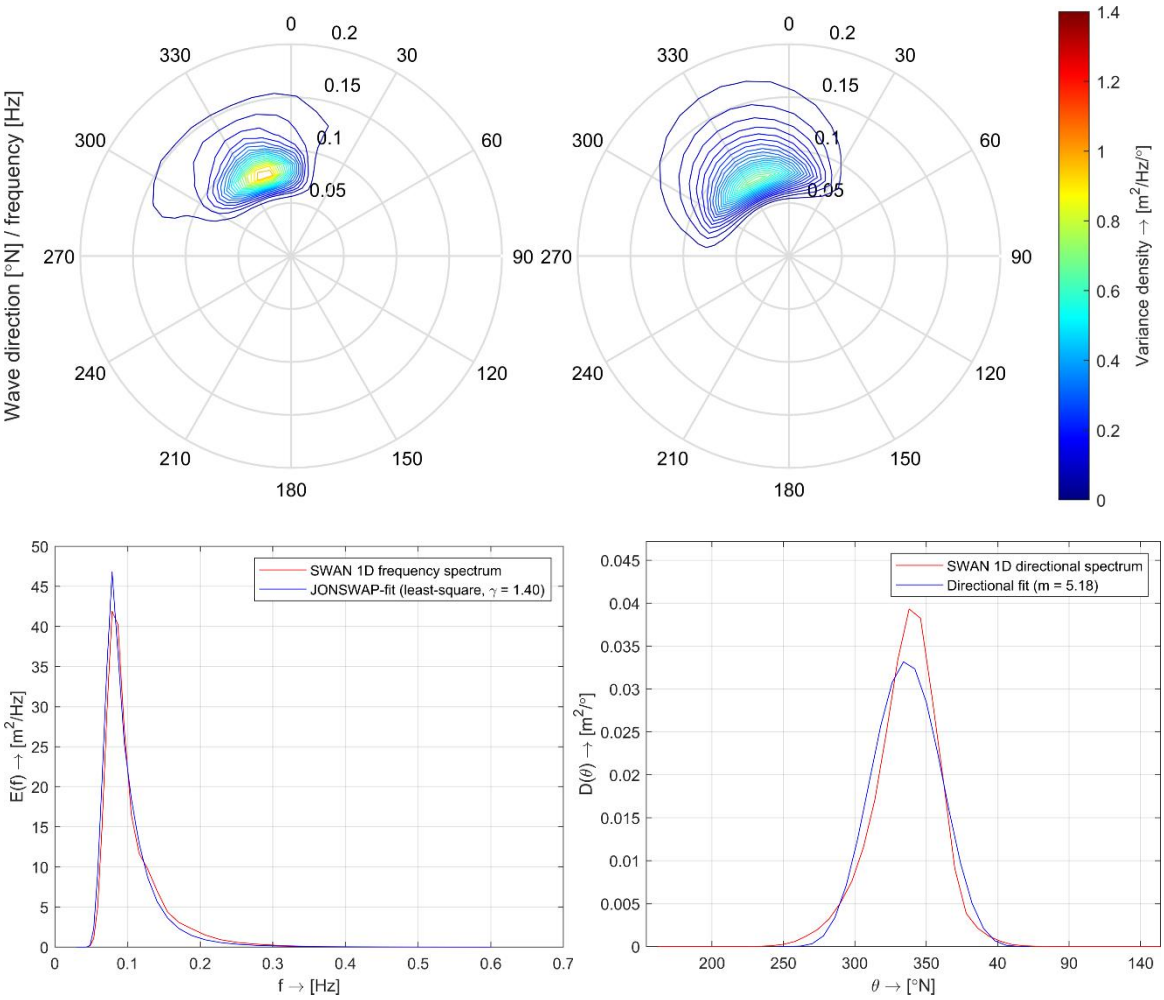

Figure C.2 As Figure C.1, now for Location 2.

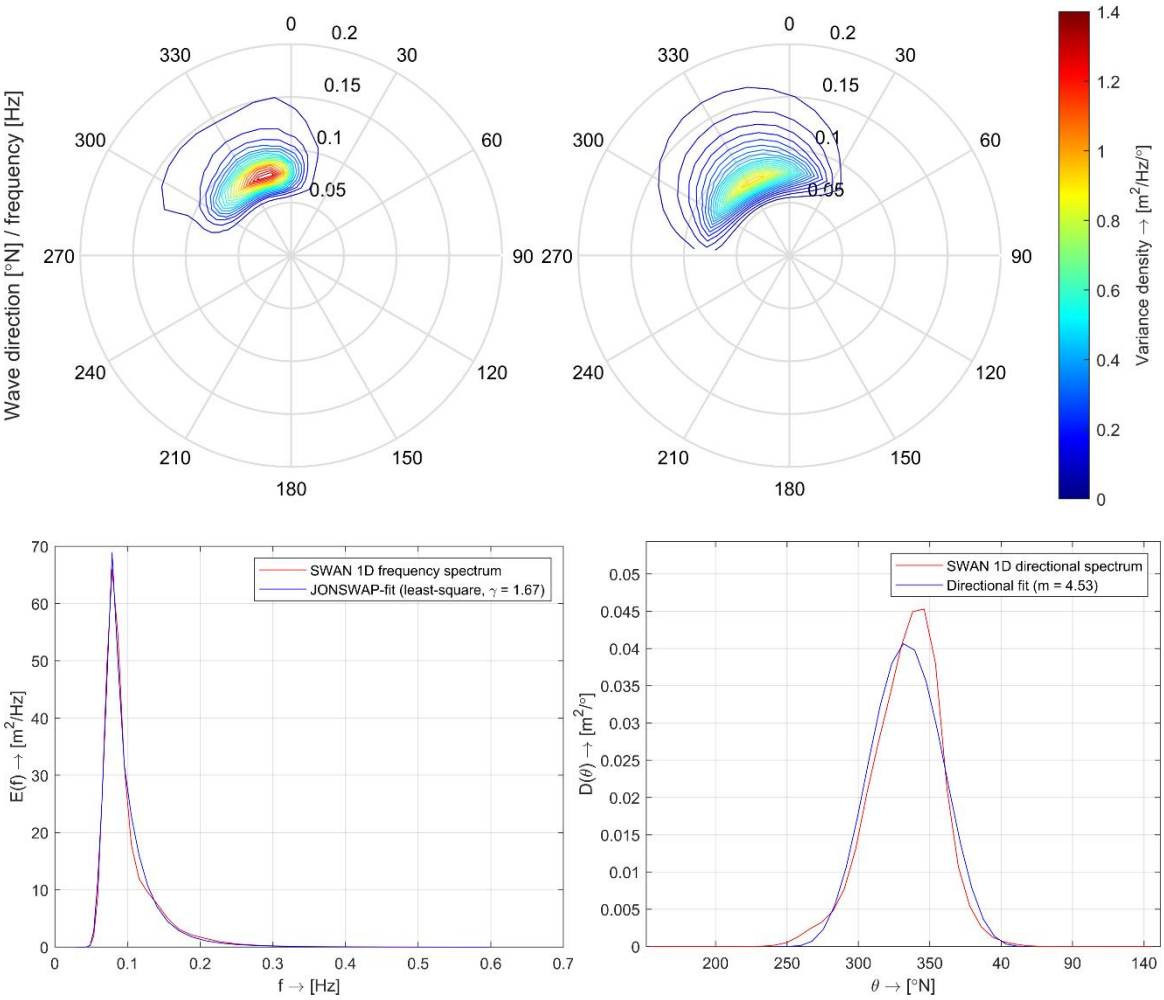

Figure C.3 As Figure C.1, now for Location 3.

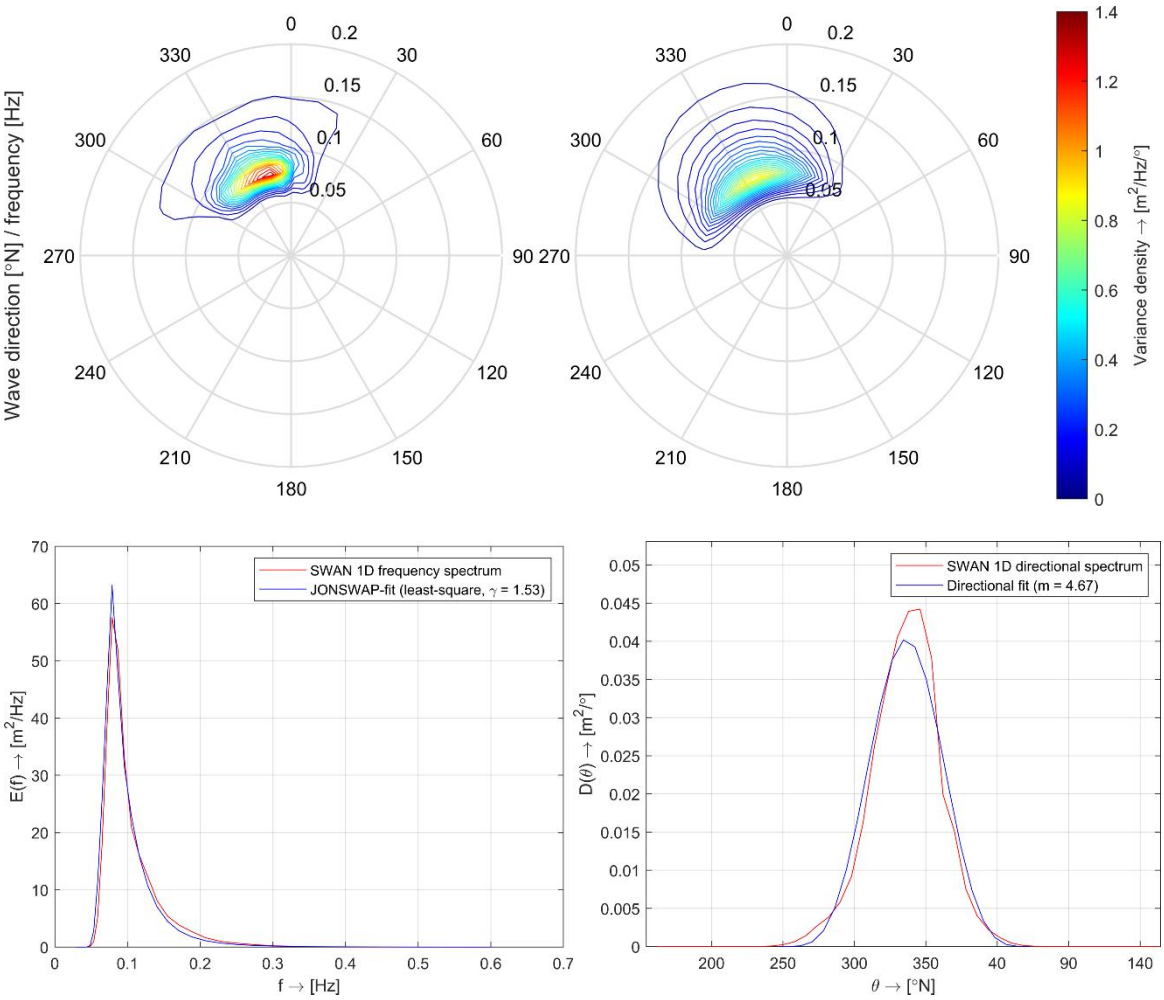

Figure C.4 As Figure C.1, now for Location 4.

D Positions of probes in physical scale model by MARIN

NORTH

WEST

EAST

SOUTH

Short crested wave probe

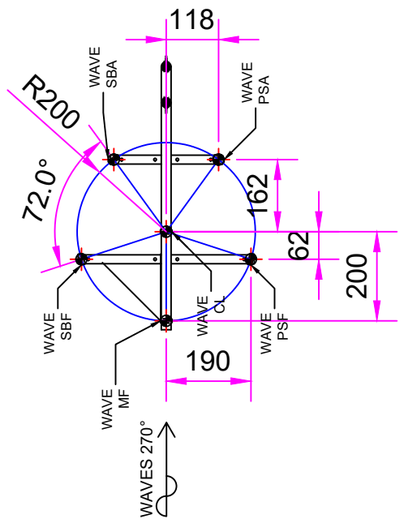

Wave splitting frame

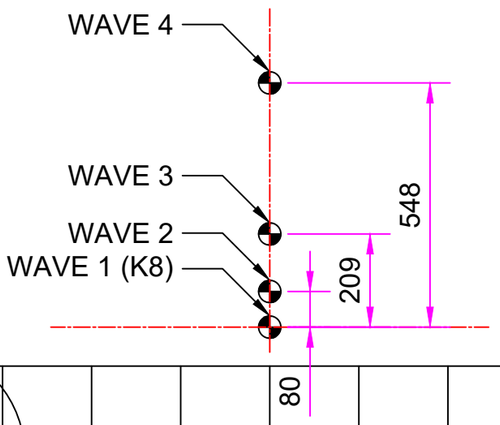

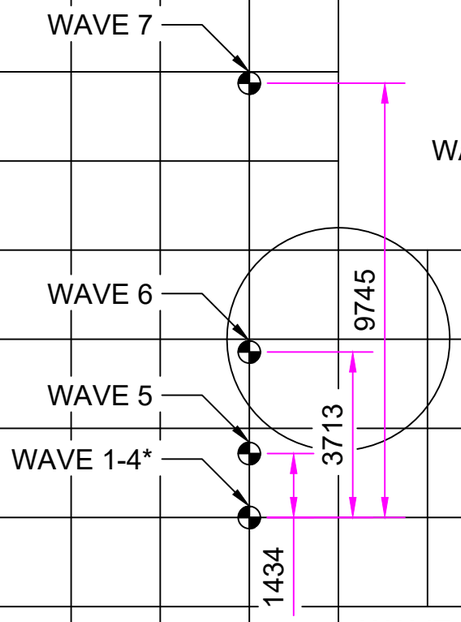

WAVES 180°

CURRENT 180°

WIND 180°

WAVE CAR

WAVE 1- 7: op statief
WAVE CL, SC1 en 8: aan meetwagen
WAVE 9 en SC2: op statief
WAVE CAR: aan subwagen (ook tijdens proeven)

22249

WAVE 9

WAVE 8

WAVE CL

WAVE SC1 (kortkammig rekje)

WAVE SC2 (kortkammig rekje)

1000

Vooraan meetwagen

11891

WAVES 270°

15 14 13 12 11 10 9 8 7 6 5 4 3 2 1

U T S R P O N M L K I H G F E D C B A